RICE UNIVERSITY

**Biodegradable Branched Polycationic Polymers as
Non-viral Gene Delivery Vectors for Bone Tissue Engineering**

by

Sue Anne Chew

A THESIS SUBMITTED
IN PARTIAL FULFILLMENT OF THE
REQUIREMENTS FOR THE DEGREE

Doctor of Philosophy

APPROVED, THESIS COMMITTEE:

Antonios G. Mikos, Professor, Chair
Bioengineering and Chemical and
Biomolecular Engineering
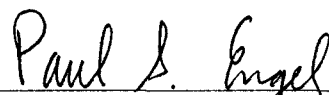
Paul S. Engel, Professor
Chemistry

Jeffrey D. Hartgerink, Professor
Bioengineering and Chemistry

F. Kurtis Kasper, Faculty Fellow
Bioengineering

HOUSTON, TEXAS
MAY 2010

UMI Number: 3421390

UMI®

Dissertation Publishing

ProQuest®

ABSTRACT

Biodegradable Branched Polycationic Polymers as

Non-viral Gene Delivery Vectors for Bone Tissue Engineering

by

Sue Anne Chew

In this work, biodegradable branched triacrylate/amine polycationic polymers (TAPPs) were synthesized from different amine and triacrylate monomers by Michael addition polymerization and incorporated into a composite scaffold to evaluate these polymers in a bone tissue engineering system. The effects of the hydrophilic spacer lengths in the polymer on characteristics which are important for gene delivery were evaluated by varying the triacrylate monomer used in the synthesis. The results demonstrated that hydrophilic spacers can be incorporated into polycationic polymers to reduce their cytotoxicity and enhance their degradability. The effects of amine basicities in the polymer on characteristics which are important for gene delivery were also evaluated by varying the amine monomers used in the synthesis. The results indicated that polycationic polymers with amines that dissociate above pH 7.4, which are available as positively charged groups for plasmid DNA (pDNA) complexation at pH 7.4, can be synthesized to produce stable polyplexes with increased zeta potential and decreased

hydrodynamic size that efficiently transfect cells. TAPP/pDNA polyplexes were then incorporated into a composite containing gelatin microparticles (GMPs) and a porous poly(propylene fumarate) scaffold. The release of pDNA *in vitro* was not affected by the crosslinking density of the GMPs but depended, instead, on the degradation rates of the TAPPs. Besides the initial burst release of polyplexes not bounded to the GMPs and the minimal release of pDNA through diffusion and dissociation from the GMPs, the pDNA was likely released as naked pDNA or in an incomplete polyplex as fragments of the polymer had to degrade to release the pDNA. The results indicated that polymeric vectors with a lower degradation rate can prolong the release of pDNA from the composite scaffold. Composite scaffolds loaded with TAPP/pDNA polyplexes may not have delivered enough intact polyplexes, as enhanced bone formation was not observed in a critical-size rat cranial defect at 12 weeks postimplantation compared to those loaded with naked pDNA. A gene delivery system consisting of biodegradable polycationic polymers should be designed to release the pDNA in an intact polyplex form.

ACKNOWLEDGEMENTS

on analyzing the histological results. I also recognize Dr. L. Scott Baggett for his patience and guidance on statistical analysis.

I extend my appreciation to my parents, Chin-Swee and Stephanie Chew and my sister, Sandee Chew, for believing in me and allowing me to explore anything I wanted in life while giving me their continuous support, love and encouragement. I also thank my family, friends, church and co-workers in the Mikos Lab for their prayers, encouragement and friendship. I especially extend my appreciation to my husband, Khon-Whey Tay for his never ending patience, love and constant reminder to have faith in the Lord and to not give up when things were not going as planned. Above all, I thank God, for the abundant blessings and hope He has given me throughout my time in Rice University.

TABLE OF CONTENTS

LIST OF FIGURES

LIST OF TABLES

LIST OF ABBREVIATION

^{1}H-NMR	proton nuclear magnetic resonance
A_{260}	UV absorbance at a wavelength of 260 nm
A_{260}/A_{280}	ratio of UV absorbance at wavelengths of 260 nm and 280 nm
AEPZ	1-(2-aminoethyl)piperazine
ANOVA	analysis of variance
API	1-(3-aminopropyl)imidazole
BDA	1,4-butanediol diacrylate
BMP	bone morphogenetic protein
CHO	Chinese hamster ovary
CMV	cytomegalovirus
D_2O	deuterium oxide
ddH_2O	double distilled water
DED	N,N-dimethylethylenediamine
DLS	dynamic light scattering
DMEM	Dulbecco's modified Eagle's medium
DMSO	dimethylsulfoxide
E. coli	Escherichia coli
E/M	number of ethyleneoxy groups in the triacrylate monomer
EDTA	ethylenediaminetetraacetic acid
eGFP	enhanced green fluorescent protein
FACS	fluorescence activated cell sorting
FBS	fetal bovine serum
FGF	fibroblast growth factor
GFP	green fluorescent protein
GMP	gelatin microparticles
H&E	hematoxylin and eosin
HCl	hydrochloric acid
HDO	deuterium protium oxide
Hyd	hydrazine
$I_{4.2}/I_{1.6}$	ratio of the integral of the methylene protons in the α-position to the ester to the integral of the methyl protons in the triacrylate monomers
IGF	insulin-like growth factor
MicroCT	microcomputed tomography
MIP	maximum intensity projections
MMA	methylmethacrylate
Mn	number average molecular weight
mRNA	messenger RNA
MSCs	mesenchymal stem cells
MTT	methyl tetrazolium
Mw	weight average molecular weight

N:P	ratio of amine groups in the polymer to phosphate groups in the pDNA
NaCl	sodium chloride
NaOH	sodium hydroxide
NIH	National Institute of Health
NLS	nuclear localization sequence
OH⁻	hydroxide ion
OPF	oligo(poly(ethylene glycol)fumarate)
PBS	phosphate buffer solution
pCMV-eGFP	plasmid-cytomegalovirus-enhanced green fluorescent protein
pCMV-hBMP-2	plasmid-cytomegalovirus-human bone morphogenetic protein-2
PDGF	platelet-derived growth factor
PDI	polydispersity
pDNA	plasmid DNA
PEG	poly(ethylene glycol)
PEI	polyethylenemine
PET	pentaerythritol triacrylate
PLGA	poly(lactic-co-glycolic acid)
PPF	poly(propylene fumarate)
PVA	poly(vinyl alcohol)
PVP	poly(vinyl pyrrolidone)
ROI	region of interest
SEC	size exclusion chromatography
TAE	tris-acetate-EDTA
TAPP	triacrylate/amine polycationic polymer
TGF	transforming growth factor
TMPETA	trimethylolpropane ethoxylate triacrylate
TMPTA	trimethylolpropane triacrylate
Tukey's HSD	Tukey's Honestly Significantly Difference
V	total volume of the volume of interest
v/v	volume per volume
V_m	volume of scaffold material
VOI	volume of interest
V_{pore}	pore volume
$V_{shrink-wrap}$	shrunk volume of interest
w/v	weight per volume
wt. %	weight percent
ρ	density

CHAPTER I

OBJECTIVE AND SPECIFIC AIMS

The overall objective of this research is to synthesize and evaluate biodegradable branched polycationic polymers with different hydrophilic spacer lengths and amine basicities for non-viral gene delivery and to incorporate these polymers into a composite scaffold carrier to investigate them in a bone tissue engineering system.

1. *Synthesis and Characterization of Biodegradable Branched Triacrylate/Amine Polycationic Polymers with Varying Hydrophilic Spacer Lengths as Non-Viral Gene Delivery Vectors*

- *Synthesis of biodegradable branched triacrylate/amine polycationic polymers with varying hydrophilic spacer lengths by altering the triacrylate monomer used in the synthesis.*

- *Evaluation of the effects of the hydrophilic spacer lengths on characteristics of the polymer which are important for gene delivery (i.e., molecular weight, amine equivalents dissociating within different pH ranges, degradability and cytotoxicity).*

- *Evaluation of the effects of the hydrophilic spacer lengths on characteristics of the polymer and plasmid DNA polyplexes which are important for gene delivery (i.e., polyplex diameter, zeta potential and transfection efficiency).*

2. *Synthesis and Characterization of Biodegradable Branched Triacrylate/Amine Polycationic Polymers with Varying Amine Basicities as Non-Viral Gene Delivery Vectors*

- *Synthesis of biodegradable branched triacrylate/amine polycationic polymers with varying amine basicities by altering the amine monomer(s) used in the synthesis.*

- *Evaluation of the effects of the amine basicities on characteristics of the polymer which are important for gene delivery (i.e., molecular weight, amine equivalents dissociating within different pH ranges, degradability and cytotoxicity).*

- *Evaluation of the effects of the amine basicities on characteristics of the polymer and plasmid DNA polyplexes which are important for gene delivery (i.e., polyplex diameter, zeta potential and transfection efficiency).*

3. *Fabrication and Evaluation of Composites Containing Triacrylate/Amine Polycationic Polymers and pDNA Polyplexes, Acidic Gelatin Microparticles and a Porous Poly(propylene fumarate) Scaffold for Bone Tissue Engineering*

- *Fabrication of composite scaffolds containing triacrylate/amine polycationic polymers and gelatin microparticles with different degradation rates.*

- *Evaluation of the effects of the triacrylate/amine polycationic polymers and gelatin microparticles degradation rates on the pDNA release kinetics in vitro.*

- *Evaluation of the ability of the composite scaffolds to enhance bone formation in a critical-size rat cranial defect in vivo.*

CHAPTER II

INTRODUCTION: NON-VIRAL GENE DELIVERY FOR BONE TISSUE ENGINEERING

Abstract

Aid is usually needed to repair bone defects with a large amount of bone loss or insufficient vascularity. Using a bone tissue engineering system that delivers a bioactive factor is a promising approach to repair such bone defects. Bone morphogenetic protein (BMP) is a bioactive factor that is capable of enhancing bone formation. Instead of delivering BMP in the protein form, BMP can also be delivered via gene therapy as a DNA encoding the BMP. There are a lot of barriers associated with the delivery of DNA *in vivo*. However, a vector such as a polycationic polymer can be used to help overcome some of these barriers. In addition to the polycationic polymer vector, the carrier that will be used to deliver the vector/DNA complexes is also an important factor that should be taken into consideration and incorporated when designing a successful gene delivery system for bone tissue engineering.

Bone

Bone Anatomy

Bone is a connective tissue that is firm and has sufficient strength to bear load. Bone forms the skeleton of the body and provides sites for the attachment of muscles. Bone also functions to protect certain organs in the body such as the brain, heart and lungs, and is a source of calcium, phosphate and other minerals. Bone is made out of an

organic phase that consists of mostly collagen type 1 and an inorganic phase[1] that consists of about 30% amorphous calcium phosphate and a little less than 70% crystalline hydroxyapatite[2]. Bone is also made out of a cellular element which consists of osteoblasts, osteocytes and osteoclasts.

Bone can be divided into two morphological types, cortical or cancellous bone. Cortical bone, which is also known as compact bone, is very dense and acts as a shell that covers the entire long bone to provide biomechanical support and fulfill homeostatic demands[3-5]. Alternatively, cancellous bone, which is also known as trabecular bone, is less dense and has a network structure with a spongy texture. Cancellous bone is present in the inner region of bone to provide biomechanical support and protective properties.

Bone Formation

The formation of bone occurs by either intramembranous or endochondral ossification. Intramembranous ossification takes place in flat bones such as the shell of cortical bones, cranial and mandible[6], and occurs without going through a cartilage intermediate[7]. Endochondral ossification, on the other hand, takes place in long bones and occurs through a cartilage intermediate.

The two stages of bone development are matrix formation and mineralization. In intramembranous ossification, immature progenitor cells progress into preosteoblasts and then into osteoblasts[7]. Osteoblasts, which are 15-30 μm cuboidal-shaped cells, synthesize and secrete collagen to form unmineralized bone matrix (i.e., osteoids) and arrange side-by-side to form a sheet that covers the bone forming surface[6]. After depositing osteoids, osteoblasts will regulate the deposition of calcium phosphate in the osteoids which results

in mineralization. The osteoblasts that are surrounded in the mineralized bone matrix then turn into osteocytes which have a stellate morphology. The osteocytes, which make up to 95% of total bone cells, play a part in bone matrix mineralization by regulating the movement of mineral ions from the extracellular fluid to form hydroxyapatite crystals[6]. Bone is a very unique tissue because it is the only tissue in the body that continuously remodels itself[8] through cycles of bone formation by osteoblasts and bone resorption by osteoclasts[8,9]. Osteoclasts, which are 20-100 μm multinucleated cells, adhere to mineralized matrix and form a small chamber that is sealed from the extracellular fluid to maintain a suitable microenvironment for bone resorption. Once they complete their resorptive function, osteoclasts move into marrow spaces close by and undergo apoptosis[6].

In endonchondral ossification, cartilage, which is an avascular tissue, is converted into bone, which is one of the most highly vascularized tissues in the body[10]. The chondrocytes in the cartilage become hypertrophic and begin secreting alkaline phosphatase which is essential for matrix calcification. The calcified hypertrophic cartilage is then penetrated by capillary vascular buds. Hypertrophic chondrocytes undergo apoptosis and the cartilage matrix is degraded, resulting in a vascularized cavity. Osteoblasts, formed from osteoprogenitor cells that enter the cavity, deposit osteoids in the area which are then replaced by trabecular bone.

Repairing Bone Defects

Effective approaches are much needed to repair bone defects caused by trauma, cancer, congenital abnormalities or age-related degeneration[11-14]. The repair of these

defects is still a challenge for orthopedic and reconstructive surgeons. The healing of a defect involves a very complex cascade of events. When an injury occurs as in a bone defect, the body responds by going through hemostasis (i.e., process that causes bleeding to stop), clearing cellular debris from the defect site and forming fibrous vascularized connective tissue[15,16]. The formation of a scar or regeneration of the tissue then takes place at the defect site. The cells at the defect site are mostly fibroblasts and inflammatory cells such as macrophages, lymphocytes, plasma cells and neutrophils, depending on the stage of the fibrous connective tissue development and whether infection is present[17]. Cytokines and growth factors in the local environment control the migration, proliferation and differentiation of the cells at the defect. Vascularization at the defect site is important for the recruitment of osteoprogenitor cells[18]. For bone, defects that have large bone loss or insufficient vascularity will not be conducive to regenerating by themselves[19]. Thus, aid is needed in healing such bone defects and different strategies are currently being investigated to guide the complex bone healing process in these defects.

Current Methods for Bone Repair

Current approaches for repairing bone defects include artificial prostheses and bone grafts[20]. Treatment of bone defects using artificial prostheses made from materials such as metal alloys and ceramics has been widely tested, however, there are several disadvantages associated with them. Before surgically placing these prostheses, a large amount of bone near the defect site has to be removed. Furthermore, non-

biocompatibility of the artificial materials[21] and the high cost of these prostheses are also limiting factors associated with this bone treatment method[20].

Among the strategies that are currently being applied to repair bone defects, bone grafting is the method that is most prominently used[22]. Bone grafts are usually harvested from the iliac crest of the patient or a donor[23]. In autogenous bone grafting, grafts from the same patient are used, whereas in allogenous bone grafting, grafts from donors are used[24]. The success of these grafts lies in the fact that they are comprised of components that are necessary for enhancing bone formation such as bone and progenitors cells and appropriate growth factors[25]. Due to problems faced when using bone grafts such as pain at the donor site, the need for two surgeries, availability of appropriate grafts with the right shape and volume as well as the risk of infection, other methods are being investigated to replace this current preferred method of healing bone defects[22].

Bone Tissue Engineering

Researchers have been focusing on the application of tissue engineering as an alternative approach to the current methods for treating bone defects. Tissue engineering, as defined by Boyan et al., is the "design, construction, modification, growth and maintenance of living tissue and organs from native or synthetic materials using scientific engineering principles with resources from molecular developmental biology, cell biology and biomaterial sciences"[26]. The ultimate goal of tissue engineering is to use the body's own capacity instead of grafts or artificial prostheses, to guide the wound healing process toward tissue regeneration.

Bone tissue engineering has been investigated to treat isolated bone defects which include fractures and non-unions[27] as well as bone diseases such as osteoporosis and osteogenesis imperfecta[28,29]. The ideal bone tissue engineering material should be osteoconductive as well as osteoinductive. An osteoconductive material is inert and allows the ingrowth of host tissue[20]. Alternatively, an osteoinductive material has the ability to induce osteogenic differentiation of mesenchymal stem cells (MSCs)[30]. The tissue engineering paradigm for bone and other tissues includes three general factors which are scaffolds, cells and bioactive molecules such as growth factors or genes encoding the growth factors. These three factors can be used singly or in combination to develop a tissue engineering system for a particular defect.

Delivery of Growth Factors to Promote Bone Formation

Tissue engineering systems, which deliver bioactive factors such as growth factors, can be a promising bone treatment method to replace the existing strategies for repairing bone defects. Growth factors are cell secreted proteins that can modulate cell activity by stimulating or inhibiting cellular proliferation, differentiation, migration, adhesion, apoptosis or gene expression[31]. Growth factors can interact with cell surface receptors of either the cell that produced and secreted the protein itself or a neighboring cell[32]. It has been shown in the literature that clinical fractures treated with growth factors had no significant difference after a 9-month healing period compared to those treated with autogenous cancellous bone grafts[33]. However, patients treated with the grafts had increased hospitalization, surgery time and blood loss from the donor site during surgery.

The delivery of growth factors to the local site can aid in fracture healing while avoiding the complications associated with bone grafts

Growth factors are typically delivered as recombinant proteins produced using microbes such as Escherichia coli (E. coli)[34] or a mammalian cell line such as Chinese hamster ovary (CHO) cells[35]. The gene that encodes the growth factor of interest is transfected into the cells where the gene is then transcribed and translated to produce the recombinant protein of interest. Fibroblast growth factors (FGFs), platelet-derived growth factors (PDGFs), insulin-like growth factors (IGFs), bone morphogenetic growth factors (BMPs) and transforming growth factors (TGFs)[8] are examples of growth factors that are capable of promoting the differentiation of MSCs into different lineages.

Bone Morphogenetic Protein

BMPs are members of the TGF-β superfamily and are osteoinductive factors that have been identified to facilitate skeletal development and the formation of bone[8,36]. BMPs can stimulate angiogenesis, which is the formation of new capillary vessels from existing vessels[37], as well as promote proliferation of MSCs[38-40]. BMPs can also behave as chemotactic agents by initiating the recruitment of osteoprogenitors and MSCs toward the defect site and stimulate the differentiation of these cells into an osteochondroblastic lineage[41]. Fifteen BMPs have been identified to date and they have varying capabilities of inducing osteogenesis in different types of cells[42]. Among them, BMP-1 has been shown to be incapable of inducing bone formation[43] and BMP-2, 4 and 7 have been established as successful osteoinductive factors[42]. A sufficient amount and duration of BMP expression at the defect site is needed to induce bone formation[25,44]. Many

researchers in bone tissue engineering have investigated the delivery of these osteoinductive factors in the form of the protein itself or the gene that encodes for the protein of interest.

Gene Therapy

The original objective of gene therapy is to deliver a gene to replace a defective gene[19]. However, the field of gene therapy has evolved to encompass introducing a new gene that encodes a specific therapeutic protein to a defect site in order to alter or control the path of cellular action[45]. Researchers have successfully identified growth factors that can enhance the formation of particular tissues, which has led to the production of these proteins for therapeutic purposes. A lot of research has been focused on delivering these growth factors for bone tissue engineering. However, shortcomings associated with delivering growth factors in the protein form have led to the use of gene therapy as an alternative approach to deliver the gene that encodes the growth factor of interest. Compared to the delivery of proteins, gene therapy allows for a longer bioavailability of the growth factor as DNA has a longer half-life compared to proteins[46]. Furthermore, manufacturing growth factors is expensive and more difficult compared to manufacturing the genes that encode the growth factors. By using gene therapy, the growth factors are synthesized *in vivo*, and as a result, the growth factors can be delivered in a more biologically active form[34] with more precise post-translational modification and tertiary structure formation[47,48]. Using gene therapy instead of delivering the BMP in the protein form for bone tissue engineering has been proven to result in higher total bone volume[49],

more efficient and organized bone formation[50] while requiring a smaller dose to enhance

bone formation[51].

Barriers of Gene Therapy

In gene therapy system for bone tissue engineering, a gene is usually delivered to

the cells at a defect site either by itself (i.e., naked DNA) or using a viral or non-viral

gene delivery vector. DNA that is delivered for gene therapy has to face many obstacles

before it can be transcribed into a messenger RNA (mRNA) and translated into the

protein of interest in the cell nucleus. Some of these barriers can be overcome by

delivering the DNA using a gene delivery vector

When designing a gene delivery system, several gene delivery barriers have to be

taken into consideration to ensure that the DNA is delivered successfully. The first barrier

or rate limiting step is to deliver the DNA to the desired area of interest without it

interacting with the reticular endothelial system[52]. This barrier can be overcome by

delivering the DNA directly to the site of interest via injection or using an implanted

carrier, rather than finding a method to circumvent the clearance of the DNA as it flows

systemically to the site of interest.

Once at or near the site of interest, the DNA has to face the obstacle of entering

cells as the cell membrane limits the transport of undesired molecules like DNA. DNA

can be interacted with a gene delivery vector to form a complex that can be delivered

using the same method that is used by cells to transport waste and nutrients to and from

the environment. These vector/DNA complexes are transported into the cells using

clathrin-coated pits which are internalized from the plasma membrane through a process

called endocytosis[53]. To ensure successful delivery through endocytosis, the complexes have to be around 100 nm or less in diameter to be able to fit in the clathrin-coated pits[54]. Although complexes larger than 100 nm are unable to get endocytosed by cells, they have been shown to transfect cells successfully[55,56] through an unknown mechanism[57,58].

Once successfully in the cell, the endocytosed DNA has to then face the obstacle of escaping from the endosomal compartment to avoid getting degraded in the lysosome[52]. pH sensitive gene delivery vectors that can buffer between pH 5.0 to 7.4 can help facilitate the release of DNA from the endosome through the proton sponge effect[59]. At low pH, as vectors buffer the pH by accepting hydrogen ions, the endosome will try to maintain the osmotic and charge balances, which will results in an influx of water and chloride counterions into the endosome. This causes the endosome to burst and results in the release of the DNA into the cytoplasm.

When the DNA successfully escapes from the endosome, it has to face the obstacle of translocation into the cell nucleus where its genetic code can then be read to produce the protein of interest[52]. The nuclear pores only allow particles of about 70 kDa (DNA with ~117 base pairs) to enter through free diffusion[60]. To deliver DNA larger than 70 kDa through the nuclear pores, a nuclear localization sequence (NLS) can be incorporated into the DNA sequence which functions to direct the complex into the nucleus[53]. However, instead of entering through the nuclear pores, DNA can be transferred into the nucleus during mitosis where the nuclear membrane is broken down[61].

Once in the nucleus, the DNA has to face the barrier of incorporating itself into the cell's DNA in order for the gene to be actually expressed by the cell. The complete DNA sequence that encodes all the proteins in an organism is known as the genomic

DNA[34]. This set of DNA is the same in each cell of the individual organism and it is replicated at every somatic cell division. DNA sequences are transcribed into mRNA which are then translated into specific proteins. Since mRNA are unstable, there is usually only transient production of protein from a specific mRNA[32]. In gene therapy, the DNA that encodes a particular growth factor to be delivered is considered exogenous DNA which does not get replicated in each somatic cell division. This DNA sequence consists of a promoter region which determines whether the gene will be expressed along with coding region for the protein of interest[62]. The promoter is regulated by the local environment in the host cell and the gene will only be expressed if it receives the required stimuli in the cell. If the gene does not receive the correct stimuli, the promoter will remain inactive[63], thus, the protein of interest will not be produced. Ideally for gene therapy, the DNA sequence should incorporate the promoter that is generally activated in the cell that will internalize the DNA to ensure that the desired protein is expressed when the exogenous gene is delivered into that cell. However, such promoters of cellular proteins are often large in size and not well characterized[64]. Therefore, promoters that resemble the promoters for viruses such as cytomegalovirus (CMV) or retrovirus are used instead as cells are known to respond to these promoters[63]. These viral promoters are often inactivated by methylation because they are recognized as foreign by the host cell, thus, eventually resulting in a decrease in gene expression after some time[65]. Therefore, a continuous delivery of the exogenous DNA is needed to ensure that the protein of interest is continuously produced.

Non-Viral Gene Delivery Vectors

Viral vectors such as adenovirus, adeno-associated virus, lentivirus and retrovirus have been shown to be very efficient at delivering DNA. However, due to the disadvantages such as immune and toxic responses, production complexity and cost of these vectors[66,67], non-viral vectors are increasingly being investigated as an alternative to replace viral vectors. Unlike viral carriers, DNA delivered using a non-viral vector is inserted into a plasmid which does not have a limitation on the size of the gene it can carry. The idea behind designing a successful non-viral gene delivery vector is to develop a material that will mimic the viral infection process[68] which has been shown to be very efficient at delivering a gene. The non-viral vector must be able to condense the DNA and protect it from degradation by nucleases. It also must form complexes that can transfect cells successfully and assist in endosomal escape.

One type of non-viral vectors currently being investigated is cationic lipids. These lipids are usually composed of a hydrophilic lipid anchor that is made out of a cholesterol or fatty acid group, and a cationic head group[19]. These two groups are connected by an intermediate group which is able to control the chemical stability and biodegradability of the cationic lipids, and can be used to attach targeting, cell uptake and intracellular trafficking moieties[69]. The hydrophilic portion of the cationic lipids plays a role in determining the flexibility and kinetics of the lipid exchange in the bilayer[70]. Tightly condensed complexes known as lipoplexes are formed when DNA and cationic lipids interact with each other. This interaction occurs as a result of the increase in entropy that

is derived when water molecules and counter ions are released from the surfaces of the DNA and the lipids[71].

Beside lipids, polymeric materials have also been investigated for application as non-viral gene delivery vectors. Neutral charged polymers such as poly(vinyl pyrrolidone) (PVP) and poly(vinyl alcohol) (PVA) have been used to deliver DNA[72]. These polymers are amphiphilic molecules that have hydrophobic backbones and hydrophilic side chains which can participate in hydrogen bonding. These polymers can interact with and stabilize DNA by hydrogen bonding as well as protect the DNA from nuclease degradation[73].

Positively charged polymers can also serve as gene delivery vehicles by electrostatically interacting with negatively charged DNA. Amines are basic groups and the lone pair electrons on the nitrogen of the amines can gain a proton which results in a positive charge. DNA has a negatively charged backbone made out of phosphodiseter groups that is highly extended due to the repulsion of the negative forces. This results in the large size of DNA which causes a problem for cellular uptake[74]. Polycationic polymers can be used to address this problem by acting in a similar way as nucleosomal proteins, such as histones, to condense and compact DNA[59]. Through electrostatic interactions with the polycationic polymers, the negative charges on the DNA are shielded, thus, reducing the repulsion between the negative charges on the DNA backbone. This capability of polycationic polymers make them more advantageous as non-viral gene delivery vectors compared to uncharged polymers. Furthermore, polymer/DNA polyplexes with a net positive charge, are able to enhance cell adhesion by interacting with the negatively charged phospholipids and sulfate groups of proteoglycans

on the cells[59,75]. Delivering DNA with a polycationic polymer instead of by itself (i.e., as naked DNA) significantly reduced the required dose of DNA to induce a biological response from the milligram range[76] to the microgram range[77].

Various types of polycationic polymers have been synthesized and evaluated as vectors for non-viral gene delivery. These polymers can be in the form of linear, branched or dendrimeric molecules, and have different advantages and disadvantages associated with them. Polyethylenimine (PEI)[78] is a polycationic polymers that have been highly investigated. Although PEI is known to be an effective non-viral gene delivery vector, its toxicity and non-degradability present a problem with repeated dosage and long-term usage due to its accumulation in the endosomal compartment or cell nucleus[79,80]. Thus, biodegradable polymers with high transfection efficiencies and low cytotoxicity are much needed to replace current non–biodegradable polycationic polymers such as PEI.

Biodegradable Polycationic Polymers

Biodegradability of polycationic polymers is important to facilitate the release of an encapsulated DNA once it is delivered into a cell. Furthermore, biodegradation of the polymers is key in the excretion of the polymers and their degradation products to avoid accumulation in the endosomal compartment or cell nucleus[81]. In designing a biodegradable polycationic polymer for gene delivery, the optimal degradation rate of the side chains or part of the main chain of the polymers is an important criterion to consider. The polymer should not degrade too quickly to avoid the disassembling of the DNA from the polyplex too early during the delivery process, making the DNA susceptible to

enzymatic degradation and reducing the DNA transfection efficiency. Alternatively, the polymer should degrade fast enough for the DNA to disassemble from the polyplex once the polyplex has reached the cytoplasm or nucleus to allow for DNA expression[81,82]. By degrading into lower molecular weight fragments, the density of positive charges in the polymer is decreased. This results in a decrease in the cytotoxicity of the polymer as interaction with cellular compartments is reduced[83,84].

Biodegradable polymers consist of degradable functional groups such as esters[85-91], disulfides[92] and urethanes[93-95]. These polymers can be synthesized from different monomers where the degradable unit is in one of the monomers or is formed during the reaction. Biodegradable polymers can also be synthesized by reacting low molecular weight molecules of existing non-biodegradable polymers such as PEI, with a degradable linker consisting of esters[96] or disulfide[92] bonds. High molecular weight PEI, which is currently one of the most effective polymers for gene delivery, forms polyplexes with high transfection efficiency but exhibits high toxicity to the cells. Alternatively, low molecular weight PEI exhibits lower toxicity but forms polyplexes which are not efficient at transfection[78,97]. By linking low molecular weight PEI with a degradable linker, a highly branched polymer with high transfection efficiency and improved toxicity can be obtained.

DNA can also be delivered with biodegradable micro- or nanoparticles which can be synthesized from biodegradable natural as well as synthetic materials. Particles synthesized from PLGA are the most studied gene delivery particles in the literature[98]. Although PLGA is a commercially available material that is FDA approved and widely used for medical applications and drug delivery, the material has several drawbacks for

DNA delivery. The large size and hydrophilic nature of DNA make it difficult to be encapsulated in the hydrophobic PLGA material. Furthermore, hydrolysis of PLGA results in the release of acidic byproducts that can lower the pH in the particles which may be detrimental to the encapsulated DNA[99,100].

A class of biodegradable polycationic polymers that has been highly investigated recently is poly(amino ester)s. One method to synthesize this class of polymers is by Michael addition polymerization of diacrylate[85,86,88] or triacrylate[87,90,91] monomers with amine monomers. This synthesis as well as the resulting polymers formed from this synthesis has many advantages associated with them. The synthesis of these polymers is performed in a one–pot reaction that does not require a catalyst, which would need to be removed through a purification process. The resulting polymers are degradable by ester hydrolysis which results from the ester groups in the acrylate monomers. Unlike polycondensation or amidation reactions, Michael addition polymerization preserves the basicity of the amine groups, even when they participate in the reaction. Thus, the amines that participate in the reaction can still be beneficial to the gene delivery process.

Lynn et al. have synthesized such polycationic polymers from diacrylate and amine monomers[88,89]. In one of their studies, they synthesized polymers from 1,4-butanediol diacrylate (BDA) and three different amine monomers which were N,N'-dimethylethylenediamine, piperazine and 4,4'-trimethylenedipiperidine. They demonstrated that these polymers were successfully degradable hydrolytically in acidic and alkaline media[89]. In another study, Lynn et al. synthesized a library containing a total of 140 structurally unique polymers[88]. Seventy of these polymers were sufficiently water-soluble and were able to bind DNA. They found that polymers containing 1-(3-

aminopropyl)imidazole (API) were similar in structure to other histidine containing polymers and the imidazole groups, which have buffering capacity, allowed these polymers to mediate endosomal escape. The linear polycationic polymer synthesized with BDA and API successfully resulted in a transfection efficiency that was 4-8 times higher than PEI.

In contrast to Lynn et al., some groups have synthesized biodegradable poly(amine ester)s by reacting triacrylate monomers, instead of diacrylate monomers, with amine monomers via Michael addition polymerization resulting in branched polymers instead of linear polymers. Linear polycationic polymers usually have a much faster degradation rate compared to branched polymers. This causes them to release the encapsulated DNA too early during the delivery process which may be detrimental to the DNA[101]. Compared to linear polymers, branched polymers have degradative sites that are more hidden inside the numerous branches of the polymer, thus, the degradation rates of these polymers can be prolonged. Furthermore, amines in branched polymers are more sterically hindered compared to those in linear polymers. As a result, the amines in branched polymers are more difficult to protonate which increases their buffering capacity and ability to assist in endosomal escape.

Wu et al. are among the groups that have successfully synthesized these poly(amine ester)s with a triacrylate monomer. Wu et al. synthesized a hyperbranched polymer using trimethylolpropane triacrylate (TMPTA) and 1-(2-aminoethyl)piperazine (AEPZ) by Michael addition polymerization[87]. The polymer contained primary, secondary and tertiary amines similar to those in the well established polymer PEI. Although PEI has been shown to be very efficient at transfecting cells, its non-

degradability can be a problem. Wu et al. demonstrated that they were able to synthesize a polymer with amine constitutions similar to PEI that formed polyplexes with higher transfection efficiency and was degradable and non-toxic compared to PEI. Kim et al. have also successfully synthesized hyperbranched poly(amine ester)s with a triacrylate monomer[91]. To synthesize their polymers, they used pentaerythritol triacrylate (PET) which is a triacrylate monomer that has an additional hydroxyl functional group compared to TMPTA, to allow further modification of the synthesized polymer and enhance water solubility. Kim et al. reacted PET with amine monomer N,N-dimethylethylenediamine (DED), and modified the hydroxyl group on PET by reacting it with aminohexanoic acid or lysine that contains amines to increase the amount of positive charges in the polymers. Kim et al. showed that the polymer that was modified with aminohexanoic acid goes through a stepwise degradation process as a result of the differences in susceptibility of the ester bonds to hydrolysis.

Delivery of Polymer/DNA Polyplexes with a Carrier

Unlike the delivery of DNA *in vitro*, there are more issues that have to be taken into consideration when designing a vector that will be successful in transfecting cells *in vivo*. Delivery of DNA *in vivo* can be performed systemically through the blood circulation or locally to a particular site of interest. Systemic delivery can be advantageous for the delivery of DNA to sites that are inaccessible or difficult to access for local applications[102]. This delivery method is more suitable for the treatment of patients with diseases where a particular gene has to be delivered to every host cell such as for osteogenesis imperfecta or Gaucher's disease. For osteoporosis where multiple

sites have a deficiency in mineralization, systemic delivery may also be a more suitable treatment compared to local delivery[103]. Although more suitable for some applications, systemic delivery of the DNA is much more challenging than local delivery as the DNA will have to traverse harsh environments to get to the specific target site. Thus, local delivery of the gene at or near the defect site using a bone tissue engineering system may be more beneficial for some applications. By using this method, there will be a higher chance that the DNA will be delivered to the targeted area successfully. Thus, a lower dose of DNA will be required to illicit a therapeutic response as compared to delivering the DNA systemically.

In developing a successful gene therapy system for bone tissue engineering, the gene delivery vector is not the only important factor to take into consideration. The carrier (i.e., scaffold or composite scaffold) that is used to deliver the vector/DNA complexes also plays a critical role in the gene therapy strategy[104]. In a gene therapy system, the gene delivery vector is important for the complexation and condensation of the DNA. The vector also protects the DNA from degradation, facilitates the interaction of the DNA with the negatively charged cells and assists in the endosomal escape of the DNA once in the cells. Alternatively, the carrier plays an important role in delivering the vector/DNA complexes to a specific site, controls the release kinetics of the complexes and protects the vector from degradation before the complexes are delivered into the cells. Furthermore, an ideal carrier for bone tissue engineering should have strong mechanical properties that are similar to bone, high porosity and interconnectivity, good biocompatibility and should be biodegradable. The carrier should also provide a three-dimensional environment for the proliferation and differentiation of osteoprogenitor

cells[104]. Certain properties of the carrier such as the degradation rate, porosity and mechanical strength can be tailored to fit the defect site of interest.

The delivery of DNA using this two level (i.e., vector and carrier) delivery system approach have been investigated by many groups[46,77,105,106]. A delivery system with just one of these components will not be as efficient as when both components are incorporated. Without the vector, the DNA will be delivered as uncondensed DNA which is not protected from degradation. Delivery of naked DNA has been shown by many groups, including ours, to be less efficient at transfecting cells[107,108]. Alternatively, without the carrier, the entire dose of vector/DNA complexes will be delivered as a bolus delivery at the site of interest. This may not result in a therapeutic effect when a sustained release of the growth factor such as BMP-2 is required to heal the defect site[36]. Appropriate concentrations of growth factors delivered for sufficient time is important to avoid retarded or no improvement in the rate of bone healing[34]. For gene delivery, the DNA encoding the growth factor will be delivered instead of the protein itself. For successful bone formation, the DNA should be delivered in a controlled manner so that the cells will be able to produce a sufficient concentration of the protein in a sustained manner.

Several research groups have used PEI as the vector to deliver DNA in a biodegradable carrier system since PEI is a well established vector that has been shown to be a very efficient non-viral gene delivery vehicle. Lim et al. delivered PEI/DNA polyplexes by electrostatically encapsulating them into water-soluble chitin and alginate fibers which have a net positive and net negative charge, respectively[105]. Polyplexes of PEI with DNA encoding basic FGF that were released from these scaffolds were able to

retain their bioactivity and transfect cells seeded on the scaffolds. The escape of polyplexes from the fiber scaffolds depended on the electrostatic interaction of the charges on the scaffolds with ions in the culture medium and the degradation rate of the scaffolds. Lim et al. found that human dermal fibroblasts transfected with polyplexes released from these 3D scaffolds had prolonged secretion of basic FGF for 2 weeks with levels that were significantly higher than the baseline. However, 2D controls with a bolus delivery of PEI/DNA polyplexes showed expression for only 3 days. The highest concentration of secreted basic FGF in the 2D controls was notably lower than for the 3D scaffolds. The results from this study showed that by incorporating a 3D scaffold carrier, continuous delivery of the PEI/DNA polyplexes could be achieved and the polyplexes could be delivered directly into the cellular microenvironment in the scaffold which enhanced the bioavailability of the DNA.

Huang et al. also delivered PEI/DNA polyplexes in a sustained and localized approach using a biodegradable carrier. They incorporated these polyplexes in a PLGA scaffold and delivered the composite scaffold in a critical-size rat cranial defect[77]. Naked DNA encoding BMP-4 delivered in the PLGA scaffolds and blank PLGA scaffolds produced bone formation mainly on the edges of the defect. DNA that was condensed with PEI and then encapsulated in the PLGA scaffolds, however, showed bone formation at the edges as well as within the defect site. Furthermore, the total bone formation was at least 4.5-fold more than the other two types of scaffolds. Delivery of condensed DNA with a vector led to more complete mineralized tissue formation as shown by an increase in osteoid and mineralized tissue density in the defect site. These results demonstrated the

advantage of using a non-viral polycationic vector to deliver DNA from a scaffold carrier compared to delivering DNA in the naked, uncondensed form.

Conclusions

Due to the limitations and problems associated with current bone repair strategies, a lot of research has been focused on using tissue engineering as an alternative approach. Bone tissue engineering systems incorporating plasmid DNA (pDNA) encoding BMP-2 complexed with a polycationic polymer is a promising application for repairing bone. Although current polycationic polymers such as PEI are known to be effective non-viral gene delivery vectors, their toxicity and non-degradability present a problem with repeated dosage and long-term usage due to their accumulation in the endosomal compartment or cell nucleus[79,80]. Thus, biodegradable polycationic polymers are being designed and synthesized to replace these non-degradable vectors. In this work, triacrylate/amine polycationic polymers (TAPPs) with different hydrophilic spacer lengths and amine basicities were synthesized by Michael addition polymerization. We hypothesized that by altering the hydrophilic spacer lengths and amine basicities in the TAPPs, the polymer and polymer/pDNA polyplex characteristics which are important for gene delivery can be tailored. To evaluate these TAPPs in a bone tissue engineering system, TAPPs/pDNA polyplexes were incorporated into a composite containing acidic gelatin microparticles (GMPs) and a porous poly(propylene fumarate) (PPF) scaffold. We hypothesized that the degradation rates of the TAPPs and GMPs can affect the release kinetics of the pDNA and that composite scaffolds containing TAPP/pDNA polyplexes will result in enhanced bone formation compared to those containing naked pDNA.

CHAPTER III

SYNTHESIS AND CHARACTERIZATION OF BIODEGRADABLE BRANCHED POLYCATIONIC POLYMERS WITH VARYING HYDROPHILIC SPACERS FOR NON-VIRAL GENE DELIVERY[†]

Abstract

Biodegradable branched polycationic polymers with varying hydrophilic spacer lengths were synthesized from different triacrylate monomers and the amine monomer 1-(2-aminoethyl)piperazine by Michael addition polymerization. The hydrophilic spacers were varied by the number of ethyleneoxy groups in the triacrylate monomer (E/M) that ranged from 0 to 14. The polymer degradation depended on the spacer length and pH; the amount of ester degraded as determined by ^{1}H-NMR after 14 days was $43.4 \pm 2.1\%$ (pH 5.0) and $89.7 \pm 1.3\%$ (pH 7.4) for the polymer with 0 E/M compared to $55.7 \pm 2.6\%$ (pH 5.0) and $98.5 \pm 1.6\%$ (pH 7.4) for the polymer with 14 E/M. Cell viability of rat fibroblasts after exposure to polymer solutions of concentrations up to 1000 μg/mL remained high (above $66.9 \pm 12.1\%$ compared to below $7.6 \pm 1.1\%$ for polyethylenimine at a concentration of 50 μg/mL or higher) and increased with the spacer length. The polyplexes made with all the synthesized polymers showed higher transfection efficiency ($4.5 \pm 1.7\%$ to $9.4 \pm 2.0\%$, dependent on the polymer/pDNA weight ratio) with an enhanced green fluorescent protein reporter gene compared to naked pDNA ($0.8 \pm 0.4\%$) as quantified by flow cytometry. This study demonstrates that hydrophilic spacers can be

incorporated into polycationic polymers to reduce their cytotoxicity and enhance their degradability for non-viral gene delivery.

Introduction

Gene therapy can be used to alter or control the path of cellular action[19] by replacing a defective gene or introducing a new gene that encodes for a specific therapeutic protein[45]. Viral vectors have been shown to be very efficient at delivering DNA. However, due to safety concerns such as immune and toxic response, production complexity and cost of these vectors[66,67], non-viral vectors such as polycationic polymers are increasingly being investigated as an alternative method for gene delivery. Such polymers, which frequently contain positively charged protonated amine groups, are able to interact electrostatically with the negative charges of the phosphate groups on the DNA backbone leading to DNA condensation and protection against DNA degradation. Furthermore, positively charged polymer/DNA polyplexes may better adhere to cells by interacting with the negatively charged phospholipids and sulfate groups of the proteoglycans on the cells[59,109], which ultimately helps with the internalization of the polyplexes by endocytosis. The pH in such newly formed endosomes gradually decreases and reaches values of 4.5 when the endosome becomes a lysosome[53,59]. Any amine groups that buffer between pH 7.4 to 5.0 can assist in the escape of the DNA from the endosome and prevent DNA degradation by nucleases in the lysosome through the proton sponge effect[59].

Biodegradable polymers with high transfection efficiencies are much needed as more cytocompatible alternatives to current non–biodegradable polycationic polymers,

such as polyethylenimine (PEI)[78] and poly(dimethylaminoethylmethacrylate) (PDMAEM)[110]. Although PEI and PDMAEM are known to be effective non-viral vectors, their toxicity and non-degradability presents a problem with repeated dosage and long-term usage due to their accumulation in the endosomal compartment or cell nucleus[79,80]. Biodegradability of polycationic polymers is important to facilitate the release of encapsulated DNA once in the cell and to excrete the polymers and their degradation products to avoid accumulation in the endosomal compartment or cell nucleus[81]. An optimal degradation rate of the side chains or part of the main chain of the polymers is a key design criterion of polymers for non-viral gene delivery. If the polymer degrades too quickly, the DNA will disassemble from the polyplex too early during the delivery process. As a result, the degraded polymer will not complex with and condense the DNA, thus making the DNA susceptible to enzymatic degradation. On the other hand, the polymer should degrade fast enough for the DNA to disassemble from the polyplex once the polyplexes have reached the cytoplasm or nucleus to allow for plasmid expression[81,82]. Degradation of the polymer into lower molecular weight fragments is further desirable as it decreases the cytotoxicity of the polymer by decreasing the density of positive charges, thus, reducing any interaction with cellular compartments[83,111].

Biodegradable polymers synthesized by Michael addition polymerization of acrylate and amine monomers have been previously investigated as non–viral gene delivery vectors[85-91]. These polymers can be synthesized from either diacrylate[85,86,88,89] or triacrylate[87,90,91] monomers, to produce either linear or branched polymers, depending on the type of amine monomer used in the synthesis. The acrylate monomers contain ester groups, which contribute to the hydrolytic biodegradability of the polymers. The

/'polymers are synthesized in a one–pot reaction that does not require a catalyst, which would have to be isolated during the purification process. In contrast to polycondensation or amidation reactions, addition polymerization preserves basicity of the amine groups, even when they participate in the reaction.

In this work, a series of polymers were synthesized by chemically conjugating different triacrylate monomers with a single amine monomer, 1-(2-aminoethyl)piperazine (AEPZ) to test the hypothesis that hydrophilic spacers can be incorporated into polycationic polymers to produce gene delivery vectors with reduced cytotoxicity and enhanced degradability. The hydrophilic spacers in these polymers consist of ethyleneoxy groups, equivalent to those found in poly(ethylene glycol) (PEG), which is often incorporated into polymers to increase the hydrophilicity and chain flexibility of the polymers[93] as well as to decrease the cytotoxicity of polymeric non-viral vectors[112,113]. To test this hypothesis, we investigated the effects of the hydrophilic spacer lengths (different triacrylate monomers) on the molecular weight, amine equivalents protonating at different pH values, degradability and cytotoxicity of the synthesized polymers as well as the diameter, zeta potential and transfection efficiency of the polyplexes formed by these polymers with plasmid DNA (pDNA), all of which are relevant parameters in designing a gene delivery vector.

Materials and Methods

Materials

Trimethylolpropane triacrylate (TMPTA), 3 types of trimethylolpropane ethoxylate triacrylates (TMPETA) that differ in the average number of ethyleneoxy

groups per molecule (TMPETA with 3 ethyleneoxy groups per monomer (3E/M), TMPETA with 7 ethyleneoxy groups per monomer (7E/M) and TMPETA with 14 ethyleneoxy groups per monomer (14E/M)), AEPZ, branched PEI (typical weight average molecular weight, Mw ~ 25 kDa, polydispersity (PDI) of 2.5), chloroform (ACS grade), sterile-filtered dimethyl sulfoxide (DMSO), methyl tetrazolium (MTT) powder, phenol red free Dulbecco's modified Eagle medium (DMEM), ethidium bromide and Tris-Acetate-EDTA (TAE) were purchased from Sigma-Aldrich (St. Louis, MO). Deuterium oxide (D_2O) was obtained from Cambridge Isotope Laboratories, Inc. (Andover, MA). Acetone (ACS grade), isopropanol (ACS grade) and Fisher Certified Buffer pH 5.0 and 7.4 were purchased from Fisher Scientific (Pittsburgh, PA). Fischer rat fibroblast 3T3-like cell line (CRL 1764) was obtained from American Type Culture Collection (Manassas, VA). DMEM, phosphate-buffered saline (PBS), penicillin, streptomycin and amphotericin B were purchased from Gibco Life (Grand Island, NY). Fetal bovine serum (FBS) was obtained from Gemini Bio-Products (Calabasas, CA). Trypsin-ethylenediaminetetraacetic acid (EDTA) (0.25% trypsin/0.02% EDTA) was obtained from Invitrogen (Carlsbad, CA). Poly(ethylene glycol) (PEG) standards with number average molecular weights (Mn) ranging from 102 to 82,500 Da were obtained from Waters (Milford, PA). Plasmid DNA (pDNA) with a cytomegalovirus (CMV) promoter and enhanced green fluorescent protein (eGFP) reporter gene (pCMV-eGFP, 4.7 kb, cat no. 6085-1) was obtained from Clontech (Palo Alto, CA). Qiagen Endofree Plasmid Giga Kit was purchased from Qiagen (Valencia, CA).

Polymer Synthesis

Four sets of polymers (P-0E/M, P-3E/M, P-7E/M, P-14E/M) (Table III-1) were synthesized by reacting AEPZ with TMPTA (0E/M), TMPETA (3E/M), TMPETA (7E/M), and TMPETA (14E/M) using a synthetic approach published previously[87].

Table III-1 Polymer composition and structures of the triacrylate and amine monomer building blocks. P-0E/M, P-3E/M, P-7E/M and P-14E/M vary in hydrophilic spacer length. l = m = n = 1 for TMPETA (3E/M), l + m + n = 7 for TMPETA (7E/M) and l + m + n = 14 for TMPETA (14E/M).

Group	Triacrylate Monomer	Amine Monomer
P-0E/M	TMPTA	AEPZ
P-3E/M	TMPETA (3E/M)	AEPZ
P-7E/M	TMPETA (7E/M)	AEPZ
P-14E/M	TMPETA (14E/M)	AEPZ
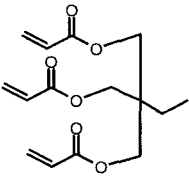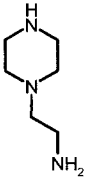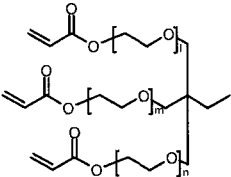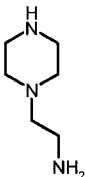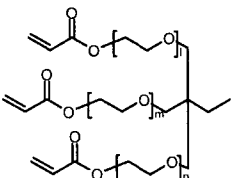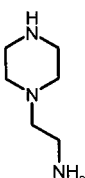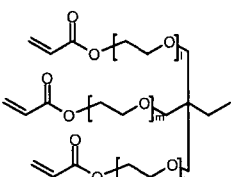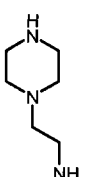
All polymers were synthesized at a 2:1 molar ratio of amine to triacrylate monomer, which is the same ratio applied previously in the synthesis of polymers with similar architecture and polymerization mechanism[87,90,91]. Typically, 10.8 mmole of the amine monomer and 5.4 mmole of the triacrylate monomer were dissolved in 20 mL of chloroform in a round bottom flask. The solution was allowed to react for 8 days at ambient temperature. The polymer was then purified by precipitation in 400 mL of acetone and 5 mL of hydrochloric acid (HCl) (12 M). The product was washed with excess acetone and vacuum dried to remove any remaining solvent. The NMR spectra revealed the following characteristic signal: **P-0E/M**: 0.9 ppm (t, C–CH$_2$–CH_3), 1.4 ppm (m, C–CH_2–CH$_3$), 2.5–3.5 ppm (t, –CH$_2$–CH_2–NR$_2$– and t, –CH$_2$–CH_2–COO–CH$_2$–), 4.0–4.1 ppm (s, C–CH_2–OOC–CH$_2$–). **P-3E/M, P-7E/M and P-14E/M**: 0.9 ppm (t, C–CH$_2$–CH_3), 1.4 ppm (m, C–CH_2–CH$_3$), 2.5–3.5 ppm (t, –CH$_2$–CH_2–NR$_2$– and t, –CH$_2$–CH_2–COO–CH$_2$–), 3.6–3.9 ppm (s, C–CH_2–O– and t, –O–CH_2–CH_2–O–), 4.0–4.1 ppm (t, –CH$_2$–CH_2–OOC–CH$_2$–).

Polymer Characterization

Proton Nuclear Magnetic Resonance (^{1}H-NMR)

^{1}H-NMR spectra of the polymers were obtained using a 400 MHz Bruker spectrometer (Bruker Avance 400, Zurich, Switzerland). The samples were dissolved in D$_2$O and analyzed using MesRe-C, an NMR processing software package (Mestrelab Research S. L., Spain). The proton peak of deuterium protium oxide (HDO) was used as the internal shift reference (δ = 4.8 ppm).

Molecular Weight Determination by Size Exclusion Chromatography (SEC)

The weight average molecular weight (Mw), number average molecular weight (Mn) and polydispersity index (PDI) (Mw/Mn) of the polymers were obtained using a Waters Alliance® HPLC system (Waters, Milford, PA) equipped with a differential refractometer. The samples were run through a Shodex OHpak SB-G (6.0 x 50 mm) guard column, a Shodex OHpak SB803 HQ (8.0 x 300 mm) and a Shodex OHpak SB802.5 HQ (8.0 x 300 mm) analytical column placed in series. PEG standards with Mn ranging from 102 to 82,500 Da were used to generate the calibration curve[87]. A 0.5 M sodium acetate buffer containing 0.1 M sodium nitrate was used as the mobile phase (pH 4.5). The flow rate was set to 0.5 mL/min, with the temperature of the column and sample chamber set at 25°C and 12°C, respectively. The polymer samples were dissolved in the mobile phase and filtered through a 0.2 μm cellulose filter (Alltech, Deerfield, IL). Data analysis was performed using the Empower™ software (Waters, Milford, PA) provided with the instrument. The theoretical average compositions of the polymers were calculated based on the Mn values obtained from SEC by assuming that the reaction occurred at the molar feed ratio of amine to triacrylate monomers of 2:1.

Hydrogen Ion Titration

The number of amine equivalents in a given mass of polymer was evaluated by hydrogen ion titration. In a typical experiment, 50 mg of polymer were dissolved in 10 mL of 150 mM sodium chloride (NaCl) solution. The polymer solution was adjusted to a pH of 2.0 using 0.1 or 1 M HCl solution and/or 0.1 N sodium hydroxide (NaOH) solution. The polymer solution was then titrated by stepwise (200 μL) addition of 0.1 N NaOH

under continuous stirring. The pH of the solution was measured after each addition of 0.1

N NaOH solution using an accumet* AP63 Portable pH meter (Fisher Scientific,

Pittsburgh, PA). Each titration was done in triplicate, and average pH values were

calculated and reported. The amine equivalents (which corresponds to the amount of

amines in the polymer) that dissociated in different pH ranges were determined by

calculating the amounts of hydroxide ion (OH⁻) that were required to change between two

pH values[114].

Polymer Degradation by ^{1}H-NMR Analysis

The rate of hydrolytic ester degradation of the polymers was determined at pH 5.0

and 7.4 by ^{1}H-NMR analysis[87,115,116]. In a typical experiment, a polymer sample (7.5 mg)

was dissolved in 750 µL of pH 5.0 or 7.4 Fisher Certified Buffer[117]. Throughout the

degradation study, the samples were incubated at 37°C while shaking at 75 rpm. At

predefined time points (0 h, 6 h, 12 h, 1 d, 3 d, 7 d and 14 d), the samples were frozen and

lyophilized. The dried samples were then dissolved in D_2O and analyzed by ^{1}H-NMR.

This study was done in triplicate (n=3). At each time point, percent ester degradation was

obtained by evaluating the change in the ratio of the integral of the methylene protons in

the α-position to the ester to the integral of the methyl protons in the triacrylate

monomers in the polymers ($I_{4.2}/I_{1.6}$). The integral of the protons in the α-position to the

ester decreased as the esters degraded. The integral attributed to the methyl protons in the

polymers remained unchanged during the hydrolytic ester degradation process. Equation

1 was used to calculate the percentage of ester that was degraded at each time point, and

the data was reported as percent ester degraded[87,115,116].

$$\% \text{ Ester Degraded} = \frac{(\text{Ratio at } 0\,h - \text{Ratio at time point})}{\text{Ratio at } 0\,h} * 100 \qquad (\text{Equation 1})$$

Cytotoxicity Analysis by MTT Assay

The cytotoxicity of the polymers was evaluated using an MTT viability assay[118]. CRL 1764 rat fibroblasts were expanded in T-75 culture flasks with DMEM supplemented with 10% (v/v) FBS and antibiotics (100 µg/mL penicillin, 100 U/mL streptomycin, and 0.5 µg/mL amphotericin B) and cultured at 37°C in 5% CO_2 and 95% relative humidity. Typically, rat fibroblasts were trypsinized with trypsin-EDTA solution (2 mL/flask) and replated on 96–well plates with a density of 8000 cells/well. The plates were incubated (37°C in 5% CO_2 and 95% humidity) for 24 hours to allow the cells to reach 80–90% confluency. Polymer solutions with a pH of 7.4 and an osmolarity of 280–320 mosm/kg were prepared in DMEM at six polymer concentrations (10, 50, 100, 250, 500 and 1000 µg/mL). Branched PEI (25 kDa) at the same concentrations was used as a negative control. PEI 25 kDa has been extensively characterized in the literature and is often used as a control in the development of polymers for non-viral gene delivery[87,119]. As cytotoxicity and transfection efficiency can vary depending on the cell type and source, PEI was included in this study for experiments that involved cells (i.e., cytotoxicity and transfection efficiency experiments) to allow for direct comparison with the synthesized polymers under the same conditions. To start the experiment, culture media was removed and 100 µL of the polymer solution was added to individual wells of the 96-well plates. The plates were then incubated for 2 and 24 h at 37°C. At each time point, the polymer solution was removed, and the wells were washed twice with PBS to remove any residual polymer solution. 100 µL of MTT solution (1 mg/mL in phenol red

free DMEM) was added to each well. After 3 h of incubation under exclusion of light, the MTT solution was removed and 100 µL of DMSO/2–propanol 1:1 (v/v) solution was added to each well to dissolve the formazan crystals formed by the live cells. The plates were agitated to help dissolve the formazan crystals. The absorbance was measured at 570 nm using a microplate reader (Powerwave X340, BIO–TEK Instruments, Winooski, VT). The cell viability was obtained by normalizing the absorbance of the wells containing cells cultured in the presence of polymer solution to the absorbance of the wells cultured with plain media. The average number of live cells was calculated from 5 different samples.

Polymer/pDNA Polyplex Characterization

<u>Amplification and Purification of Plasmid DNA</u>

pCMV-eGFP was amplified in Escherichia coli (E. coli) bacterial cultures and purified using a Qiagen Endofree Plasmid Giga Kit according to the protocols provided by the manufacturer. The yield of the pDNA was determined from the UV absorbance at a wavelength of 260 nm (A_{260}) (NanoDrop^{TM} 1000 Spectrophotometer, Thermo Scientific, Wilmington, DE). To evaluate the plasmid purity, the ratio of the UV absorbance at wavelengths of 260 nm and 280 nm (A_{260}/A_{280}) was determined to be between 1.8 and 2.0. The pCMV-eGFP was used in all the polymer/pDNA polyplex characterization experiments.

<u>Zeta Potential</u>

Polymer/pDNA polyplexes were prepared at different polymer to pDNA weight ratios (5:1, 10:1, 50:1, 100:1, 200:1 and 300:1). The polyplexes were prepared by adding various amounts of polycationic polymer solution in PBS (300 µL) drop-wise to 10 µg of pDNA also dissolved in 300 µL PBS. The mixture was vortexed and then incubated for 1 h at room temperature to allow for polyplex formation. The zeta potential of the resulting particles or larger aggregates was obtained using a Zen 3600 Zetasizer (Malvern Instruments, Worcestershire, UK). Disposable cuvettes were filled with the polyplex solution and run in the zetasizer for a minimum of 10 cycles and a maximum of 100 cycles at 25°C. The zeta potential was calculated using the Smoluchowski equation based on the electrophoretic mobility[120]. This study was done in triplicate.

<u>Band Retardation with Gel Electrophoresis</u>

Different weight ratios (10:1, 20:1, 30:1, 40:1, 60:1, 80:1 and 100:1) of polycationic polymer to pDNA solutions were prepared. The polyplexes were prepared from 10 µL polymer solution in PBS and 10 µl of a solution of 1 µg pDNA in PBS as described above. A 0.5% (w/w) of agarose gel containing 5 µL of ethidium bromide solution (10 mg/mL) was prepared in TAE buffer (1x). The polyplex sample (20 µL) containing bromophenol blue loading solution was loaded into the wells. The gel was run for 1 h at 80 mV in TAE buffer (1x) and an image of the gel was captured in an UV transillumination box.

Hydrodynamic Polyplex Sizes by Dynamic Light Scattering (DLS)

The hydrodynamic diameter of the polycationic polymers/pDNA polyplexes was evaluated at different polymer to pDNA weight ratios (10:1, 50:1, 100:1, 200:1, 300:1 and 500:1) using a 90PLUS Particle Size Analyzer (Brookhaven Instruments Corporation, Holtsville, NY) with an incident beam of 660 nm wavelength and scattering angle set at 90°. The data were collected using the BIC 32 Bit Software (Brookhaven Instruments Corporation, Holtsville, NY). The polyplexes were prepared from 300 μL polymer solution in PBS and 300 μL of a solution of 10 μg pDNA in PBS as described above. The solution was allowed to equilibrate to 25°C inside the analyzer before the analysis was started. The diameter of the polyplexes or aggregates thereof was obtained using Laplace inverse program Non-Negative Least-Squares (NNLS)[119]. This study was done in triplicate.

eGFP Transfection of Rat Fibroblasts

CRL 1764 rat fibroblasts were grown in T-75 culture flasks using DMEM supplemented with 10% (v/v) FBS and antibiotics (100 μg/mL penicillin, 100 U/mL streptomycin, and 0.5 μg/mL amphotericin B) at 37°C in an incubator (5% CO_2, 95% relative humidity). In a typical experiment, rat fibroblasts were trypsinized (2 mL trypsin-EDTA solution/flask) and replated in 6-well plates at a seeding density of 250,000 cells/well. After 24 h of cell attachment, media was aspirated and 100 μL of the plasmid polyplex solution containing 5 μg of pDNA complexed at different polymer/pDNA weight ratios (10:1, 50:1, 100:1, and 300:1) was added drop-wise to the cells. The

following solutions served as controls: PEI/pDNA at a weight ratio of 2:1, naked pDNA and FBS-free media without pDNA. The weight ratio of 2:1 for PEI/pDNA polyplexes corresponds to a ratio of amine groups in the polymer to phosphate groups in the pDNA (N:P) of 11.5:1, which is similar to that used by Wu et al. (N:P of 10:1) as the optimal N:P for transfection with PEI[87]. The polyplexes were prepared from 50 μL polymer solution in PBS and 50 μl of a solution of 5 μg pDNA in PBS as described before. Immediately after the addition of 100 μL of the polyplex solution, 400 μL of DMEM (FBS free) was added. After 24 h, 2 mL of DMEM/FBS (10% (v/v)) was added to the cells, and the flask was incubated for an additional 48 h. The cells were then washed twice with PBS, trypsinized (500 μL of trypsin-EDTA solution per well), washed with PBS, fixed with chilled formaldehyde solution (1%) and placed on ice for 1 h. After washing with PBS, samples were analyzed using a flow cytometer (Becton Dickenson FACS Scan, BD Biosciences, San Jose, CA) at high flow. CellQuest Pro software (BD Biosciences, San Jose, CA, v 5.1) was used to collect the data. A total of 5000 cells were counted for each sample. The location of the cells on the dot plot was confirmed by running untreated cells in PBS through the cytometer. Markers were placed at 5% of control samples (untreated cells) and the relative rightward shift of the intensity was observed as the percentage of transfected cells. This study was done at n=5. Fluorescence images of selected samples were taken with a confocal microscope (Zeiss LSM 510, Carl Zeiss Jena, Germany) to confirm transfection and expression of the green fluorescent protein. The cells were imaged with a 20x objective after excitation by an argon laser. The transfection study was designed to ensure that a lower mass of polymer per unit area of culture well compared to that tested in the cytotoxicity experiment was

used. In the cytotoxicity experiment, cells exposed to the highest mass of polymer per unit area of culture well tested, 300 μg/cm^2 (polymer concentration of 1000 μg/mL), were still viable. In the transfection experiment, the highest mass of polymer per unit area of culture well that was tested was 150 μg/cm^2 (weight ratio of 300:1).

Statistical Methods

The results were presented as means ± standard deviation. Single-factor analysis of variance (ANOVA) was used to identify if there were any significant differences among groups ($p < 0.05$). Tukey's Honestly Significantly Difference (HSD) test was then conducted to identify the specific groups that differed statistically significantly.

Results and Discussion

Polymer Synthesis

Polymers were synthesized and precipitated from acetone through the addition of HCl. The precipitates were solid or rubbery and sticky. The protonated polymers were insoluble in organic solvents, thus all characterizations were done in aqueous solutions. A general structure of the synthesized branched polymers is shown in Figure III-1. The end groups in the polymer are primary amines from the amine monomer, AEPZ, that did not react with the triacrylate monomer[87]. Once protonated, these primary amines can participate in the complexation with pDNA. The yields of the polymerization were between 70-85%.
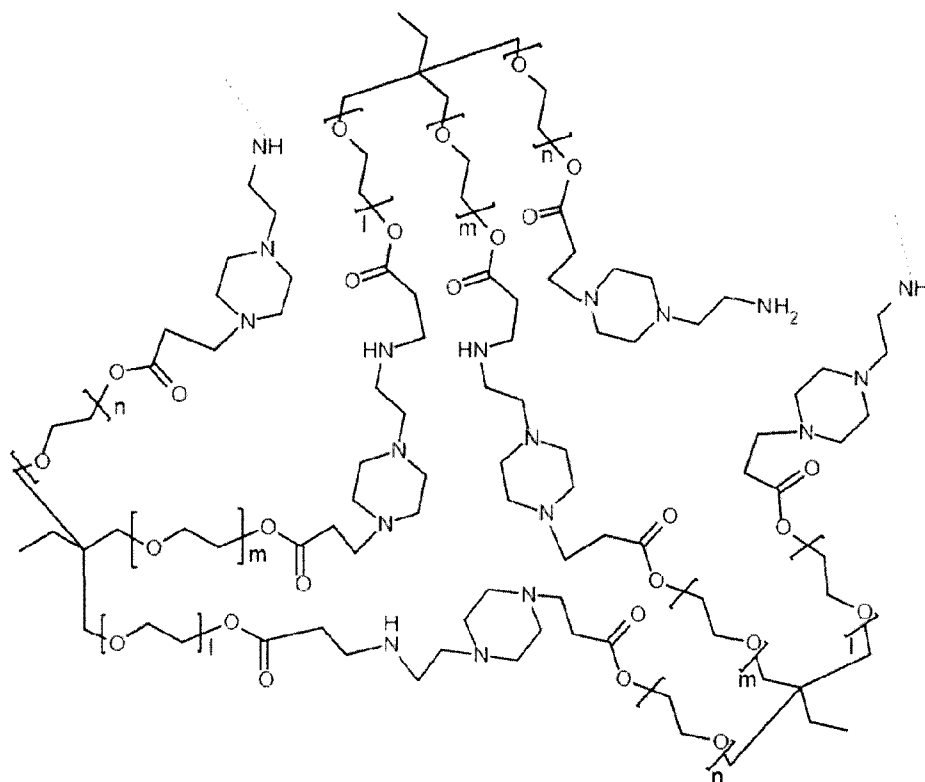
Figure III-1 General structure of a branched polymer obtained by Michael addition reaction of AEPZ with a triacrylate monomer.

Polymer Characterization

Proton Nuclear Magnetic Resonance (^{1}H-NMR)

^{1}H-NMR confirmed that all acrylate groups of the triacrylate monomers converted during the reaction, as the typical signals for olefinic protons (5.8-6.6 ppm) were absent for the polymeric products (not shown). Since the presence of unreacted acrylate groups would contribute to polymer cytotoxicity, it is important to achieve complete reaction of the acrylate groups[121].

^{1}H-NMR data was also used to verify that the polymer building blocks, amine and triacrylate monomers, reacted in a molar ratio of 2:1. The integral of the peaks between

2.5–3.5 ppm (derived from six protons: $-CH_2-CH_2-NR_2$ in the amine monomer, $-CH_2-$ CH_2-NR_2 formed through the reaction, and $-CH_2-COO-CH_2-$ from the triacrylate monomer) was compared to the integral of the peak at 0.9 ppm (derived from three methyl protons in the triacrylate monomers). These calculations yielded molar ratios for P-0E/M, P-3E/M, P-7E/M and P-14E/M of 1.8, 2.1, 1.9, and 2.3, respectively.

Molecular Weight Determination

Table III-2 presents Mn, Mw and PDI of the polymers as obtained by SEC, as well as the theoretical average composition of the polymers calculated based on the experimental Mn and Mw values.

Table III-2 Number average molecular weight, weight average molecular weight, polydispersity index (PDI), estimated average number of triacrylate and amine monomers per polymer molecule and pKa values of the polymers examined in this study.

Polymer	Mn (Da)*	Mw (Da)*	PDI*	Number of Triacrylate Monomers[†]	Number of Amine Monomers[†]	pKa
P-0E/M	2,700	6,670	2.47	4 (10)	8 (20)	7.85
P-3E/M	1,980	4,800	2.42	3 (7)	6 (14)	7.93
P-7E/M	2,310	8,660	3.75	3 (10)	6 (20)	8.02
P-14E/M	3,180	10,070	3.17	3 (9)	6 (18)	8.08

* Measured by size exclusion chromatography

[†] Estimated from number average molecular weight, numbers in brackets estimated from weight average molecular weight

The SEC traces of the synthesized polymers are shown in Figure III-2. It was found that on average the polymers consisted of 6 or 8 amine and 3 or 4 triacrylate monomers. Low molecular weights were obtained for the synthesized polymers. The molecular weights of the polymers were obtained with SEC using linear PEG standards to generate the calibration curve. The calibration with a linear polymer may not account for the effect of branching that may be present in the polymers; thus an underestimation of the molecular weights may have occurred.
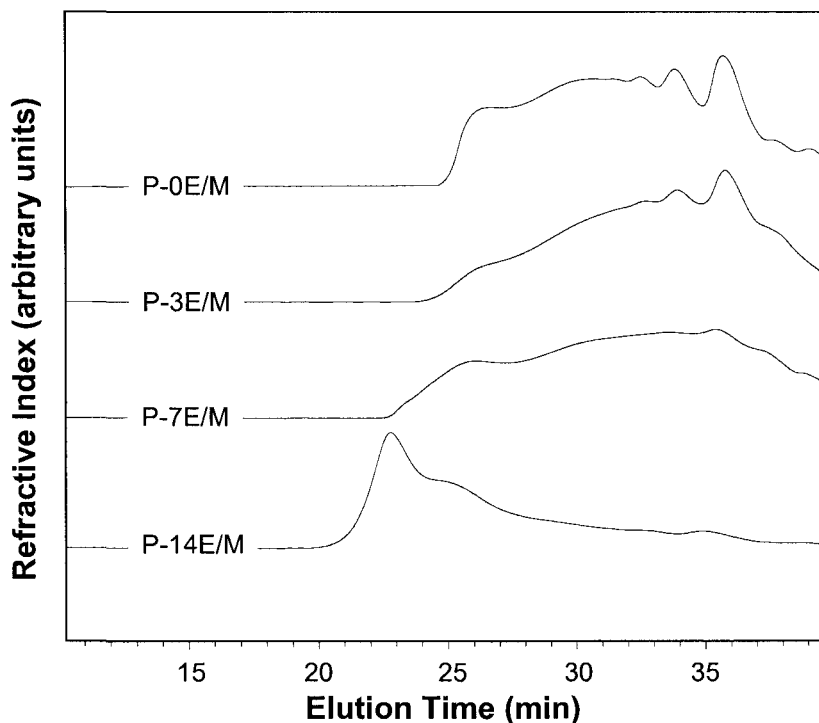
Figure III-2 Size exclusion chromatography traces of the synthesized polymers.

As the variable in this study (i.e., hydrophilic spacer length) was altered, the molecular weight and degree of branching in the polymers were potentially affected as well. The molecular weight (Mn and Mw) of the polymers was found to increase with the

hydrophilic spacer length of the triacrylate monomer (P-14E/M > P-7E/M > P-3E/M). P-0E/M, which was synthesized from the smallest acrylate precursor (TMPTA), showed comparably high molecular weights and a low PDI and consisted on average of 1 triacrylate and 2 amine monomers more than the other polymers. Although there was an increase in molecular weight as the hydrophilic spacer increased, all the polymers were formed from a similar amount of amine and triacrylate monomer (Table III-2). Thus, a large effect of degree of branching on the parameters and polymers investigated in this study is not expected. The difference in Mw likely resulted from the difference in the mass of the triacrylate monomer (i.e., molecular weight of monomer increases with the increase in hydrophilic spacer length) rather than from the amount of potential branching in the polymers. Although this study provided initial insight on the effects of the hydrophilic spacer lengths, further investigation will facilitate a more complete understanding of the individual effects of the various parameters (hydrophilic spacer length, polymer MW and degree of branching).

Determination of Amine Equivalents and Polymer pKa Values by Hydrogen Ion Titration

Hydrogen ion titration of the polymers was conducted from pH 2 to pH 12, instead of from pH 12 to pH 2, to avoid degradation of the polymers at basic pH. The titration curves obtained are shown in Figure III-3. Table III-2 lists the pKa values determined for the polymers. For the amine monomer AEPZ, which contains a primary, secondary and tertiary amine, a pKa value of 9.30 was obtained.
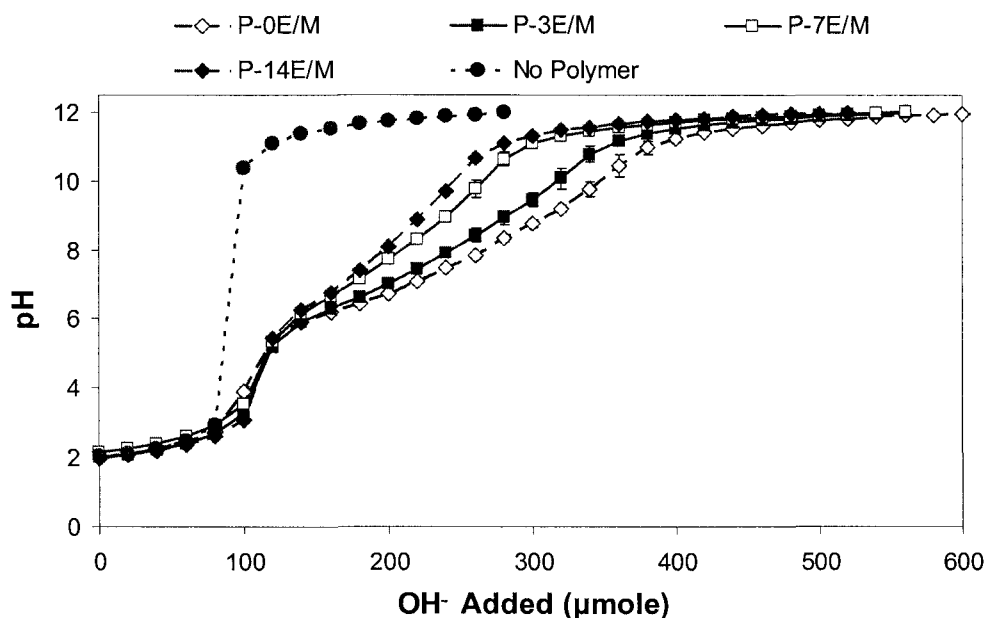
Figure III-3 Titration curves (0.1 N NaOH) of the polymers. The results are expressed as means ± standard deviations for n=3.

The pKa values of the amines changed upon conversion in the addition reaction. During the Michael-type reaction the alkyl substitution of the amines is increased, i.e., a primary amine becomes secondary and a secondary amine becomes tertiary. Besides increased alkyl substitution, sterically hindered accessibility also contributes to the observed changes in amine pKa. The synthesized polymers displayed pKa values in a small range between 7.85 and 8.08. pKa values of the polymers increased with the hydrophilic spacer lengths in the triacrylate monomers, likely due to improved accessibility of the amines. The titration curves for the four synthesized polymer types were very similar in shape (Fig. III-3) which was expected because they all consist of the same amine monomer (Table III-1). The polymers in this study were synthesized from an amine monomer, AEPZ, that has a primary, secondary and tertiary amine, where the reaction occurs first at the secondary amine and then at the primary amine[86,87]. The

synthesized polymers have amine groups that have different degrees of substitution and chemical environments and dissociate at different pH values. The buffering by the different amine groups blended into a broad buffering range, where distinct plateau and equivalent points for the different types of amines were not observed, which resulted in one pKa value for the whole polymer. Figure III-3 shows that the buffering pH ranges of polymers with shorter hydrophilic spacers were wider as compared to those determined for polymers with longer hydrophilic spacers. This indicates that polymers with shorter hydrophilic spacers have higher buffering capacities.

For a given mass of polymer (typically 50 mg), the amine equivalents dissociating in four different ranges were evaluated (Fig. III-4). The amine equivalents that dissociate between pH 2.5 and 5.0 were evaluated in order to compare the availability of unprotonated amines at pH 5.0 that may catalyze hydrolytic ester degradation[122]. Similarly, the amine equivalents that dissociate between pH 2.5 and 7.4 were determined to compare the availability of unprotonated amines which can catalyze the hydrolytic ester degradation at pH 7.4. The amine equivalents that dissociate at pH 5.0 - 7.4 were obtained to estimate the buffering capacity of the polymers at the endosomal/lysosomal pH range and thus, the polymer's ability to aid in pDNA escape from the endosome prior to lysosomal degradation by nucleases[6]. The amine equivalents dissociating above pH 7.4 were calculated to determine the amounts of protonated amines that could help with polymer/pDNA complexation when the polyplexes are assembled at pH 7.4.
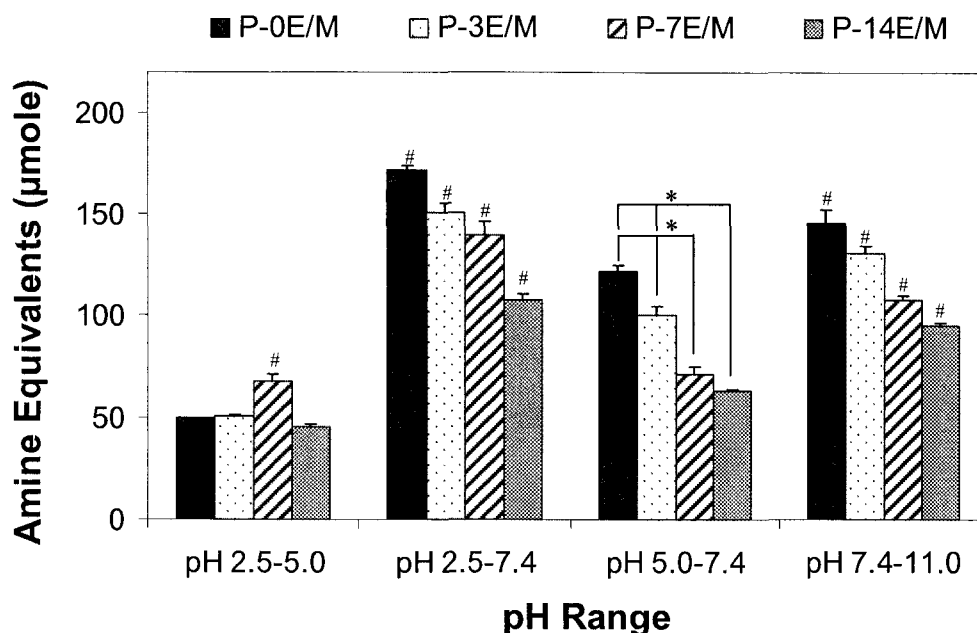
Figure III-4 Amine equivalents that dissociate at different pH ranges. The results represent means ± standard deviations for n = 3. # indicates a statistically significant difference between one polymer and the other polymers within the same pH interval (p<0.05). * represents a statistically significant difference between two polymers within the same pH interval (p<0.05).

For a given mass of polymer (50 mg), polymers with shorter hydrophilic spacer lengths, which contain a higher density of amines per molecular weight by design, had higher buffering capacities between pH 5.0 and 7.4 as well as between pH 7.4 and 11.0 (Fig. III-4). Consequently a higher number of protonated amines is available in the polymers with short spacer lengths to aid in pDNA escape from the endosome and for the assembly of polymer/pDNA polyplexes at pH 7.4. In these polymers, a comparably large number of unprotonated amines is available below pH 7.4 that could assist with polymer hydrolytic ester degradation.

Polymer Degradation (^{1}H-NMR)

In this study, the rate of hydrolytic ester degradation of the polymers, which occurs in the body when the polymers are exposed to the aqueous environment, was investigated. The hydrolytic ester degradation profiles of the polymers at pH 5.0 and 7.4 are shown in Figures III-5A and III-5B, respectively. Figure III-5C compares the polymers at two time points (3 and 14 days). Polymers with longer hydrophilic spacers degraded faster than those with shorter spacers at both tested pH values. This is explained by the hydrophilic spacers attracting water molecules to the ester sites. Furthermore, polymers with longer hydrophilic spacers likely form looser structures with more flexible chains and more easily accessible ester sites[93]. Comparing the polymers synthesized from the different triacrylate monomers, the amount of ester degraded increased as the length of hydrophilic spacer increased. P-3E/M had a significantly higher amount of esters degraded compared to P-7E/M and P-14E/M at pH 5.0 after 3 and 14 days. At pH 7.4, P-3E/M had a significantly higher amount of esters degraded compared to P7E/M and P-14E/M after 3 days, however the amount of ester degraded in the three TMPETA polymers were not significantly different after 14 days. The amount of esters degraded for P-0E/M (no spacer) and P-14E/M (longest spacer) were significantly different from each other at day 14. The percent of ester degraded increased from 43.4 ± 2.1% to 55.7 ± 2.6% at pH 5.0 and 89.7 ± 1.3% to 98.5 ± 1.6% at pH 7.4 with the increase in hydrophilic spacer length. P-0E/M, which was synthesized from TMPTA and contained no ethyleneoxy groups, degraded faster than P-3E/M for most of the time points and conditions observed. Due to its lower molecular weight compared to P-0E/M, P-3E/M
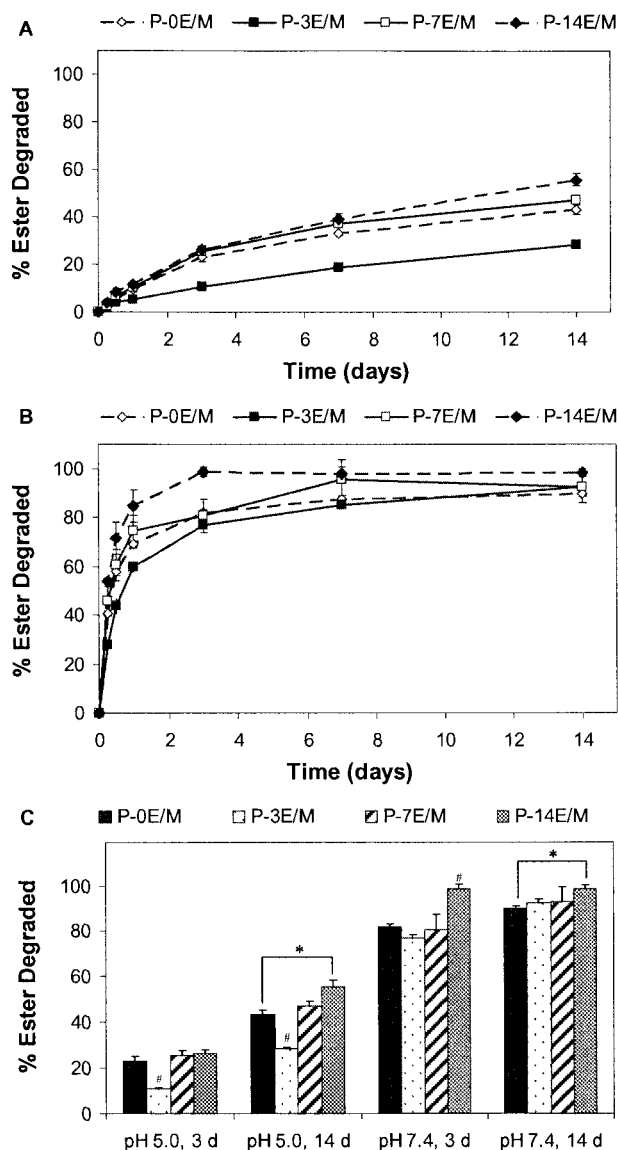
Figure III-5 Ester degradation profiles of the polymers at 37°C and (A) pH 5.0 simulating lysosomal pH and (B) pH 7.4 simulating cytoplasmic pH and (C) degree of degradation after 3 and 14 days at pH 5.0 and 7.4 at 37°C as observed by ^{1}H-NMR. The extent of degradation is expressed as means ± standard deviation for n = 3. # indicates a statistically significant difference between one polymer and the other polymers degraded under the same conditions (p<0.05). * represents a statistically significant difference between two polymer compositions degraded under the same conditions (p<0.05).

chains may have formed tighter structures and their ester groups might have been more effectively shielded from hydrolytic degradation. In summary, hydrophilic spacers can be incorporated into the polymers to increase their hydrolytic degradation rates. All polymers showed a higher rate of hydrolytic ester degradation at pH 7.4 (cytoplasmal pH) than at pH 5.0 (lysosomal pH). This is explained by a higher number of unprotonated amine groups that are present at the higher pH to catalyze hydrolysis of the ester groups, which is consistent with previous work on poly(ester amine)s[79,122]. Olefinic protons (5.8-6.6 ppm), which would contribute to polymer cytotoxicity[121], were not present in the ^{1}H NMR spectra of polymer degradation samples over the course of the hydrolytic ester degradation study (data not shown), indicating that a reverse Michael addition reaction, which would yield free acrylate groups, did not occur.

Cytotoxicity Analysis

Cells remained viable after incubation with polymer solutions for 2 and 24 h at all concentrations tested. PEI, which was tested in comparison, however, caused significant cell death (Fig. III-6). After 2 h, more than 70% of the cells exposed to the polymers with different hydrophilic spacers were viable (Fig. III-6A). After 24 h, more than 70% of the cells were viable except for the cells that were exposed to P-3E/M at 1000 µg/mL concentration (66.9 ± 12.1% viability) (Fig. III-6B). In general, polymers with longer hydrophilic spacers (P-7E/M and P-14E/M) were less cytotoxic as compared to those with shorter or no spacer (P-0E/M and P-3E/M) after 24h. This is likely due to the decrease in the charge density in the polymers[93].
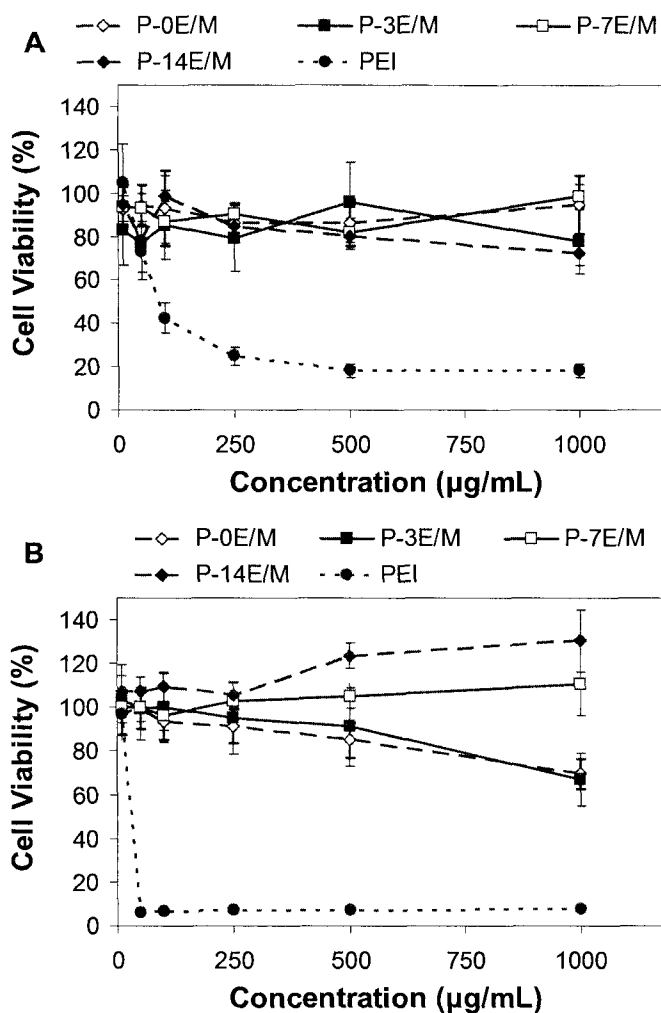
Figure III-6 Cytotoxicity of the polymers (with polyethylenimine (PEI) as negative control) on CRL 1764 rat fibroblasts after (A) 2 h and (B) 24 h as evaluated by an MTT assay. The results are expressed as means ± standard deviation for n = 5.

The slow degradation rates observed for P-0E/M and P-3E/M may also contribute to the observed toxicity[111]. PEI, in contrast, caused significant cell death after 2 h with less than 25% cell viability at a concentration of 250 μg/mL or higher. After 24 h, less than 8% of the cells were viable when exposed to PEI at a concentration of 50 μg/mL or higher. PEI has an 8-13 times higher molecular weight and 2-3 times higher charge density compared

to the synthesized polymers. Both parameters certainly contribute to the high toxicity of PEI[123,124]. The improved cytocompatibility of the developed polycationic polymers will allow for use at high concentrations and high N:P ratios.

Polymer/pDNA Polyplex Characterization

Zeta Potential

The surface charge of the polyplexes formed by the polymers was evaluated to determine optimal polymer to pDNA ratios, which result in a positively charged polyplex that can interact with, instead of repulsing, the negative charges on the cell membrane[59,75]. The pCMV-eGFP plasmid, which was used in this study, has a zeta potential of -33.1 ± 0.5 mV. All the polyplexes formed at a polymer/pDNA weight ratio of 5:1 had a negative zeta potential ranging from -8.5 ± 0.4 mV to -27.5 ± 2.9 mV (Fig. III-7). At a weight ratio of 10:1, P-0E/M, P-3E/M and P-7E/M formed polyplexes that were neutral. P-14E/M, which of all tested polymers provides the least amines per molecule and therefore will form polyplexes at the lowest N:P ratio at a given weight ratio of polymer to DNA, formed a negative polyplex (-4.3 ± 1.9 mV) at a weight ratio of 10:1 and a positive polyplex (7.3 ± 0.5 mV) at a weight ratio of 50:1. The zeta potential of all the polyplexes formed increased as the weight ratio of polymer to pDNA increased, which corresponds with the changing N:P ratios within the polyplexes. Consequently, the polyplexes formed from polymers with shorter hydrophilic spacer lengths had higher zeta potentials compared to polyplexes with polymers with longer hydrophilic spacers at all tested weight ratios.
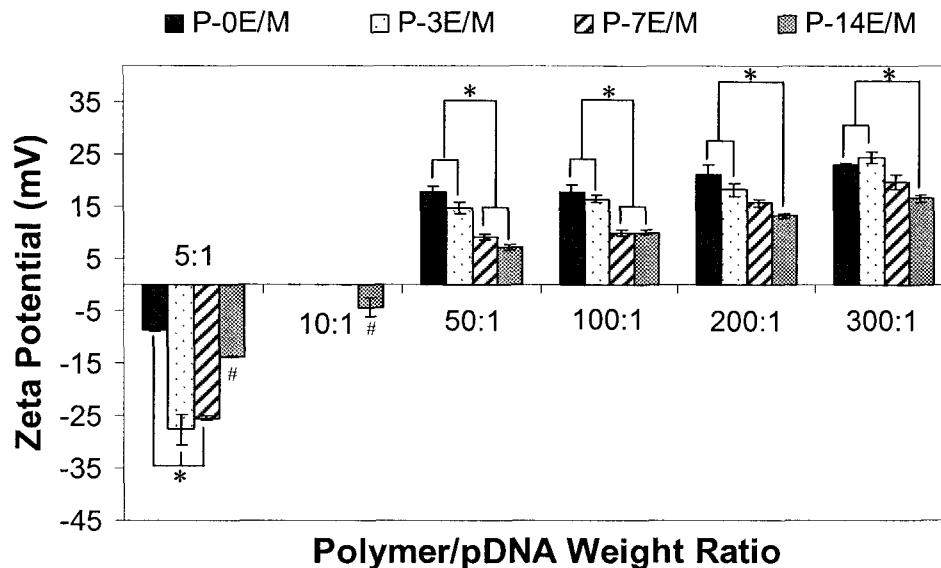
Figure III-7 Zeta potential of the polyplexes formed with 10 µg pCMV-eGFP DNA at different polymer/pDNA weight ratios. The results are expressed as means ± standard deviation for n = 3. # indicates statistically significant difference between a polyplex and other polyplexes in the same weight ratio (p<0.05). * represents a statistically significant difference between two polyplexes within the same weight ratio (p<0.05).

Band Retardation with Gel Electrophoresis

The electrophoretic patterns of the polymer/pDNA polyplexes were obtained by gel electrophoresis in agarose gel and UV light detection (Fig. III-8). Lane 8 in all images represents uncomplexed pDNA (naked pDNA) and shows migration of the plasmid to the positive end of the gels. P-0E/M, P-3E/M and P-7E/M were able to retard the migration of the pDNA at polymer/pDNA weight ratios of 10:1 and higher.
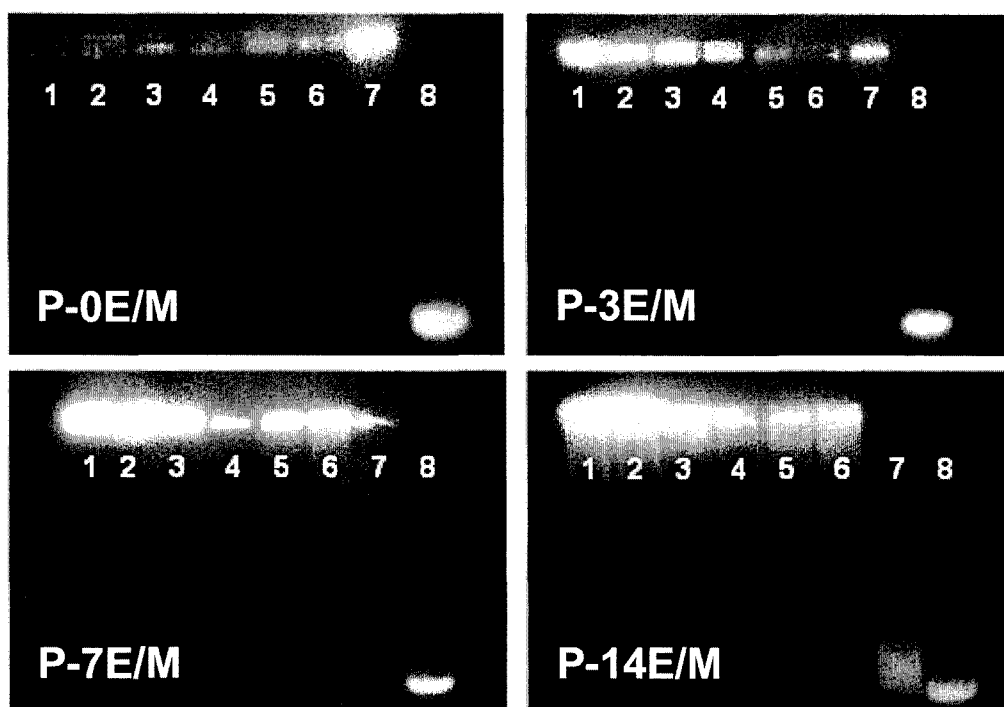
Figure III-8 Gel retardation assay of pDNA/polymer polyplexes at different polymer/pDNA weight ratios: (1) 100:1, (2) 80:1, (3) 60:1, (4) 40:1, (5) 30:1, (6) 20:1, (7) 10:1, and (8) naked pDNA.

In correspondence with the zeta potential results (Fig. III-7), the polymers neutralized the charges of the pDNA at a ratio of 10:1. At these ratios, zeta potential measurements revealed neutrality of the polyplexes, which favors particle aggregation as electrostatic repulsion is minimal. The zeta potential of P-14E/M was negative at a weight ratio of 10:1 and positive at a ratio of 50:1. Neutral polyplexes are consequently expected within this range. Through gel electrophoresis, P-14E/M was found to retard the migration of pDNA at weight ratios of 20:1 or higher. The higher amount of P-14E/M needed to neutralize the charges on the pDNA is explained by the low molar content of amine groups.

Hydrodynamic Polyplex Sizes by Dynamic Light Scattering (DLS)

The hydrodynamic size (diameter) of the polyplexes formed by the polymers and pDNA at different weight ratios was obtained by DLS (Fig. III-9). At low polymer/pDNA weight ratios (10:1 for all the polymers, also 50:1 for P-0E/M), aggregation of the polyplexes was observed as shown by large particle diameters ranging between 923.4 ± 75.6 nm and 1910.5 ± 17.2 nm.
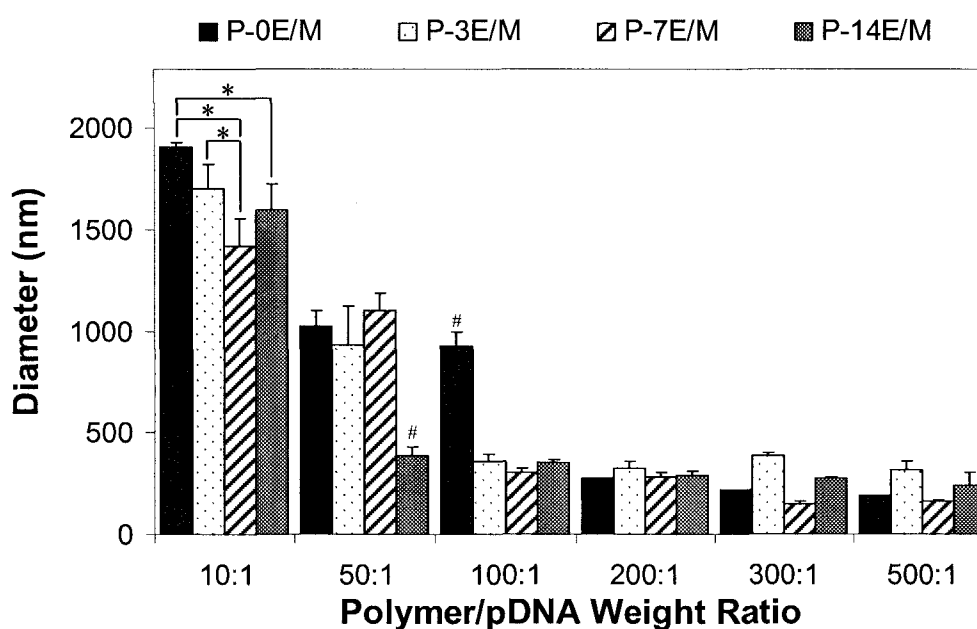
Figure III-9 Diameter of the polyplexes formed with 10 μg pCMV-eGFP DNA at different polymer/pDNA weight ratios as evaluated by DLS. The results are expressed as means $\pm$ standard deviation for $n = 3$. # indicates statistically significant difference between a polyplex and other polyplexes in the same weight ratio ($p < 0.05$). * represents a statistically significant difference between polyplexes within the same weight ratio ($p < 0.05$).

The zeta potential increased as the polymer/pDNA ratios were increased (Fig. III-7) and individual polyplexes were electrostatically stabilized[54]. Consequently, the diameters of the polyplexes decreased to 147.2 ± 14.1 nm (P-7E/M, polymer/pDNA weight ratio of 300:1). Naked pDNA, in comparison, had a diameter of around 751.6 ± 111.8 nm (data not shown). The results indicate that all the polymers were able to complex with and condense the pDNA at certain weight ratios, which is essential for DNA stabilization and transfection efficiency[73]. Although the polyplexes formed with the polymers developed in this study may not be as small as those formed by branched PEI (25 kDa) (~20-40 nm)[125], the polyplexes formed with the polymers developed in this study are promising, as larger sized particles have been found to sediment onto cells, increasing the interaction with the cells, which can enhance particle uptake[57,126]. Larger polyplexes may not get internalized through clathrin coated endocytosis[54], however they have been shown to get internalized successfully by other mechanisms which have not been elucidated[57,58].

Transfection Efficiency with Enhanced Green Fluorescent Protein Reporter Gene

The results from the transfection study are shown in Figure III-10. At low polymer/pDNA weight ratios (10:1 and 50:1), only P-3E/M resulted in a significantly higher number of transfected cells than naked pDNA. At a polymer/pDNA weight ratio of 100:1, P-0E/M, P-3E/M and P-14E/M resulted in significantly higher transfection rates (7.2 ± 0.5% to 8.0 ± 1.5%) than naked pDNA (0.8 ± 0.4%). At the highest weight ratio (300:1), P-0E/M, P-3E/M and P-7E/M resulted in significantly higher transfection (6.7 ± 2.0% to 9.4 ± 2.0%) than naked pDNA. The transfection efficiency of polyplexes formed at weight ratios 100:1 and 300:1 were not significantly different from each other. Above

a certain weight ratio, no increase in surface charge (Fig. III-7) or reduction in the size

(Fig. III-9) of the polyplexes formed were observed within a polymer group, as also

observed in a study by Wu et al.[87].
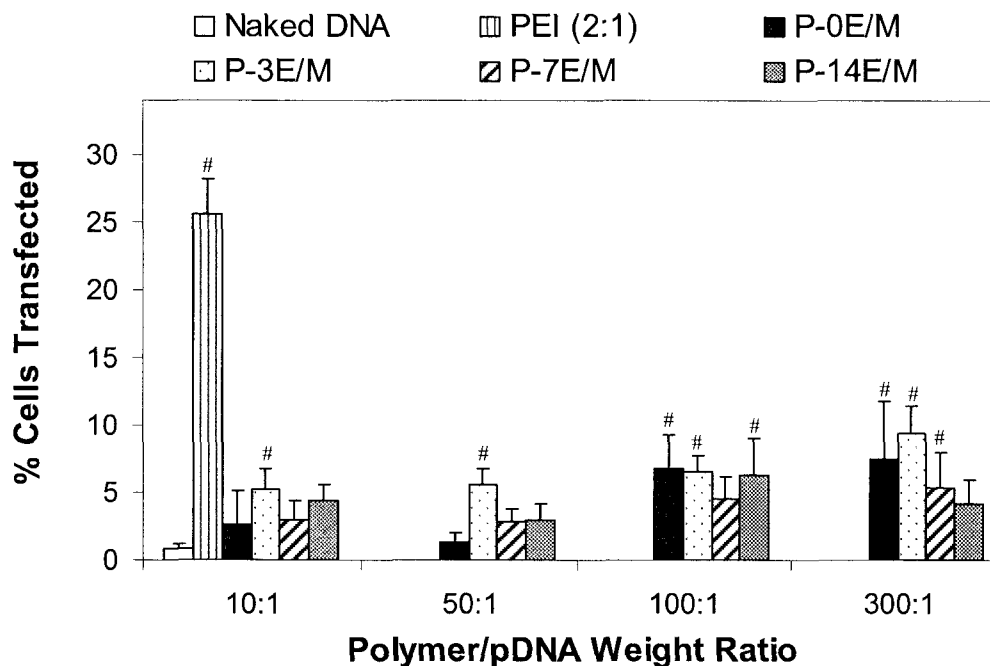
Figure III-10 Efficiency of CRL 1764 cell transfection with polyplexes formed with 5

μg pCMV-eGFP DNA at different polymer/pDNA weight ratios. Naked pDNA and

polyplexes formed from PEI at a polymer/pDNA weight ratio of 2 served as controls. The

results are expressed as means ± standard deviation for n = 4-6. # indicates a statistically

significant difference between a polyplex and naked pDNA (p<0.05).

This suggests that at a certain polymer/pDNA weight ratio, the amount of polymer that

participates in the polyplex formation may reach a critical point where any polymer

subsequently added to the polyplex solution will remain uncomplexed. Thus, above that

critical point, the addition of polymer will not facilitate additional complexation.

Determination of the amount of uncomplexed polymer was not part of the design of this study. However, quantification of the amount of uncomplexed polymer in the future will give more insight on the polymer/pDNA complexation.

At all the weight ratios tested, the percent of cells transfected by polyplexes made from the synthesized polymers was significantly lower than obtained for polyplexes with PEI at a weight ratio of 2:1. The low molecular weights and charge densities of the synthesized polymers as compared to PEI are factors explaining the lower transfection efficiencies observed[123,127]. Although low transfection efficiencies were observed *in vitro* for the synthesized polymers under the conditions explored in this study, they were higher at certain weight ratios than those associated with naked pDNA.

Fluorescence micrographs were taken to confirm the transfection results obtained by flow cytometry. As a negative control, a fluorescence image of cells treated with just media was taken (Fig. III-11A). There were no transfected cells observed when exposed to naked pDNA (Fig. III-11B). Cells transfected with polyplexes of P-0E/M at a polymer/pDNA weight ratio of 300:1 had overall faint eGFP expression as seen in Figure III-11C. Arrows point to cells that expressed eGFP. Cells that were transfected with PEI/pDNA (2:1) polyplexes had a more intense expression of eGFP (Fig. III-11D).

A very low number of live cells, however, were observed after exposure to PEI polyplexes, as seen by light microscopy (data not shown). The cytotoxicity of PEI is well described in the literature and likely attributed to the high MW and charge density of PEI[123]. Wells treated with the polymers synthesized in this study, even at polymer/pDNA weight ratios as high as 300:1, revealed a high number of live, well spread cells as seen by light microscopy.

The results indicate that the synthesized polycationic polymers degrade well under physiological and lysosomal conditions and can efficiently complex pDNA and transfect cells.
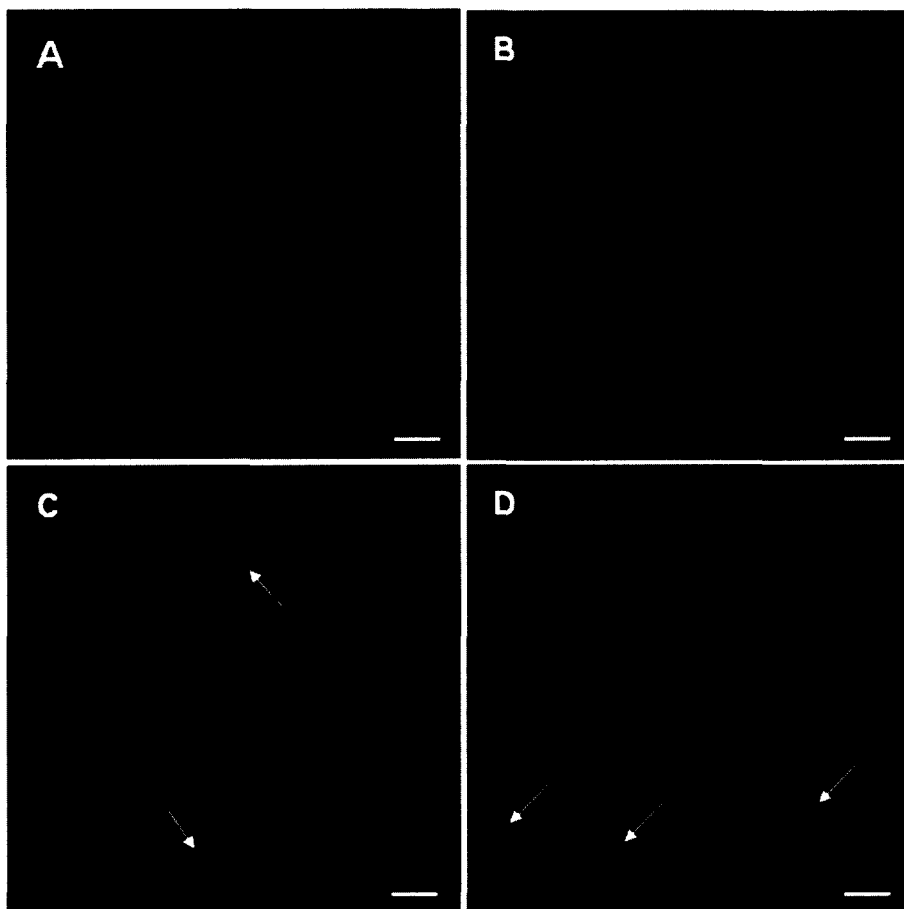
Figure III-11 Representative fluorescence images of CRL 1764 cells after exposure to the following media: (A) plain medium, (B) naked pDNA (CMV-eGFP), (C) P-OE/M/pDNA (300:1), and (D) PEI/pDNA (2:1). An amount of 5 μg pCMV-eGFP DNA was used for each media consisting of pDNA (B-D). Green fluorescence in cells represents expression of GFP. Brightly fluorescing cells are indicated by arrows. Scale bars represent 50 μm.

As a result of the low molecular weight of the polymers and the lower charge density than PEI, effective DNA complexation is achieved at high N:P ratios, and the transfection efficiencies are comparably low. At the same time, these parameters contribute to the low cytotoxicity of the developed polymers, which makes them potential vectors for non-viral gene delivery applications. This study suggests that the polymers can be used at higher concentrations compared to PEI and for repeated dosage.

In this study, a limited effect of hydrophilic spacer length on the transfection efficiency of the polymers was observed. However, there were other parameters, such as degradation rate, which were significantly affected by the length of the hydrophilic spacers. In this study, the cells were directly exposed to the polyplexes, but for *in vitro* or *in vivo* gene therapy approaches where the polyplexes are first released from a scaffold, the polyplexes may take a longer time to reach the cells. Thus, the significant differences in degradation rates of polymers with different spacer lengths may result in pDNA being released at different times and in different forms (i.e., intact complexes or free pDNA), which could in turn result in significant differences in transfection. Rat fibroblasts were chosen as an initial model cell line in this study, and transfection was performed in the absence of serum; however, transfection efficiency can vary between cell lines and with the absence or presence of serum. Future transfection studies *in vitro* in different cell lines as well as *in vivo* in an appropriate animal model will yield a more comprehensive analysis of the transfection capabilities of these polymers.

Conclusions

This study confirmed our hypothesis that the introduction of hydrophilic spacers to branched biodegradable polycationic polymers yields effective gene delivery vectors with reduced cytotoxicity and increased polymer degradation rates. Polymers with shorter hydrophilic spacers yielded polyplexes with higher N:P ratios, which resulted in polymer/pDNA polyplexes with higher zeta potentials. The percent of cells transfected by polyplexes of the synthesized polymers at certain weight ratios was significantly higher than that associated with naked pDNA, however, not comparable to polyplexes with branched PEI with a weight ratio of 2:1. The lower transfection observed could have resulted from the lower molecular weight and reduced charge density of these polymers compared to PEI. However, a higher density of cells was observed after exposure to the synthesized polymers at high concentration, indicating the capability of the polymer to be used at high concentration as needed for transfection with these polymers. Further work will be done to optimize the Michael addition synthesis to produce polymers with higher molecular weight to study the effect of molecular weight on transfection. The findings of this work can be used for the design of non-viral vectors with tailored structural and degradative characteristics as needed for specific applications.

CHAPTER IV

SYNTHESIS AND CHARACTERIZATION OF BIODEGRADABLE BRANCHED POLYCATIONIC

POLYMERS WITH VARYING AMINE BASICITIES FOR NON-VIRAL GENE DELIVERY[†]

Abstract

In this work, biodegradable branched polycationic polymers were synthesized by Michael addition polymerization from different amine monomers and the triacrylate monomer trimethylolpropane triacrylate. The polymers varied in the amount of amines that dissociate in different pH ranges, which are considered to be beneficial to different parts of the gene delivery process. P-DED, a polymer synthesized from trimethylolpropane triacrylate and dimethylethylenediamine, had the highest number of protonated amines that are available for plasmid DNA (pDNA) complexation at pH 7.4 of all polymers synthesized. P-DED formed a positive polyplex (13.9 ± 0.5 mV) at a polymer/pDNA weight ratio of 10:1 in contrast to the other polymers synthesized, which formed positive polyplexes only at higher weight ratios. Polyplexes formed with the synthesized polymers at the highest polymer/pDNA weight ratio tested (300:1) resulted in higher transfection with enhanced green fluorescent protein reporter gene (5.3 ± 1.0% to 30.6 ± 6.6%) compared to naked pDNA (0.8 ± 0.4%), as quantified by flow cytometry. Polyplexes formed with P-DED (weight ratio of 300:1) also showed higher transfection (30.6 ± 6.6%) as compared to polyplexes formed with branched polyethylenimine (weight ratio of 2:1, 25.5 ± 2.7%). The results from this study demonstrated that

polymers with amines that dissociate above pH 7.4, which are available as positively charged groups for pDNA complexation at pH 7.4, can be synthesized to produce stable polyplexes with increased zeta potential and decreased hydrodynamic size that efficiently transfect cells. This work indicated that polymers containing varying amine functionalities with different buffering capabilities can be synthesized by using different amine monomers and used as effective gene delivery vectors.

Introduction

Polycationic polymers have been widely investigated as non-viral vectors for gene delivery. In contrast to viral vectors, which are known to be efficient gene carriers, polycationic polymers generally lack drawbacks commonly associated with viral vectors, such as immune response, production complexity and cost[66,67]. Depending on the chemical structure and environment of the amine functionalities in polycationic polymers, these amines dissociate at different pH values resulting in pH dependent charge densities of the polymers. During the various steps involved in the gene delivery process, different buffering profiles are considered to be beneficial. For DNA complexation and polyplex formation, the number of amines dissociating above pH 7.4 is important, as only charged amines are able to electrostatically interact with the negative charges of the phosphate groups along the DNA backbone[53,128]. The process of DNA complexation aids with condensing and protecting plasmid DNA from degradation. An excess of positive charges ultimately results in the formation of positively charged polymer/DNA polyplexes, which can effectively adhere to target cells by interacting with the negatively charged phospholipids and sulfate groups of the proteoglycans on the cells[59,109]. This interaction

may also improve the chance for endocytotic internalization of the polymer/DNA polyplexes. Upon internalization, amine functionalities that dissociate in the pH range between 5.0 and 7.4 play an important role, as they buffer the pH in the endosome. A material with buffering capacity in this pH range can assist in the escape of the DNA from the endosome and prevent DNA degradation by nucleases in the lysosome through the proton sponge effect[59]. During the delivery process, an optimal degradation rate of main or side chains is another vital component of the polycationic polymer to ensure the release of the encapsulated pDNA and the excretion of the polymer and its side products[81]. Polymer degradation should not occur too rapidly to avoid premature disassembly of the DNA from the polyplex. On the other hand, the polymer should degrade quickly enough to facilitate DNA disassembly from the polyplex once the polyplex reaches the cytoplasm or nucleus, so that free DNA is available for expression in the nucleus[82]. The degradation of the polymer is also beneficial in lowering the cytotoxicity of the polymer, as the polymer's charge density decreases when the polymer degrades into fragments of low molecular weight, which interact less with cell compartments[83,84]. It has been shown for poly(ester amine)s that unprotonated amines have the capability to autocatalyze degradation[122]. Thus, for poly(ester amine)s, amine groups that are in an unprotonated state at pH 5.0 (lysosomal pH) and 7.4 (cytoplasmal pH) play important roles during the delivery process.

Biodegradable polycationic polymers can be synthesized by a variety of polymerization methods, such as Michael addition[85-91,107] and reversible addition–fragmentation chain transfer (RAFT)[129,130] polymerization. Biodegradable polymers synthesized from acrylate and amine monomers by Michael addition

polymerization as non–viral gene delivery vectors have been previously investigated by many groups, including ours. The acrylate monomers can be either bifuctional[85,86,88,89] or trifunctional[87,90,91,107] yielding linear or branched poly(ester amine)s, depending on the type of amine monomer used during the addition reaction. The ester groups in the acrylate monomers allow for hydrolytic biodegradation of the polymers. In our previous work, we synthesized a series of polymers with different types of triacrylate monomers and with a single amine monomer, 1-(2-aminoethyl)piperazine (AEPZ), to investigate the effects of hydrophilic spacer lengths on polymer properties relevant for the gene delivery process[107]. It was found that the incorporation of hydrophilic spacers into the polymers decreased polymer cytotoxicity and accelerated hydrolytic degradation. These alterations of the triacrylate monomer chemistry, however, resulted in a decrease of amine group density and affected the contribution of the amines to key steps of the gene delivery process, namely DNA complexation, endosomal escape and polymer degradation. In addition, variations of the hydrophilicity of the triacrylate monomers did not significantly affect the dissociation properties of the polymers. Consequently, this study focuses on altering the amine monomers used during polymer synthesis with the objective to yield polymers with buffering profiles and pKa values different from those investigated in our previous work[107]. It is hypothesized that by changing the density, degree of substitution and chemical environment of the polymeric amine groups through altering the amine monomers used for polymer synthesis, polymer characteristics relevant for gene delivery can be altered and controlled.

In this study, a series of polymers was synthesized by chemically conjugating different amine monomers with a single triacrylate monomer, trimethylolpropane

triacrylate (TMPTA), to evaluate the effects of altering amine basicities on parameters important for gene delivery. The specific objectives of this work were to investigate the effects of chemically different amine groups on characteristics of the polymer synthesized (molecular weight, basicity determined as amine equivalents dissociating within different pH ranges, degradability and cytotoxicity) and of polyplexes with pDNA (polyplex hydrodynamic diameter, zeta potential and transfection efficiency) to determine design parameters for effective non-viral gene delivery vectors.

Materials and Methods

Materials

TMPTA, AEPZ, 1-(3-aminopropyl) imidazole (API), N,N-dimethylethylenediamine (DED), hydrazine (Hyd), branched polyethylenimine (PEI) (typical weight average molecular weight, Mw ~ 25 kDa, PDI of 2.5), chloroform (ACS grade), sterile-filtered dimethyl sulfoxide (DMSO), methyl tetrazolium (MTT) powder, phenol red free Dulbecco's modified Eagle medium (DMEM), ethidium bromide and Tris-Acetate-Ethylenediaminetetraacetic acid (EDTA) (TAE) were purchased from Sigma-Aldrich (St. Louis, MO). Deuterium oxide (D_2O) was obtained from Cambridge Isotope Laboratories, Inc. (Andover, MA). Acetone (ACS grade), isopropanol (ACS grade) and Fisher Certified Buffer pH 5.0 and 7.4 were purchased from Fisher Scientific (Pittsburgh, PA). Fischer rat fibroblast 3T3-like cell line (CRL 1764) was obtained from American Type Culture Collection (Manassas, VA). DMEM and phosphate-buffered saline (PBS) were purchased from Gibco Life (Grand Island, NY). Fetal bovine serum (FBS) was obtained from Gemini Bio-Products (Calabasas, CA). Trypsin-EDTA (0.25%

trypsin/0.02% EDTA) was obtained from Invitrogen (Carlsbad, CA). Poly(ethylene glycol) (PEG) standards with Mn ranging from 102 to 82,500 Da used for SEC were obtained from Waters (Milford, PA). pDNA with a cytomegalovirus (CMV) promoter and enhanced green fluorescent protein (eGFP) reporter gene (pCMV-eGFP, 4.7 kb, cat no. 6085-1) was obtained from Clontech (Palo Alto, CA). Qiagen Endofree Plasmid Giga Kit was purchased from Qiagen (Valencia, CA).

Polymer Synthesis

Synthesis at Room Temperature (P-AEPZ)

P-AEPZ (Table IV-1) was synthesized by reacting AEPZ with TMPTA as previously described[87,107]. Briefly, the polymer was synthesized at a 2:1 mole ratio[87,90,91] of amine to triacrylate monomer in chloroform. The mixture was allowed to react for 8 days under ambient temperature and then purified by precipitation in a solution of 400 mL of acetone and 5 mL of hydrochloric acid (HCl) (12 M). The product was washed with excess acetone and finally vacuum dried to remove any remaining solvent. The ^{1}H-NMR spectra revealed the following characteristic signals: **P-AEPZ**: δ 0.9 (t, C–CH$_2$–CH_3), 1.4 (m, C–CH_2–CH$_3$), 2.5–3.5 (t, –CH$_2$–CH_2–NR$_2$– and t, –CH$_2$–CH_2–COO–CH$_2$–), 4.0–4.1 (s, C–CH_2–OOC–CH$_2$–).

Table IV-1 Polymer composition and structures of the triacrylate and amine monomer building blocks. P-AEPZ, P-API, P-DED, P-Hyd, P-AEPZ/Hyd, and P-API/Hyd vary in the type of amines they comprise.

Group	Triacrylate Monomer	Amine Monomer
P-AEPZ	TMPTA	AEPZ
P-API	TMPTA	API
P-DED	TMPTA	DED
P-Hyd	TMPTA	Hydrazine
P-AEPZ/Hyd	TMPTA	AEPZ Hydrazine
P-API/Hyd	TMPTA	API Hydrazine

Synthesis at 50°C (P-API, P-DED, P-Hyd, P-AEPZ/Hyd and P-API/Hyd)

All other polymers (Table IV-1) were synthesized by reacting TMPTA with API (P-API), DED (P-DED), Hyd (P-Hyd), AEPZ and Hyd (1:1 mole ratio) (P-AEPZ/Hyd) and API and Hyd (1:1 mole ratio) (P-API/Hyd) on the basis of previous methods[90,91]. The polymers were synthesized at a 2:1 mole ratio of amine to triacrylate monomer. Typically, 10.8 mmole of the amine monomer and 5.4 mmole of the triacrylate monomer were mixed in 20 mL of chloroform in a round bottom flask. For P-AEPZ/Hyd and P-API/Hyd, 5.4 mmole of each type of amine monomer was used, which resulted in a total of 10.8 mmole of amine monomer. The mixture was allowed to react for 3 days at 50°C. The polymer was then purified by precipitation in a solution of 400 mL of acetone and 5 mL of concentrated hydrochloric acid (12 M). The product was washed with excess acetone and finally vacuum dried to remove any remaining solvent. The ^{1}H-NMR spectra revealed the following characteristic signals: **P-DED**: δ 0.9 (t, C–CH$_2$–C*H$_3$*), 1.4 (m, C–C*H$_2$*–CH$_3$), 2.5–3.7 (t, –CH$_2$–C*H$_2$*–NR$_2$–, s, –C*H$_3$*–N– and t, –CH$_2$–C*H$_2$*–COO–CH$_2$–), 4.0–4.1 (s, C–C*H$_2$*–OOC–CH$_2$–). **P-Hyd**: δ 0.9 (t, C-CH$_2$–C*H$_3$*–), 1.4 (m, –C*H$_2$*–CH$_3$–), 2.3–3.6 (t, –CH$_2$–C*H$_2$*–NH–NH– and t, –CH$_2$–C*H$_2$*–COO–CH$_2$–), 4.0–4.1 (s, C–C*H$_2$*–OOC–CH$_2$–). **P-AEPZ/Hyd**: δ 0.9 (t, C–CH$_2$–C*H$_3$*), 1.4 (m, C–C*H$_2$*–CH$_3$), 2.5–3.6 (m, –CH$_2$–C*H$_2$*– NR$_2$, t, –CH$_2$–C*H$_2$*–NH–NH– and t, –CH$_2$–C*H$_2$*–COO–CH$_2$–), 4.0–4.1 (s, C–C*H$_2$*–OOC–CH$_2$–). **P-API/Hyd**: δ 0.9 (t, C–CH$_2$–C*H$_3$*), 1.4 (m, C–C*H$_2$*–CH$_3$–), 2.1 (m, –NR$_2$–CH2–C*H$_2$*–CH$_2$–NR$_2$–), 2.1–3.5 (t, –CH$_2$–C*H$_2$*–NR$_2$–, t, –CH$_2$–C*H$_2$*–NH–NH– and t, –CH$_2$–C*H$_2$*–COO–CH$_2$–), 4.0–4.1 (s, C–C*H$_2$*–OOC–CH$_2$–). 4.3 (t, –CH$_2$–C*H$_2$*– imidazole–), 7.2–7.4 (d, –N–C*H*=C*H*–N–), 8.3 (s, –N=C*H*–N–).

Polymer Characterization

The results reported for P-AEPZ in this study (i.e., polymer molecular weight, hydrogen ion titration and ester degradability and polymer/pDNA polyplex zeta potential, band retardation and hydrodynamic diameter) are adopted from a previous study (represented as P-0E/M)[107]. Experiments that involve cells (i.e., cytotoxicity and transfection efficiency studies) were repeated to avoid variations between different cell pools.

Proton Nuclear Magnetic Resonance (^{1}H-NMR)

^{1}H-NMR spectra of the polymers were obtained using a 400 MHz Bruker spectrometer (Bruker Avance 400, Zurich, Switzerland). The samples were dissolved in deuterium oxide (D_2O) and the resulting spectra were analyzed using MestRe-C, a NMR processing software package (Mestrelab Research S. L., Spain). The proton peak of deuterium protium oxide (HDO) was used as the internal shift reference and therefore set to $\delta = 4.8$ ppm.

Molecular Weight Determination by Size Exclusion Chromatography (SEC)

The weight average molecular weight (Mw), number average molecular weight (Mn) and polydispersity index (PDI) (Mw/Mn) of the polymers were determined by SEC using a Waters Alliance® HPLC system (Waters, Milford, PA) equipped with a differential refractometer as previously described[107]. Briefly, the samples were run through a Shodex OHpak SB-G (6.0 x 50 mm) guard column, a Shodex OHpak SB803

HQ (8.0 x 300 mm) and a Shodex OHpak SB802.5 HQ (8.0 x 300 mm) analytical column placed in series using PEG standards with Mn ranging from 102 to 82,500 Da to obtain a calibration curve (as previously done by Wu et al.[87] and our group[107] for polymers with similar architecture to those synthesized in this study). A 0.5 M sodium acetate buffer containing 0.1 M sodium nitrate was used as the mobile phase (pH 4.5) with a flow rate of 0.5 mL/min. The theoretical average compositions of the polymers were calculated as previously described[107].

Hydrogen Ion Titration

The number of amine equivalents in a given mass of polymer was evaluated by hydrogen ion titration as done previously[107]. Briefly, 50 mg of polymer were dissolved in 10 mL of 150 mM sodium chloride (NaCl) solution. The polymer solution was adjusted to a pH of 2.0 and then titrated by stepwise addition of 0.1 N NaOH while measuring the pH of the solution using an accumet* AP63 Portable pH meter (Fisher Scientific, Pittsburgh, PA). Each titration was done in triplicate, and average pH values were calculated and reported. The amine equivalents that dissociated in different pH ranges were determined as previously described[107,114]. The pKa values were obtained from the titration curves as the pH values at 50% ionization or half way to the equivalent point (midpoint of the plateau areas on the curves).

Polymer Degradation by ^{1}H-NMR Analysis

The rate of hydrolytic ester degradation of the polymers was determined at pH 5.0 and 7.4 by ^{1}H-NMR analysis as previously described[87,107,115,116]. Briefly, a polymer sample (7.5 mg) was dissolved in 750 μL of Fisher Certified Buffer pH 5.0 or pH 7.4[117] and incubated at 37°C with constant agitation (75 rpm). At predefined time points (0 h, 6 h, 12 h, 1 d, 3 d, 7 d and 14 d), the samples were analyzed by ^{1}H-NMR. This study was done in triplicate (n=3). At each time point, percent ester degradation was calculated as previously described[107].

Cytotoxicity Analysis by MTT Assay

The cytotoxicity of the polymers was evaluated using an MTT viability assay as described previously[107,118]. Briefly, CRL 1764 rat fibroblasts were plated on 96–well plates with a density of 8000 cells/well. Polymer solutions with a pH of 7.4 and an osmolarity of 280–320 mosm/kg were prepared in DMEM at six polymer concentrations (10, 50, 100, 250, 500 and 1000 μg/mL). Branched PEI (Mw ~ 25 kDa) solutions at the same concentrations were used as negative controls. Branched PEI 25 kDa has been widely evaluated and is often used as a control for cytotoxicity studies by other groups in the literature[87,119]. After 24 h of cell attachment, the cells were incubated for 2 and 24 h at 37°C in the presence of 100 μL of the polymer solution. MTT assay was performed immediately after the two time points and the absorbance was measured at 570 nm using an absorbance microplate reader (Powerwave X340, BIO–TEK Instruments, Winooski,

VT). The average number of live cells was calculated from 5 different samples as previously described[107].

Polymer/pDNA Polyplex Characterization

<u>Amplification and Purification of Plasmid DNA</u>

pCMV-eGFP was amplified in Escherichia coli (E. coli) bacterial cultures and purified using a Qiagen Endofree Plasmid Giga Kit according to the protocols provided by the manufacturer. The yield of pDNA was determined from the UV absorbance at a wavelength of 260 nm (A_{260}) (NanoDrop[TM] 1000 Spectrophotometer, Thermo Scientific, Wilmington, DE). To evaluate plasmid purity, the ratio of the UV absorbance at wavelengths of 260 nm and 280 nm (A_{260}/A_{280}) was determined and found to range between 1.8 and 2.0. The pCMV-eGFP plasmid was used in all of the polymer/pDNA polyplex characterization experiments.

<u>Zeta Potential</u>

The zeta potential of polymer/pDNA polyplexes at different polymer to pDNA weight ratios (5:1, 10:1, 50:1, 100:1, 200:1 and 300:1) was obtained as previously described[107]. Briefly, the polyplexes were prepared with 10 μg of pDNA in 600 μL PBS. The zeta potential of the resulting particles or larger aggregates was obtained using a Zen 3600 Zetasizer (Malvern Instruments, Worcestershire, UK) at 25°C. The zeta potential was calculated using the Smoluchowski equation based on the electrophoretic mobility[120]. This study was done in triplicate.

Band Retardation with Gel Electrophoresis

Band retardation of the polyplexes at different weight ratios (10:1, 20:1, 30:1, 40:1, 60:1, 80:1 and 100:1) of polycationic polymer to pDNA solutions was performed as previously described[107]. Briefly, the polyplexes were prepared from 1 μg pDNA in 20 μL PBS and loaded into the wells of a 0.5% (w/w) agarose gel with bromophenol blue loading solution. The gel was run for 1 h at 80 mV in TAE buffer (1x) and an image of the gel was captured in a UV transillumination box.

Hydrodynamic Polyplex Sizes by Dynamic Light Scattering (DLS)

The hydrodynamic diameter of the polycationic polymer/pDNA polyplexes was evaluated at different polymer to pDNA weight ratios (10:1, 50:1, 100:1, 200:1, 300:1 and 500:1) using a 90PLUS Particle Size Analyzer (Brookhaven Instruments Corporation, Holtsville, NY)[107]. In brief, the polyplexes were prepared with 10 μg pDNA in 600 μL of PBS and analyzed in the instrument. The diameter of the polyplexes or aggregates thereof was obtained using Laplace inverse program Non-Negative Least-Squares (NNLS)[119]. This study was done in triplicate.

eGFP Transfection of Rat Fibroblasts

The transfection of CRL 1764 rat fibroblasts was performed as previously described[107]. Rat fibroblasts were plated in 6-well plates at a seeding density of 250,000 cells/well. After 24 h of cell attachment, the cells were incubated in the presence of 100 μL of polyplex solution containing 5 μg of pDNA complexed at different polymer/pDNA

weight ratios (10:1, 50:1, 100:1, and 300:1) and 400 μL of DMEM (FBS free). PEI/pDNA at a weight ratio of 2:1, naked pDNA and FBS-free media without pDNA served as controls. After 24 h, the cells were supplemented with 2 mL of DMEM/FBS (10% (v/v)) which resulted in a solution containing 8% instead of 10% (v/v) of FBS. The slightly lower concentration of FBS was not expected to significantly affect the metabolism of the cells. After 48 h, the cells were then trypsinized and fixed with chilled formaldehyde solution (1%). Samples were then analyzed using a flow cytometer (Becton Dickenson FACS Scan, BD Biosciences, San Jose, CA). This study was conducted with n=4-6. Fluorescence images of selected samples were taken with a confocal microscope (Zeiss LSM 510, Carl Zeiss Jena, Germany) to confirm transfection and expression of the green fluorescent protein (GFP). The cells were imaged with a 20x objective after excitation by an argon laser. We ensured that the highest weight ratios tested in the transfection study had a lower mass of polymer per unit area of culture well (150 μg/cm^2, weight ratio of 300:1) compared to that tested in the cytotoxicity experiment. In the cytotoxicity experiment, cells exposed to the highest mass of polymer per unit area of culture well tested, 300 μg/cm^2 (polymer concentration of 1000 μg/mL), were still viable.

Statistical Methods

The results were presented as means $\pm$ standard deviation. Multiple-factor analysis of variance (ANOVA) was used to identify if there were any significant differences among groups ($p < 0.05$). Tukey's Honestly Significantly Difference (HSD) test was then conducted to identify the specific groups that differed statistically significantly.

Results and Discussion

Polymer Synthesis

A series of polymers were synthesized and precipitated in acetone/HCl. The sticky precipitates were solid, rubbery or a viscous liquid. In their protonated form, the polymers were insoluble in organic solvents, thus all characterizations were done in aqueous media. An exemplary structure of the synthesized branched polymers is shown in Figure IV-1 with DED as the amine monomer.
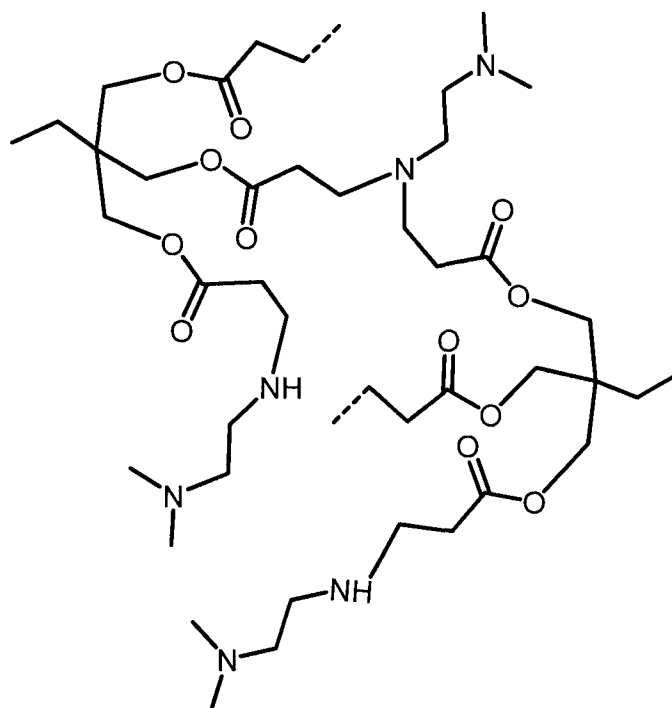
Figure IV-1 General structure of a branched polymer obtained by Michael addition reaction of TMPTA with an amine monomer (shown here: DED).

Different synthesis methods (room temperature/non-heated or heated) had to be applied to yield the different polymers. P-AEPZ was obtained at ambient temperature. If

polymerized at 50°C, the reaction solution of P-AEPZ formed a cross-linked gel. All other polymers were synthesized at an elevated temperature (50°C) because reactions at room temperature were incomplete, as indicated by the presence of olefinic proton signals (5.8-6.6 ppm) in the ^{1}H-NMR spectra of the final products. The synthesis of P-API was incomplete even when the synthesis was performed at temperatures above 50°C or at increased reaction time and amine monomer concentration. Any unreacted acrylate groups in P-API could possibly contribute to polymer toxicity[121], thus P-API was excluded from further characterizations. The synthesis of P-Hyd was complete with regard to acrylate group conversion (no olefinic proton peaks present), however, the polymeric product only dissolved in acidic solutions. Thus, P-Hyd was only characterized by hydrogen ion titration. The yields of the polymerization were between 80-90%.

The obtained ^{1}H-NMR data were also used to verify that the polymer building blocks, amine and triacrylate monomer, reacted at the intended molar ratio of 2:1, which represents the monomer ratio at initiation. The integral of the signals between 2.5–3.5 ppm (derived from $-CH_2-CH_2-NR_2-$ (of the amine monomers AEPZ, API, DED), H_3C-NR_2- (of DED), $-CH_2-CH_2-NR_2-$ formed through the reaction, and $-CH_2-COO-CH_2-$ from the triacrylate monomer) was compared to the integral of the proton signal at 0.9 ppm (derived from three methyl protons in the triacrylate monomer). The calculations yielded molar ratios for P-AEPZ, P-DED, P-AEPZ/Hyd and P-API/Hyd of 1.8, 2.3, 2.5, and 1.7, respectively.

Polymer Characterization

Molecular Weight with Size Exclusion Chromatography

The Mn, Mw and PDI of the polymers as obtained by SEC as well as the theoretical average composition of the polymers calculated based on the experimental Mn and Mw values are shown in Table IV-2. P-AEPZ, which on average consists of 4 triacrylate and 8 amine monomers, had a higher molecular weight (Mn of 2700 Da) compared to the other polymers which on average consisted of only 2 triacrylate and 4 amine monomers (Mn < 1000 Da).

Table IV-2 Number average molecular weight, weight average molecular weight, polydispersity index (PDI), estimated average number of triacrylate and amine monomers per polymer molecule and pKa values of the polymers examined in this study. Values for P-AEPZ are adopted from a previous study[107].

Polymer	Mn (Da)*	Mw (Da)*	PDI*	Number of Triacrylate Monomers†	Number of Amine Monomers†	pKa$_1$[#]	pKa$_2$[#]	pKa$_3$[#]
P-AEPZ	2700	6671	2.47	4 (10)	8 (20)	7.85	-	-
P-DED	838	946	1.13	2 (2)	4 (4)	5.56	9.56	-
P-Hyd	-	-	-	-	-	4.24	-	-
P-AEPZ/Hyd	812	888	1.09	2 (2)	4 (4)	6.34	9.61	
P-API/Hyd	796	840	1.06	2 (2)	4 (4)	4.14	6.32	8.96

* Measured by size exclusion chromatography

† Estimated from number average molecular weight; numbers in parentheses estimated from weight average molecular weight

[#] Determined from titration curve

Only P-AEPZ was synthesized at room temperature, while all other polymers were synthesized at 50°C, which may have contributed to the observed differences in molecular weight and monomer composition. Another possible explanation for the different degrees of polymerization may be the different reactivity of the amine monomers used[86]. Low molecular weights were obtained for the synthesized polymers. The molecular weights of the polymers were obtained with SEC using linear PEG standards to generate the calibration curve. The calibration with a linear polymer may not account for the effect of branching that may be present in the polymers; thus an underestimation of the molecular weights may have occurred. The molecular weight[97] and degree of branching[131] of polymers are factors that can highly affect the parameters of non-viral gene delivery polymers which in turn can affect their transfection efficiencies.

Determination of Buffering Profiles and Polymer pKa Values by Hydrogen Ion Titration

Hydrogen ion titration of the polymers was started at pH 2 with sodium hydroxide until a pH of 12 was reached, in order to avoid degradation of the polymers at basic pH. The obtained titration curves are shown in Figure IV-2. Table IV-2 summarizes the pKa values that were determined for the synthesized polymers. The building block AEPZ has a primary, secondary and tertiary amine and a specified pKa value of 9.30. API has a primary amine with a pKa of 9.81 and a basic imidazole amine with a pKa of 6.28. Imidazole polymers have been shown to exhibit buffering capacity in the endosomal/lyosomal pH range and are often incorporated into polymers as endosomal escape moieties[124,128,132].
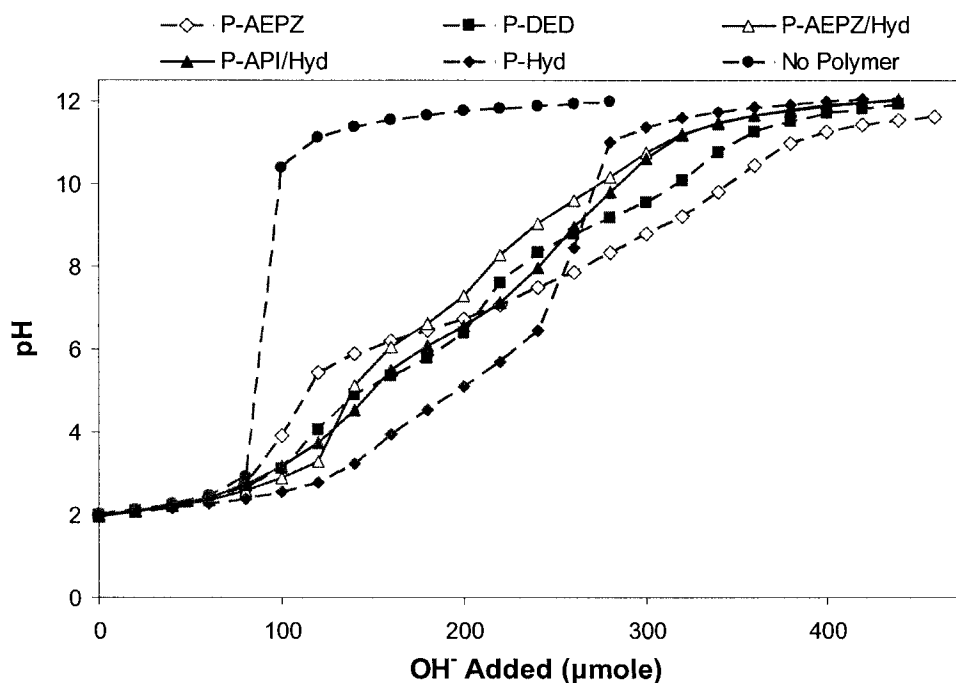
Figure IV-2 Titration curves (0.1 N NaOH) of the polymers. Values for P-AEPZ are adopted from a previous study[107]. The results are expressed as means ± standard deviations for n=3.

The ethylenediamine group in DED, used previously by Kim et al.[90,91], is a diacid molecule and forms a 5-membered ring with a gauche-anti conformational transition upon protonation[133], which results in pKa values of 9.74 and 6.36. Xiong et al. have synthesized a polymer containing hydrazide moieties, which are characterized by a low pKa of around 5.00 and therefore remain predominantly uncharged at physiological pH[134]. Xiong et al. found that polymeric hydrazide moieties do not participate in the proton sponge effect due to the low pKa[134]. These functionalities, however, may be beneficial for poly(ester amine) degradation. Amines with low pKa values, which remain unprotonated at pH 5.0 or 7.4, can autocatalyze the degradation of esters at that pH[122]. In

this work, we found that the pKa value of hydrazine decreased from 7.97 (monomer) to 4.24 upon conversion into a higher order amine during polymerization (P-Hyd).

In general, the pKa values of the amines (Table IV-2) changed upon conversion in the Michael addition reaction as a result of the increase in alkyl substitution during the reaction. Sterically hindered accessibility also contributes to the observed changes in the pKa values of the amines. The molecular weight and degree of branching of the polymers could also affect the dissociation of the amines. As seen in Table IV-1, the polymers that were synthesized cover a wide range of pKa values as intended by the choice of the different amine monomers. P-AEPZ had a single pKa of 7.85. Through the addition of amines from amine monomers DED, Hyd and API, polymers were produced that contained amine groups with pKa values above and below 7. The incorporation of the amine monomer DED resulted in a polymer (P-DED) with two pKa values, 9.56 for the primary amine of the monomer, which could have become secondary or tertiary upon polymerization, and 5.56 for the tertiary amine that dissociates through the gauche-anti conformational transition. The incorporation of the amine monomer API in P-API/Hyd resulted in a pKa of 8.96 for the primary amine of the monomer, which could have become secondary or tertiary upon polymerization, and an additional, low pKa value of 6.32 for the imidazole amine. The amine monomer Hyd which was incorporated into P-Hyd, P-AEPZ/Hyd and P-API/Hyd, resulted in an additional low pKa value of 4.24, 6.34 and 4.14, respectively. By incorporating two different amine monomers in the polymer, such as in P-AEPZ/Hyd and P-API/Hyd, the resulting polymers displayed multiple pKa values covering a wide pH range.

The titration curves for the four synthesized polymers were all different in shape (Fig. IV-2), which demonstrates that the type of amine monomer had a significant effect on the buffering capacity and profile of the polymers. In contrast, polymers made from the same type of amine monomer (AEPZ), were very similar in shape[107].

The amine equivalents dissociating in four different pH ranges were evaluated for a given mass of polymer (typically: 50 mg) as done in previous work[107] (Fig. IV-3).
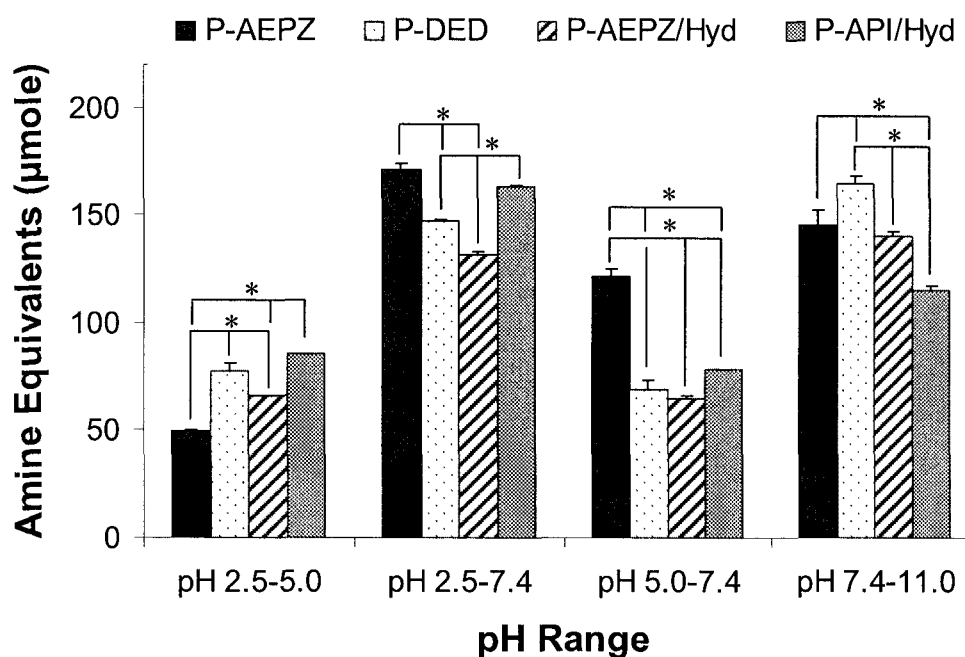
Figure IV-3 Amine equivalents that dissociate within different pH ranges. The results represent means ± standard deviations for n=3. # indicates a statistically significant difference between one polymer and all other polymers within the same pH interval (p<0.05). Values for P-AEPZ are adopted from a previous study[107]. * represents a statistically significant difference between two polymers within the same pH interval (p<0.05).

The amine equivalents that dissociate between pH 2.5 - 5.0 and pH 2.5 - 7.4 were evaluated in order to compare the availability of unprotonated amines, which may catalyze the degradation at pH 5.0 and 7.4, respectively[122]. The amine equivalents that dissociate at pH 5.0 - 7.4 were obtained to evaluate the buffering capacity of the polymers at the endosomal/lysosomal pH range, which determines the polymer's ability to aid in pDNA escape from the endosome prior to lysosomal degradation by nucleases[6]. The amine equivalents dissociating between pH 7.4 - 11.0 are charged at physiological pH and considered to aid in polymer/pDNA polyplex formation at pH 7.4.

For a given mass of polymer (50 mg), P-AEPZ had the highest buffering capacity in the range relevant to assist in endosomal escape (pH 5.0-7.4) as compared to the other polymers (Fig. IV-3). Compared to P-AEPZ, the other polymers (P-DED, P-AEPZ/Hyd and P-API/Hyd) had significantly more amines dissociating in the pH range of 2.5 to 5.0. Such amine groups can help catalyze polymer degradation at pH 5.0. P-AEPZ and P-API/Hyd had the highest amount of amines that may assist with the catalysis of hydrolytic degradation at pH 7.4 compared to the other polymers. Compared to all other polymers, P-DED had a significantly higher number of amines dissociating between pH 7.4 and 11.0; dissociation above pH 7.4 is important for polyplex assembly at this pH. The high pKa values of P-DED and P-AEPZ/Hyd were similar (9.56 and 9.61, respectively), however, the buffering profiles of the polymers at pH 7.4 (cytoplasmal pH) are significantly different. This demonstrates that it is not only important to compare the pKa values of the polymers, but also the buffering profiles and amount of amine equivalents at the different pH ranges. The data in Figure IV-3 also illustrates that the polymers synthesized from various amine monomers, which resulted in different

molecular weights and molar contents of amine groups, significantly varied in the amine equivalents dissociating in the four investigated pH ranges. When the triacrylate monomer chemistry was varied, as done in our previous work, the amount of amine equivalents dissociating in the four investigated pH ranges decreased as the hydrophilic spacer length increased and did not vary significantly between the different pH ranges[107].

Polymer Degradation with ^{1}H-NMR Analysis

The degradation profiles of the polymers at pH 5.0 and 7.4 are shown in Figure IV-4A and IV-4B, respectively. Figure IV-4C compares the polymers at two time points (3 and 14 days). Even though P-DED, P-AEPZ/Hyd and P-API/Hyd had more unprotonated amines at pH 5.0 (Fig. IV-3), their rates of degradation at day 3 were still significantly lower than those observed for P-AEPZ at pH 5.0 (Fig. IV-4C). P-DED, P-AEPZ/Hyd and P-API/Hyd may have formed polymers with structures in which the polymer chains are not as flexible, thus, the unprotonated amines in the polymers are less likely to interact with the ester groups and catalyze the degradation of the polymers. Furthermore, P-AEPZ may have formed a polymer with more accessible ester groups. P-DED, P-AEPZ/Hyd and P-API/Hyd may have more hidden ester groups, which can result in the reduction in the rate of hydrolysis[135]. The results from this study suggest that although a polymer has a higher amount of amines that may autocatalyze degradation, other factors, such as accessibility of the ester groups and flexibility of the polymer chains to allow for the interaction of the unprotonated amines and ester groups, may also affect hydrolysis and result in a lower degradation rate.
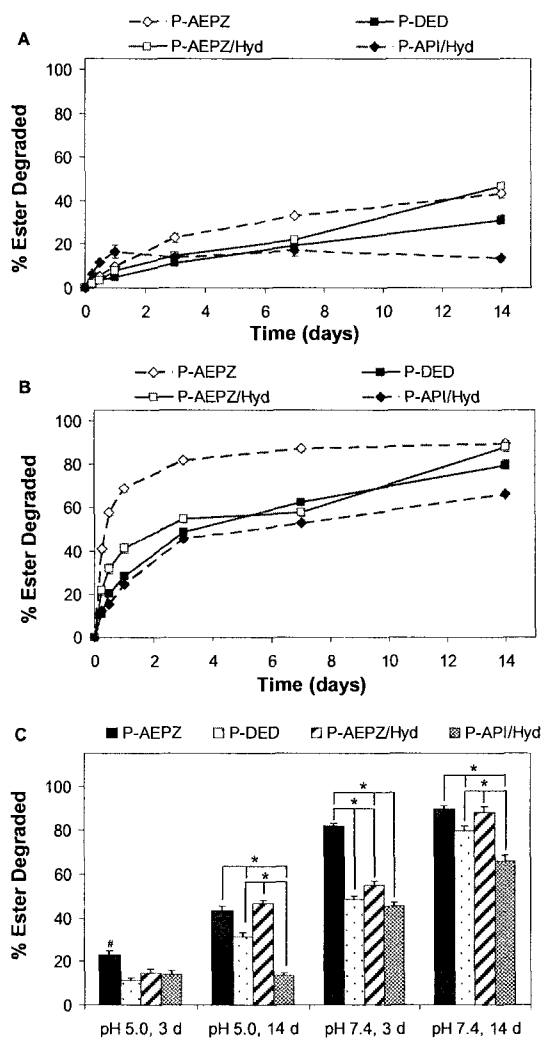
Figure IV-4 Ester degradation profiles of the polymers at 37°C and (A) pH 5.0 simulating lysosomal pH and (B) pH 7.4 simulating cytoplasmic pH and (C) degree of degradation after 3 and 14 days at pH 5.0 and 7.4 at 37°C as observed by ^{1}H-NMR. The extent of degradation is expressed as means ± standard deviation for n=3. # indicates a statistically significant difference between one polymer and all other polymers degraded under the same conditions (p<0.05). Values for P-AEPZ are adopted from a previous study[107]. * represents a statistically significant difference between two polymer compositions degraded under the same conditions (p<0.05).

Further studies that investigate the polymer architecture and topology will give a better understanding regarding the differences in degradation rates seen in this study. P-AEPZ/Hyd achieved around the same amount of degradation as P-AEPZ by day 14 (~45% and 90% at pH 5.0 and 7.4, respectively). ~80% of the esters in P-AEPZ degraded after 3 days and ~80% of the esters in P-DED degraded after 14 days at pH 7.4. These two polymers will be good candidates for evaluating pDNA release kinetics from polycationic polymers with a high (P-AEPZ) and low (P-DED) degradation rate. A higher rate of degradation was seen for all the polymers at pH 7.4 (cytoplasmal pH) than at pH 5.0 (lysosomal pH). This resulted from the higher number of unprotonated amine groups that are present at the higher pH to catalyze hydrolysis of the ester groups, which is consistent with previous work on poly(ester amine)s[79,107,122].

Cytotoxicity Analysis

Cells remained viable after incubation with the synthesized polymer solutions for 2 and 24 h at all tested concentrations. More than 85% of the cells exposed to the synthesized polymers were viable at all concentrations (Fig. IV-5). In contrast, PEI caused significant cell death after 2 h with less than 12% cell viability at a concentration of 250 μg/mL and higher and after 24 h with less than 6% cell viability at a concentration of 10 μg/mL and higher. PEI (25 kDa) has a molecular weight which is 9 times higher than that of P-AEPZ and around 30 times higher than that of all other polymers. Furthermore, PEI has a charge density which is approximately 2 times higher compared to the polymers synthesized in this study. The high toxicity of PEI may have resulted from these two parameters[123,124].
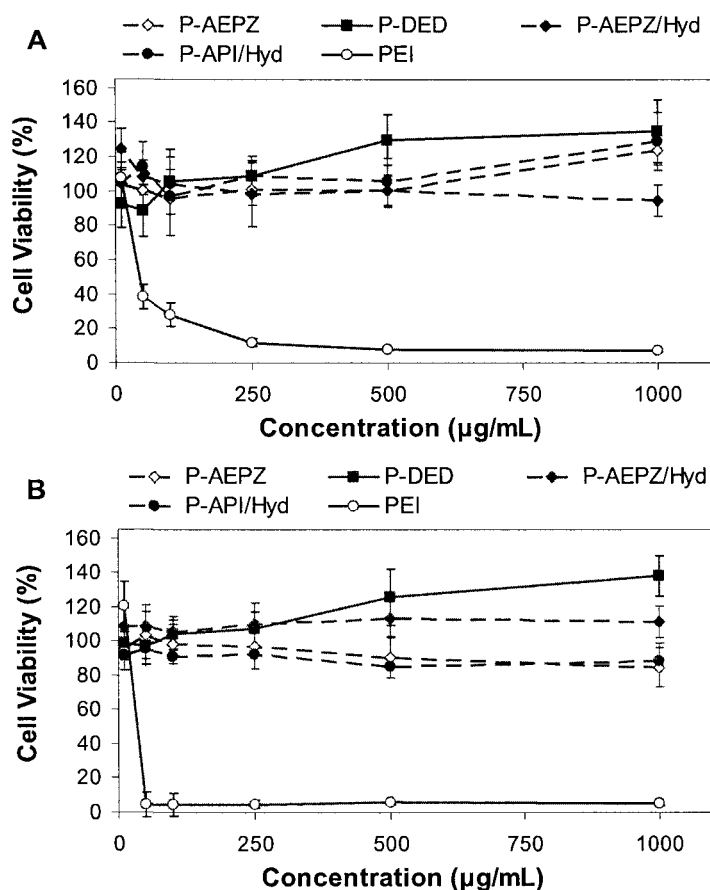
Figure IV-5 Cytotoxicity of the polymers with polyethylenimine (PEI; 25kDa) as negative control) on CRL 1764 rat fibroblasts after (A) 2 h and (B) 24 h as evaluated by an MTT assay. The results are expressed as means ± standard deviation for n=5.

The improved cytocompatibility of the developed polycationic polymers will allow for the use of these polymers at high concentrations and high N:P ratios. Especially P-DED, which contains a considerable amount of amines that dissociate at and above pH 7.4 and is therefore strongly charged at this pH, and showed good cytocompatibility even when exposed to cells at concentrations as high as 1000 µg/mL.

Polymer/pDNA Polyplex Characterization

<u>Zeta Potential</u>

The optimal polymer to pDNA ratios are those which result in a polyplex with a positive surface charge that allows the polyplex to interact with the negative charges on the cell membrane[59,75]. The pCMV-eGFP plasmid, which was used in this study, has a zeta potential of -33.1 ± 0.5 mV. All the polyplexes formed at a polymer/pDNA weight ratio of 5:1 had a negative zeta potential ranging between -8.5 and -30.0 mV (Fig. IV-6).
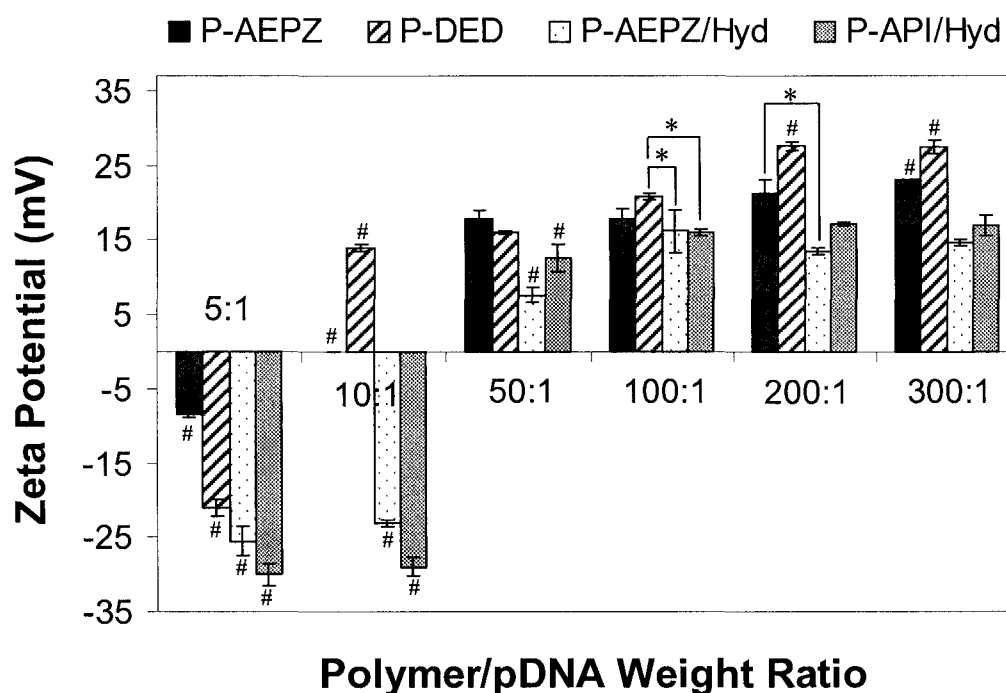
Figure IV-6 Zeta potential of the polyplexes formed with 10 μg pCMV-eGFP DNA at different polymer/pDNA weight ratios. The results are expressed as means ± standard deviation for n = 3. # indicates statistically significant difference between a polyplex and all other polyplexes formed at the same weight ratio (p<0.05). Values for P-AEPZ are adopted from a previous study[107]. * represents a statistically significant difference between two polyplexes formed at the same weight ratio (p<0.05).

At a weight ratio of 10:1, P-AEPZ and P-DED formed polyplexes characterized by a zeta potential of 0.0 ± 0.0 mV and 13.9 ± 0.5 mV, respectively. P-AEPZ/Hyd and P-API/Hyd, which contain a lower number of amines per weight of polymer that are protonated at pH 7.4 and that can participate in pDNA complexation as compared to P-AEPZ and P-DED (Fig. IV-3), formed negative polyplexes at a weight ratio of 10:1 and positive polyplexes at a weight ratio of 50:1. Half of the amine monomers in P-AEPZ/Hyd (synthesized from a 1:1:1 mole ratio of TMPTA:AEPZ:Hyd) and P-API/Hyd (synthesized from a 1:1:1 mole ratio of TMPTA:API:Hyd) are derived from hydrazine, which is characterized by a low pKa once incorporated into the polymers. Thus, the amines will not be protonated at physiological pH (7.4) and therefore cannot contribute to the complexation of pDNA. As a result, a higher polymer to pDNA ratio is needed for P-AEPZ/Hyd and P-API/Hyd to neutralize the charges of the pDNA as compared to P-AEPZ and P-DED. Polyplexes formed with P-DED generally showed higher zeta potentials as compared to all other polymers due to the polymer's high buffering capacity above pH 7.4, which results in a higher number of protonated amines at pH 7.4 that are available for pDNA complexation (Fig. IV-3). The zeta potential of all polyplexes formed by the synthesized polymers increased as the weight ratio of polymer to pDNA increased, which corresponds with the increased N:P ratios within the polyplexes.

Band Retardation with Gel Electrophoresis

The electrophoretic patterns of the polymer/pDNA polyplexes were obtained by gel electrophoresis (Fig. IV-7). Lane 8 in all images represents uncomplexed negatively

charged pDNA (naked pDNA), which migrated to the positive end of the gels. P-AEPZ

and P-DED were able to retard the migration of pDNA at polymer/pDNA weight ratios of

10:1 or higher. P-AEPZ and P-DED neutralized the charges of pDNA at a ratio of 10:1,

which is in accordance with the results for the zeta potential measurements (Fig. IV-6).
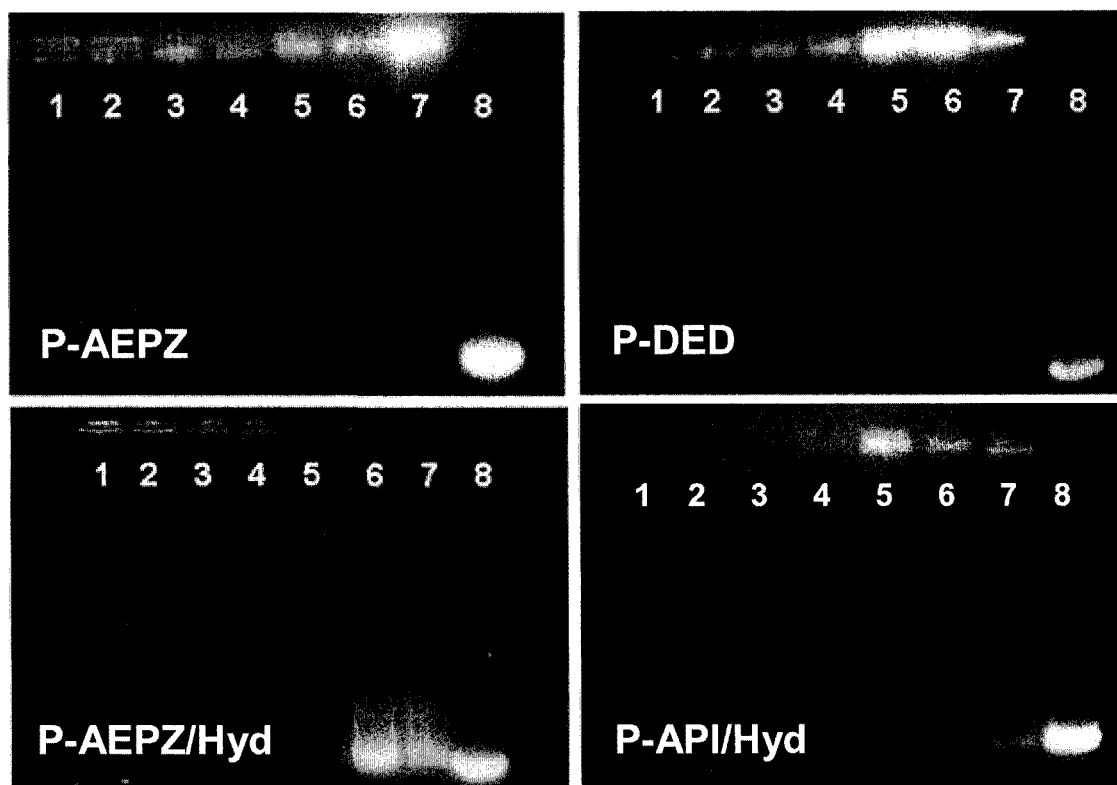
Figure IV-7 Gel retardation assay of pDNA/polymer polyplexes at different

polymer/pDNA weight ratios: (1) 100:1, (2) 80:1, (3) 60:1, (4) 40:1, (5) 30:1, (6) 20:1, (7)

10:1, and (8) naked pDNA. Results for P-AEPZ are adopted from a previous study[107].

Polyplexes with P-AEPZ/Hyd and P-API/Hyd, which exhibit lower N:P ratios at a given

polymer/pDNA weight ratio, were able to retard the migration of the pDNA at weight

ratios of 30:1 or higher and 20:1 or higher, respectively. This is also consistent with the

zeta potential data (Fig. IV-6). Polymers with a higher amount of protonated amine at pH

7.4 (i.e., P-AEPZ and P-DED) were able to retard the migration of pDNA at a lower polymer/pDNA weight ratio.

Hydrodynamic Size with Dynamic Light Scattering (DLS)

The hydrodynamic size (diameter) of the polyplexes formed at different polymer/pDNA ratios were obtained by DLS (Fig. IV-8). Naked pDNA had a diameter of 751.6 ± 111.8 nm (data not shown).
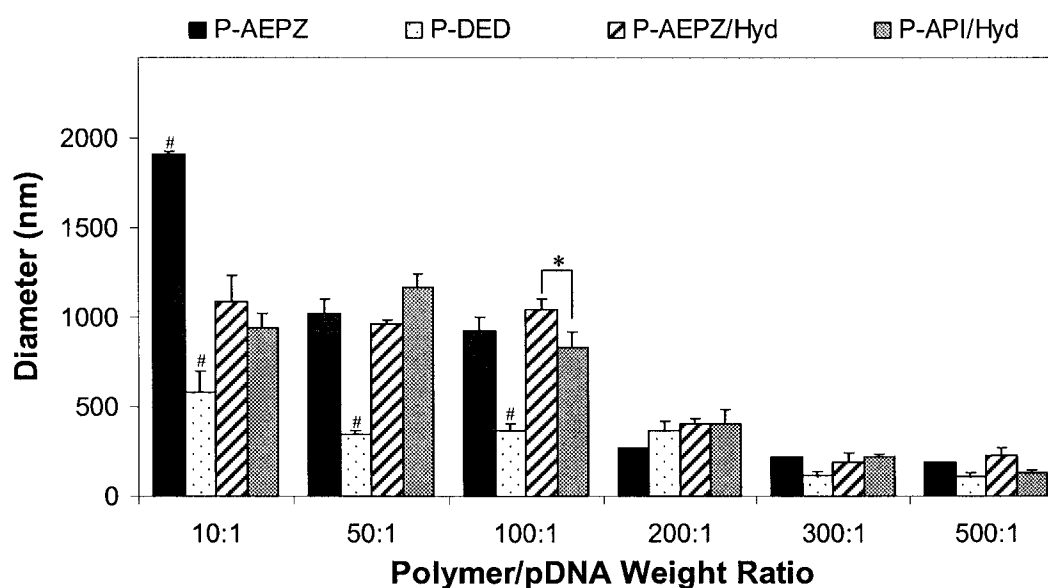
Figure IV-8 Diameter of the polyplexes formed with 10 μg pCMV-eGFP DNA at different polymer/pDNA weight ratios as evaluated by DLS. The results are expressed as means ± standard deviation for n=3. # indicates statistically significant difference between a polyplex formulation and polyplexes formed by all other polymers of the same weight ratio (p<0.05). Values for P-AEPZ are adopted from a previous study[107]. * represents a statistically significant difference between polyplexes of the same weight ratio (p<0.05).

Upon complexation, the polymer and pDNA yielded condensed particles with a diameter as small as 111.1 ± 19.9 nm (P-DED, polymer/pDNA weight ratio of 500:1). At low polymer/pDNA weight ratios (10:1, 50:1 and 100:1), aggregation of the polyplexes may have occurred as indicated by the large particle diameters ranging from 832.0 ± 85.4 nm to 1910.5 ± 17.2 nm. At low weight ratios, neutrality of the polyplexes may cause particle aggregation as electrostatic repulsion is minimal. The zeta potentials increased as the polymer/pDNA ratios were increased (Fig. IV-6) and individual polyplexes were electrostatically stabilized[54]. The large particle diameters observed for polyplexes formed with a low polymer/pDNA weight ratio could also have resulted from the inability of the polymers to condense pDNA at low polymer/pDNA weight ratios. Polyplexes formed at a polymer/pDNA weight ratio of 300:1 or higher were significantly smaller in size compared to those formed at a polymer/pDNA weight ratio of 100:1 or lower. Compared to the other polymers, P-DED formed individual particles with small particle diameters even at the lowest polymer/pDNA ratio tested (10:1). Due to the polymer's high buffering capacity above pH 7.4, the formed polyplexes were positively charged even at low weight ratios and were able to repulse each other and avoid aggregation. All synthesized polymers were able to form complexes with and condense pDNA at appropriate N:P ratios, which is beneficial for DNA stabilization and transfection[73]. The polyplexes formed by the synthesized polymers may not be as small as those formed by branched PEI (25 kDa), however, they are still promising for gene delivery. Larger sized particles have been shown to sediment onto cells, which enhances particle uptake by increasing the interaction with the cells in 2D cultures[57,126]. Although P-AEPZ/Hyd and P-API/Hyd form complexes with lower zeta potential compared to P-AEPZ and P-DED

(Fig. IV-6), P-AEPZ/Hyd and P-API/Hyd were able to condense pDNA to low hydrodynamic sizes at high polymer/pDNA weight ratios. There was no increase in surface charge of the polyplexes formed after a certain weight ratio as also observed by other groups in the literature[87]. However, improvement in the condensation of the pDNA was still observed. This suggests that above a certain polymer/pDNA weight ratio, additional polymer may not increase the surface charge of the polyplexes but it may still improve pDNA condensation.

Transfection Efficiency with Enhanced Green Fluorescent Protein Reporter Gene

The transfection efficiencies of the polyplexes formed by the synthesized polymers were evaluated using rat fibroblasts as a model cell line and the results are summarized in Figure IV-9. At low polymer/pDNA weight ratios (10:1, 50:1 and 100:1), the polyplexes formed by the synthesized polymers did not result in significantly higher numbers of transfected cells as compared to naked pDNA. We hypothesized that this resulted from the significantly larger hydrodynamic size of polyplexes formed at the lower polymer/pDNA weight ratios compared to at the higher weight ratios (300:1 and 500:1). The insufficient condensation and stabilization of the pDNA may have led to the lower transfection efficiencies observed[73]. At a polymer/pDNA weight ratio of 300:1, polyplexes formed with P-AEPZ, P-DED and P-AEPZ/Hyd resulted in significantly higher transfection efficiencies (11.8 ± 2.6%, 30.6 ± 6.6% and 5.3 ± 1.0%, respectively) than naked pDNA (0.8 ± 0.4%).
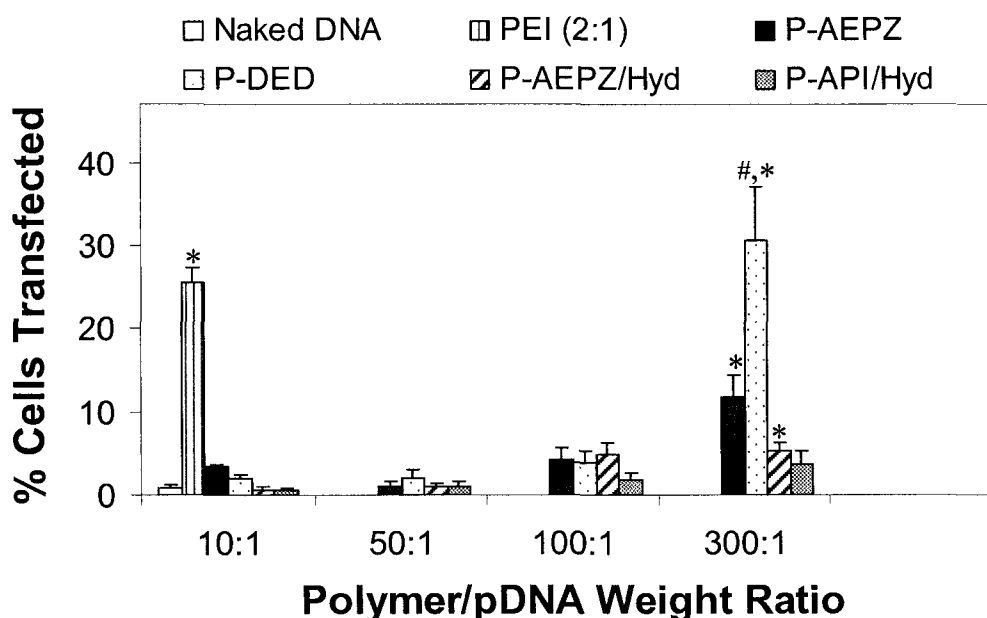
Figure IV-9 Efficiency of CRL 1764 cell transfection with polyplexes formed with 5 μg pCMV-eGFP DNA at different polymer/pDNA weight ratios. Naked pDNA and polyplexes formed by PEI at a polymer/pDNA weight ratio of 2:1 served as controls. The results are expressed as means ± standard deviation for n = 4-6. * indicates a statistically significant difference between a polyplex and naked pDNA ($p<0.05$). # indicates a statistically significant increased transfection efficacy as compared to the transfection efficacy of PEI/pDNA polyplexes ($p<0.05$).

At this weight ratio (300:1), polyplexes formed with P-DED, which has the highest number of dissociated amines available for pDNA complexation (Fig. IV-3), even resulted in a significantly higher transfection efficiency (30.6 ± 6.6%) than observed for polyplexes formed with PEI (weight ratio of 2:1, 25.5 ± 2.7%). Compared to all other synthesized polymers, P-DED had the highest amount of amines that dissociate above pH 7.4 which are available for pDNA complexation. P-DED showed more efficient pDNA

complexation and condensation and formed polyplexes with higher zeta potential (Fig. IV-6). This is especially beneficial for effective interaction with negatively charged cell membranes and cellular uptake. The high transfection efficiencies observed are a good indication that the polyplexes were successfully internalized by the cells and led to expression of GFP. As compared to PEI, a much larger excess of P-DED was required for effective pDNA complexation and cellular transfection, which is explained by the comparatively low molecular weight and low charge density of P-DED[123,127]. Due to the excellent cytocompatibility of P-DED (Fig. IV-5), such high polymer to pDNA ratios are not a concern.

Fluorescence images were taken to confirm the transfection results obtained by flow cytometry. A fluorescence image of cells treated with plain media was taken as a negative control (Fig. IV-10A). There was no transfection observed for cells exposed to media containing naked pDNA (Fig. IV-10B). Cells exposed to polyplexes formed with P-DED at a weight ratio of 300:1 had intense expression of GFP as seen by the bright green fluorescence in Figure IV-10C. Cells that were transfected with polyplexes formed with PEI (at a weight ratio of 2:1) also showed significant expression of GFP (Fig. IV-10D), however the fluorescence was not as bright and consistent as observed for transfection with P-DED (Fig. IV-10C).

Quantitative cytotoxicity evaluation was performed with an MTT assay 2 and 24 h after incubating the cells with the polymers at different concentrations. Although quantitative cytotoxicity evaluation was not performed beyond 24 h after cell treatment with the polymer/pDNA polyplexes, qualitative cytotoxicity evaluation was performed with light microscopy at the end of the transfection experiment.
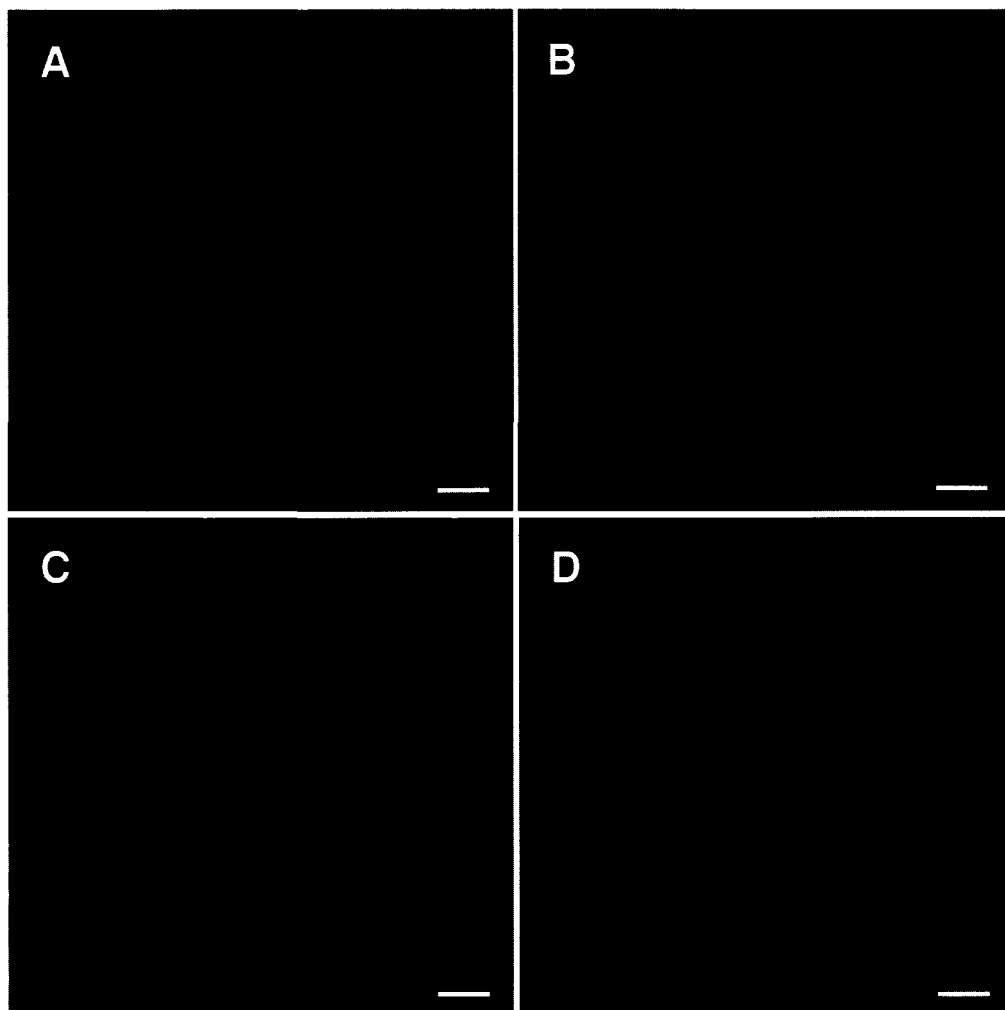
Figure IV-10 Representative fluorescence images of CRL 1764 cells after exposure to the following media: (A) plain medium, (B) naked pDNA (CMV-eGFP), (C) P-DED/pDNA (300:1), and (D) PEI/pDNA (2:1). In groups B-D, 5 µg pCMV-eGFP DNA were used.

In general, wells treated with polyplexes formed by the synthesized polymers, even at the highest polymer/pDNA weight ratio of 300:1, had a high number of live, well spread cells (data not shown). In contrast, a very low number of live cells was observed in wells

exposed to polyplexes formed with PEI. The cytotoxicity observed for PEI has been previously reported and likely resulted from the high MW and charge density of the polymer[123]. Transfection was performed in the absence of serum in this study. However, transfection efficiency can be different with the absence or presence of serum. Future transfection studies *in vivo* in an appropriate animal model will yield a more comprehensive analysis of the transfection capabilities of these polymers.

Conclusions

In this work polycationic polymers were synthesized from the triacrylate monomer TMPTA and different amine monomers by Michael addition polymerization. The hypothesis was confirmed that through variations of the amine monomers used in the reaction, the amine group density within the polymers and the basicity and buffering capacity of the polymers can be controlled. Parameters that are important in the gene delivery process were significantly influenced by these properties. It was found that amines that dissociate above pH 7.4 and are available for pDNA complexation, are a key parameter for effective pDNA condensation and transfection. P-DED, the polymer with the most amines dissociating above physiological pH, formed dense polyplexes of high zeta potential which transfected cells more efficiently than branched PEI under the conditions tested. The evaluation of the synthesized polycationic polymers further showed that the availability of unprotonated amines that can autocatalyze degradation does not exclusively predetermine the polymer degradation rate. All synthesized polymers had low cytotoxicity, which allows their use at high N:P ratios as necessary for the fabrication of poplyplexes with effective pDNA complexation and cellular

transfection. It is concluded that when designing non-viral vectors, it is important to investigate the amount of amines that dissociate in specific pH ranges relevant for autocatalytic degradation, pDNA complexation and endosomal escape instead of only examining the total amount of amines in the polymer.

CHAPTER V

DELIVERY OF PLASMID DNA ENCODING BONE MORPHOGENETIC PROTEIN-2 COMPLEXED WITH A BIODEGRADABLE BRANCHED POLYCATIONIC POLYMER FROM A COMPOSITE SCAFFOLD[†]

Abstract

This study investigated the delivery of plasmid DNA (pDNA) encoding bone morphogenetic protein-2 in the form of polyplexes with a biodegradable branched triacrylate/amine polycationic polymer (TAPP), which were complexed with gelatin microparticles (GMPs) loaded within a porous tissue engineering scaffold. More specifically, the study investigated the interplay between TAPP degradation, gelatin degradation, pDNA release and bone formation in a critical-size rat cranial defect model. The pDNA release kinetics *in vitro* were not affected by the crosslinking density of the GMPs but depended, rather, on the degradation rates of the TAPPs. Besides the initial release of polyplexes not bound to the GMPs and the minimal release of polyplexes through diffusion or dissociation from the GMPs, the pDNA was likely released as naked pDNA or as part of an incomplete polyplex, following the degradation of fragments of the polycationic polymer. After 30 days, significantly higher amounts of pDNA were released (93-98%) from composite scaffolds containing naked pDNA or pDNA complexed with P-AEPZ (a faster degrading TAPP) compared to those containing pDNA

complexed with P-DED (a slower degrading TAPP) (74-82%). Composite scaffolds containing GMPs complexed with TAPP/pDNA polyplexes did not result in enhanced bone formation, as analyzed by microcomputed tomography and histology, in a critical-size rat cranial defect at 12 weeks post-implantation compared to those loaded with naked pDNA. The results demonstrate that polycationic polymers with a slow degradation rate can prolong the release of pDNA from the composite scaffolds and suggest that a gene delivery system comprising biodegradable polycationic polymers should be designed to release the pDNA in an intact polyplex form.

Introduction

Bone defects can occur due to trauma, cancer, congenital abnormalities or age-related degeneration[11-14]. Defects that have large amounts of bone loss or insufficient vascularity are not conducive to bone regeneration and aid may be needed in healing these types of defects[19]. Thus, the search for a promising approach to repair these bone defects is very much needed. Bone tissue engineering systems delivering bioactive factors, that have the capability of inducing bone formation, such as bone morphogenetic proteins (BMPs), have been investigated by many groups. BMPs can stimulate angiogenesis[37], promote proliferation of mesenchymal stem cells (MSCs)[38-40], initiate the recruitment of osteoprogenitors and MSCs toward the defect site and stimulate the differentiation of the cells along an osteoblastic lineage[41]. Delivering the gene encoding a BMP is an alternative approach to delivering the BMP in the protein form. Gene delivery allows for a longer bioavailability of the protein[46], and the resulting protein will have a more precise post-translational modification and tertiary structure formation as it is

produced *in vivo*[136,137]. Furthermore, the production of the gene is lower in cost and easier compared to the production of the protein.

When developing a successful gene delivery system, the gene delivery vector is not the only important factor that has to be taken into consideration. The carrier that delivers the vector/DNA complexes (i.e., scaffold or composite scaffold) also plays a critical part in the gene delivery approach. In an ideal non-viral gene delivery system, the gene delivery vector has to be capable of condensing and protecting the DNA, facilitating delivery of the DNA into the cells and assisting in endosomal escape in order that the DNA can be transcribed and translated in the nucleus. Furthermore, the scaffold or composite scaffold has to be able to deliver the vector/DNA complexes to or near the defect site, control the release kinetics of the complexes and preferably protect the vector from degrading before the complexes are delivered into the cells.

Previous work in our laboratory has investigated the use of composite scaffolds comprising gelatin microparticles (GMPs) and porous poly(propylene fumarate) (PPF) to deliver BMP-2 for bone tissue engineering[18,138]. In this work, we investigated the delivery of plasmid DNA (pDNA) encoding BMP-2 complexed with a hydrolytically degradable polycationic polymer using a similar composite scaffold. The biodegradable branched triacrylate/amine polycationic polymers (TAPPs) used in this work have been extensively characterized previously in our laboratory[108]. Polymer/pDNA polyplexes formed with these polymers at certain weight ratios have been shown to result in higher transfection compared to naked pDNA[108]. Acidic GMPs, which are negatively charged at physiological pH were loaded electrostatically with net positively charged TAPP/pDNA

polyplexes. These enzymatically degradable GMPs have been used previously to deliver both growth factors[18,138,139] and pDNA[106,140,141] in a sustained manner.

The overall objective of this study was to evaluate the ability of composite scaffolds comprising pDNA complexed with a TAPP, GMPs and a porous PPF scaffold to control the release of pDNA and induce bone formation in a critical-size rat cranial defect. We hypothesized that the release of pDNA from these composite scaffolds can be controlled by the degradation rates of the TAPPs and GMPs. To test this hypothesis, composite scaffolds were fabricated with two different types of TAPPs (P-AEPZ or P-DED, synthesized with amine monomer 1-(2-aminoethyl)piperazine (AEPZ) or N,N-dimethylethylenediamine (DED), respectively) and GMPs (crosslinked with 10 mM or 40 mM glutaraldehyde and termed "10 mM" and "40 mM", respectively). The effects of the degradation rates of the TAPPs and GMPs on the release kinetics of the pDNA *in vitro* were evaluated. Furthermore, we also hypothesized that the delivery of pDNA complexed with a TAPP from the composite scaffolds will result in higher BMP-2 protein expression as reflected by greater bone formation compared to the delivery of naked pDNA from the composite scaffolds. To test this hypothesis, composite scaffolds were implanted into a critical-size rat cranial defect and the capability of these composite scaffolds to induce bone formation was evaluated at 12 weeks post-implantation.

Materials and Methods

Experimental Design

All the groups containing pDNA in this study were loaded with the same dose of pDNA (160 µg), which was derived from the dose of pDNA used for the critical-size rat

cranial defect study performed by Huang et al.[77]. Based on previous studies in our laboratory[108], we chose to investigate two different types of TAPPs (P-AEPZ and P-DED) that have different degradation rates and transfection efficiencies. At pH 7.4, ~80% of the esters in P-AEPZ and P-DED degrade after 3 and 14 days, respectively. Polyplexes formed with P-AEPZ and P-DED (polymer/pDNA weight ratio of 300:1) result in 11.8 ± 2.6% and 30.6 ± 6.6% transfection in rat fibroblasts with an enhanced green fluorescent protein (eGFP) reporter gene, respectively. Two different types of acidic GMPs (10 mM and 40 mM), which vary in the amount of glutaraldehyde used for crosslinking the GMPs during fabrication, were investigated. 10 mM acidic GMPs loaded with BMP-2 are completely degraded after 9 days in PBS containing collagenase, whereas 40 mM acidic GMPs do not show visible degradation after 28 days[142]. The difference in crosslinking density and enzymatic degradation rates of the GMPs has been shown to result in different drug release kinetics[139,142]. Porous PPF scaffolds, which have been used previously with GMPs in our laboratory to deliver growth factors[18,138], were used as the carrier for the GMPs and polyplexes in this study. PPF scaffolds can undergo bulk degradation by ester hydrolysis[143], and the high porosity of the scaffolds allows for circulation of nutrients and metabolic wastes as well as tissue ingrowth, which facilitates vascularization and a firm attachment to surrounding tissue[144,145]. The resulting groups for the studies are summarized in Table V-1.

Table V-1 Composition of pDNA, triacrylate/amine polycationic polymer and gelatin microparticles in each group

Group	Amount of pDNA (µg)	Type of TAPP	Type of GMP
Blank_10*	-	-	10 mM
Blank_40*	-	-	40 mM
Free_10	160	-	10 mM
Free_40	160	-	40 mM
P-AEPZ_10	160	P-AEPZ	10 mM
P-AEPZ_40	160	P-AEPZ	40 mM
P-DED_10	160	P-DED	10 mM
P-DED_40	160	P-DED	40 mM

*groups included in the *in vivo* bone formation study but not in the *in vitro* release kinetics study

Materials

Pluronic F-127 and bacterial collagenase type 1A were purchased from Sigma-Aldrich (St. Louis, MO). pDNA with a cytomegalovirus (CMV) promoter and human BMP-2 gene (pCMV-hBMP-2, 5.5 kb) was obtained from Invitrogen (Carlsbad, CA). PicoGreen Quantification Reagent assay kit was purchased from Molecular Probes (Eugene, OR). Fischer-344 rats were purchased from Harlan (Indianapolis, IN).

PPF Scaffold Preparation and Characterization

PPF was synthesized as previously described[146], and the resulting polymer had a number average molecular weight of 2270 and a polydispersity index of 1.53. Porous

PPF scaffolds were fabricated as previously reported[18,138], and disc-shaped scaffolds (8 mm diameter x 1 mm thickness) were obtained. Mercury porosimetry (Autoscan 500, Quantachrome Instruments, Boynton Beach, FL) was used to evaluate the porosity of the scaffolds, as performed previously[144]. Microcomputed tomography (microCT) was also used to analyze the porosity of the scaffolds as previously described[138,144], with a global binarization threshold of 60-255. The interconnectivity of the scaffolds, which is defined as the fraction of the pore volume in the scaffold that is accessible from the outside through openings of a certain minimum size[147], was also obtained with microCT according to established methods[138,144]. The porosity and interconnectivity analyses were conducted in triplicate.

Composite Scaffold Fabrication

pCMV-hBMP-2 was amplified in *Escherichia coli* bacteria as done previously[107,108]. P-AEPZ and P-DED were synthesized by reacting trimethylolpropane triacrylate (TMPTA) with AEPZ and DED, respectively, as previously described[108]. Gelatin with an isoelectric point of 5.0 was used to prepare acidic GMPs using a previously established method[148], and particles ranging from 50-100 μm in diameter were obtained. The composite scaffolds were prepared using an adaptation of previous methods for loading with growth factors[18,138]. First, a 300 μL solution of polymer/pDNA polyplexes containing 160 μg of pDNA were prepared according to established methods[107,108]. The solutions were then lyophilized to remove the liquid. Preliminary studies in our laboratory have shown that there is no significant difference in the transfection efficiency for polyplexes formed with and without lyophilization (data not

shown). Dry GMPs were then loaded with the lyophilized polyplexes and naked pDNA that were resuspended in 25 µl of PBS. For composite scaffolds from groups without pDNA (i.e., Blank_10 and Blank_40), the dry GMPs were swelled with 25 µl of PBS alone. Each solution was added drop-wise to 5 mg of GMPs, and the mixture was vortexed and left overnight for 20 hours at 4°C. The loaded GMPs were then mixed with 30 µL of 24% (w/v) aqueous solution of Pluronic F-127 and injected into the pores of a PPF scaffold.

In Vitro Plasmid DNA Release Kinetics

Composite scaffolds were prepared as stated above and placed in 1 mL of PBS containing bacterial collagenase type 1A at a physiologically relevant concentration (400 ng/mL) to allow for the enzymatic degradation of the GMPs[149]. The samples were placed on an orbital shaker (70 rpm) in a 37°C warm room throughout the duration of the study. At each time point (0.5, 1, 2, 3, 7, 10, 17, 24 and 30 d), the release solutions were collected and completely replaced with 1 mL of fresh PBS containing collagenase. The release samples from each time point were analyzed with a PicoGreen Quantification Reagent assay according to the manufacturer's guidelines. 100 µL of 1 × TE buffer, 50 µL of the release solution and 150 µL of a 200-fold dilution of the PicoGreen reagent were added to individual wells of an opaque 96-well plate. The fluorescence intensity of each well was measured in a fluorescent microplate reader (FLx800, BIO_TEK Instruments, Winooski, VT) equipped with 480/525 (excitation/emission) filter sets. Preliminary studies in our laboratory have shown that the PicoGreen reagent cannot fully bind to pDNA that is in a polyplex, as also reported by Kim et al.[150]. The assay does not

allow us to accurately differentiate between and measure the amount of pDNA with different extents of complexation (i.e., fully complexed, partially complexed and uncomplexed pDNA) at each time point. Thus, after each time point, the collected release solutions were further incubated at 37°C for an additional 14 days to allow the TAPPs to degrade and release the pDNA from the polyplexes. The PicoGreen Quantification assay was then performed on the solutions to quantify the total amount of pDNA released at each time point which would include uncomplexed or previously complexed pDNA. Standard solutions of known pDNA concentrations ranging from 0-6 µg/mL were used to form the calibration curves. The cumulative release at each timepoint was calculated using the equation below. This study was conducted at n=4.

$$\% \, Cumulative \, release \, at \, time \, X = \frac{\sum pDNA \, released \, up \, to \, time \, X}{pDNA \, loaded}$$

In Vivo Bone Formation

Animal Surgery, Euthanasia and Implant Retrieval

This study was conducted in accordance with an animal protocol approved by the Rice University Institutional Animal Care and Use Committee (IACUC). The composite scaffolds were compiled using aseptic techniques and implanted into 11-12 week old male syngeneic Fischer-344 rats weighing approximately 250-274 g. The general inhalational anesthesia, creation of an 8 mm diameter critical-size cranial defect with a trephine drill, placement of composite scaffolds in the defect site and postoperative animal care were performed as previously described[18].

The 32 animals from the 4 control groups (i.e., Blank_10, Blank_40, Free_10 and Free_40, with n=8 per group) were implanted without any complications or abnormal behavior in the animals. Three out of eight of the animals receiving composite scaffolds from Group P-AEPZ_10 experienced seizures in the immediate postoperative period. Two out of three of these animals were euthanized upon the recommendation of the consulting veterinarian. To continue the study, the animal protocol was modified and approved to include a preoperative intraperitoneal injection of fosphenytoin (60 mg/kg)[151] 30 minutes before surgery for the remaining animals implanted with composite scaffolds from Groups P-AEPZ_10 (to replace the euthanized animals), P-AEPZ_40, P-DED_10 and P-DED_40. Each animal also received intraperitoneal injections of fosphenytoin at 12 (20 mg/kg), 24 (20 mg/kg) and 36 (15 mg/kg) hours after surgery for maintenance. Some of the animals receiving a composite scaffold containing P-AEPZ (i.e., from Groups P-AEPZ_10 and P-AEPZ_40) and one animal receiving a composite scaffold containing P-DED (i.e. from Group P-DED_10), which were given fosphenytoin before surgery, still experienced seizures. However, euthanasia was not recommended for these animals. Fosphenytoin was found to be capable of reducing the occurrence, severity and length of the seizures in this study and previous studies in both rats[151] and humans[152].

The animals were euthanized and implants were harvested at 12 weeks post-implantation using a previously established method[18]. The resulting rectangular section, which included the defect site and implant, was placed into 10% neutral buffered formalin for 5 days and then placed into 70% ethanol. One of the animals implanted with a composite scaffold from Group P-AEPZ_40 had a large abdominal tumor that was discovered around 7 weeks post-implantation. The animal was euthanized upon the

recommendation of the consulting veterinarian prior to the end of the study and thus was not included in the microCT and histology evaluations.

Microcomputed Tomography

MicroCT was used to quantify the amount of bone formed within the defect. The retrieved samples were scanned, and the amount of bone volume in the defect was obtained as previously described[18,138] with a global binarization threshold of 70-255. Maximum intensity projections (MIPs) for each sample were generated. An 8 mm diameter circular region of interest (ROI) was created in the MIP, and a binary image was obtained with a global binarization threshold of 70-255. The percent of area that was bone within the circular ROI was determined with the equation below.

$$\% \text{ Bone area} = \frac{\text{Binarized object area}}{\text{ROI area}} \times 100\%$$

The extent of bony bridging and union within the defect was also determined from the MIPs by two blinded observers (J.D.K and P.P.S.) separately according to the grading scale in Table V-2 as done previously[18,138]. A consensus score was obtained for each sample.

Table V-2 Scoring guide for extent of bony bridging and union obtained using maximum intensity projections of microCT datasets

Description	Score
Bony bridging over entire span of defect at longest point (8 mm)	4
Bony bridging over partial length of defect	3
Bony bridging only at defect borders	2
Few bony spicules dispersed throughout defect	1
No bone formation within defect	0
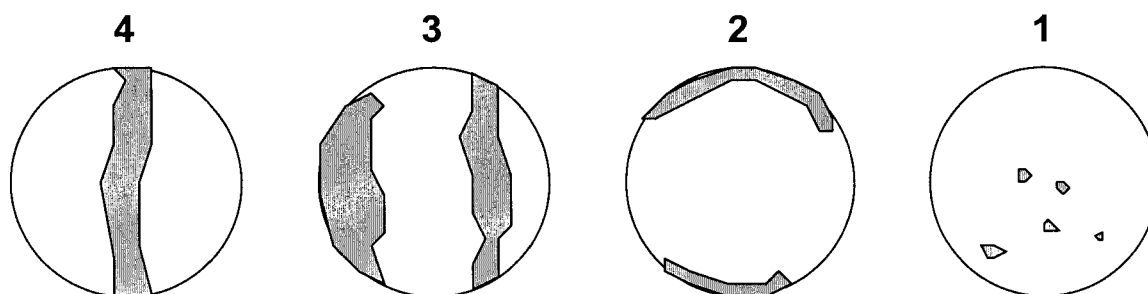
Histological Processing and Scoring

After microCT scanning, the samples were dehydrated in a graded series of ethanol solutions (70% to 100%), followed by methylmethacrylate (MMA) embedding as done previously[153]. After polymerization, 5 μm thick coronal sections were prepared from the middle of the sample using a microtome. Three sections per sample were stained with hematoxylin and eosin (H&E). One section per sample was stained with Von Kossa/Van Gieson and one section per sample was stained with Goldner's Trichrome. The sections stained with H&E were quantitatively evaluated separately by three blinded observers (F.K.K., J.D.K. and P.P.S.) using light microscopy. The hard tissue response (1) at the scaffold-bone interface and (2) within the pores of the scaffold were evaluated

using the quantitative grading scale in Table V-3 as done previously[18,138]. A consensus score was obtained for each sample.

Table V-3 Scoring guide for quantitative histological analysis

Description	Score
Hard tissue response at scaffold-bone interface	
Direct bone to implant contact without soft interlayer	4
Remodeling lacuna with osteoblasts and/or osteoclasts at surface	3
Majority of implant is surrounded by fibrous tissue capsule	2
Unorganized fibrous tissue (majority of tissue is not arranged as capsule)	1
Inflammation marked by an abundance of inflammatory cells and poorly organized tissue	0
Hard tissue response within the pores of the scaffold	
Tissue in pores is mostly bone	4
Tissue in pores consists of some bone within mature, dense fibrous tissue and/or a few inflammatory response elements	3
Tissue in pores is mostly immature fibrous tissue (with or without bone) with blood vessels and young fibroblasts invading the space with few macrophages present	2
Tissue in pores consists mostly of inflammatory cells and connective tissue components in between (with of without bone) OR the majority of the pores are empty or filled with fluid	1
Tissue in pores is dense and exclusively of inflammatory type (no bone present)	0

Statistical Methods

For the results of the release kinetics of pDNA *in vitro* in the different phases, repeated measures analysis of variance (ANOVA) was used to identify if there were significant differences among groups at an alpha level of 0.05. Tukey-Kramer multiple

comparison test was then conducted to identify the specific groups that differed statistically significantly. For the cumulative release after 30 d *in vitro* and the microCT bone volume and area results obtained from the *in vivo* study, multi-factor ANOVA was used to identify if there were significant differences among groups at an alpha level of 0.05. Tukey's Honestly Significantly Difference (HSD) test was then conducted to identify the specific groups that differed statistically significantly. For the microCT bone union and histology hard tissue response scoring results obtained from the *in vivo* study (discrete ordinal values), ordered logistic regression was used to identify if there were significant differences among groups at an alpha level of 0.05. An analysis of effects was then performed to identify the specific groups that differed statistically significantly.

Results

PPF Scaffolds Porosity and Interconnectivity

The porosity of the PPF scaffolds was determined by microCT and mercury porosimetry and was found to be 64.3 ± 1.0 and 67.1 ± 0.8%, respectively, which is comparable to what was reported by Patel et al. for the same porous PPF scaffold formulation (~70%)[18]. More than 98.8 ± 0.3% of the pores in the scaffolds were connected to the outside environment through an opening of 32 μm or larger (Fig. V-1). Pores of at least 10 μm are needed for bone cell migration[144]. The interconnectivity gradually decreased as the opening cut-off increased.
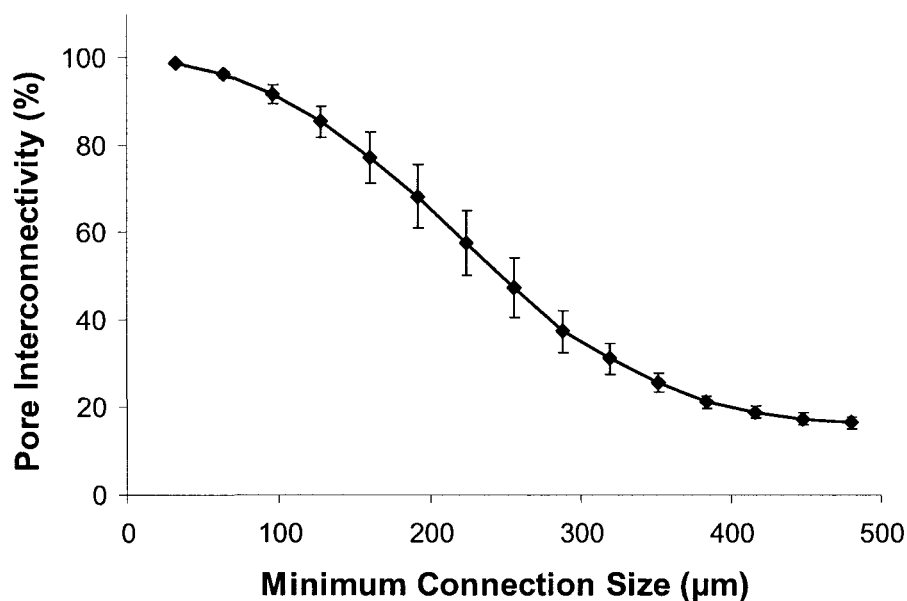
Figure V-1 Pore interconnectivity obtained by microCT analysis at different minimum connection size. The results represent means ± standard deviations of n = 3.

In Vitro Plasmid DNA Release Kinetics

The *in vitro* release of pDNA from the composite scaffolds was evaluated in PBS containing a physiological amount of collagenase over 30 days. The pDNA release profiles are shown in Figure V-2. The amount of pDNA released was divided into four time segments as done in previous studies[138,139,142,149] to facilitate the comparison of the release rates of the different groups: Phase 1 (the first 24 h), Phase 2 (days 1-3), Phase 3 (days 3-17) and Phase 4 (days 17-30) (Table V-4). The type of GMP (10 or 40 mM) did not have an overall significant effect on the pDNA release kinetics. However, the type of TAPP (no polymer (i.e., delivered as naked pDNA), P-AEPZ or P-DED) did have an overall significant effect on the pDNA release kinetics ($p < 0.0001$).
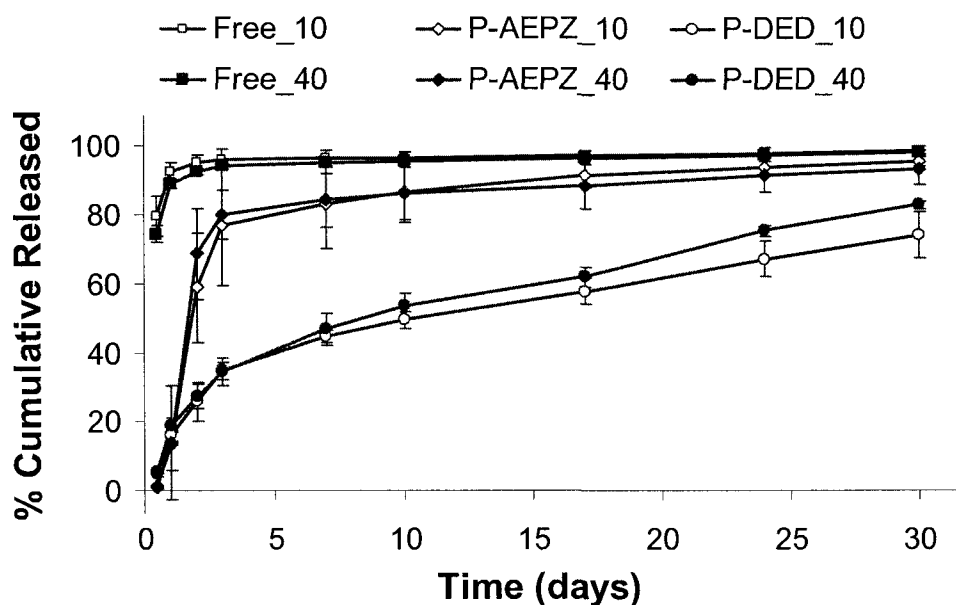
Figure V-2 Profiles of percent cumulative pDNA released *in vitro* in PBS containing collagenase. The results represent means ± standard deviations of n = 4.

Groups Free_10 and Free_40 had a large burst release of pDNA (92.6 ± 1.1 and 88.9 ± 2.5% pDNA per day, respectively) in the first 24 h (Phase 1) and significantly lower release rates in the subsequent phases (0.1 to 2.6% per day). All other groups had significantly lower release rates in Phase 1 (10.7 to 16.6% per day) compared to Groups Free_10 and Free_40. Groups P-AEPZ_10 and P-AEPZ_40 had significantly higher release rates in Phase 2 (31.7 ± 10.2 and 32.1 ± 9.2% per day, respectively) compared to the other groups (1.7 to 11.0% per day). Groups P-AEPZ_10 and P-AEPZ_40 released pDNA at significantly higher rates in Phase 2 compared to the other phases (0.3 to 14.1 % per day). Groups P-DED_10 and P-DED_40 released pDNA at significantly higher rates in Phase 1 (16.0 ± 1.6 and 19.0 ± 2.1% per day, respectively) and Phase 2 (9.4 ± 0.8 and 11.1 ± 1.9% per day, respectively) compared to Phase 3 and 4 (1.3 to 2.0% per day).

Table V-4 Release kinetics of pDNA from composite scaffolds in four different phases. The results are expressed as means ± standard deviation (% release per day) for n = 4.

Group	Phase 1 (% / day) First 24 h	Phase 2 (% / day) Days 1–3	Phase 3 (% / day) Days 3-17	Phase 4 (% / day) Day 17-30
Free_10	$92.6 \pm 1.1^{a,b}$	1.7 ± 0.4	0.1 ± 0.0	0.1 ± 0.0
Free_40	$88.9 \pm 2.5^{a,b}$	2.6 ± 0.9	0.2 ± 0.2	0.1 ± 0.0
P-AEPZ_10	13.4 ± 7.7^{b}	$31.8 \pm 10.2^{a,b}$	1.0 ± 1.1	0.3 ± 0.1
P-AEPZ_40	14.1 ± 16.6^{b}	$33.0 \pm 6.2^{a,b}$	0.6 ± 0.1	0.4 ± 0.3
P-DED_10	16.0 ± 1.6^{c}	9.4 ± 0.8^{c}	1.6 ± 0.2	1.3 ± 0.2
P-DED_40	19.0 ± 2.1^{b}	11.1 ± 1.9^{b}	2.0 ± 0.2	1.6 ± 0.2

[a] represents statistically significant difference ($p < 0.05$) between one group from all other groups excluding the group with the same TAPP treatment (i.e., Free_10 and Free_40, P-AEPZ_10 and P_AEPZ_40, P-DED_10 and P_DED_40 are not significantly different from each other) within the same phase.

[b] represents statistically significant difference ($p < 0.05$) between one phase from all other phases within the same group.

[c] represents statistically significant difference ($p < 0.05$) between one phase from Phase 3 and 4 within the same group.

Although no difference in release kinetics was observed for 10 and 40 mM GMPs, visual observation of the samples at the end of the release study demonstrated that there was more degradation of 10 mM GMPs compared to 40 mM GMPs, as expected. After 30 days, almost all of the 10 mM GMPs in samples from Groups Free_10 and P-AEPZ_10 were degraded. However, samples from Group P-DED_10 still had some 10 mM GMPs remaining in the sample tubes. For samples with 40 mM GMPs, there were still some GMPs remaining in all the sample tubes. However, samples from Groups P-

AEPZ_40 and P-DED_40 had a higher amount of 40 mM GMPs remaining in the sample tubes compared to samples from Group Free_40.

In Vivo Bone Formation

The ability of the composite scaffolds to induce bone formation was evaluated in a critical-size rat cranial defect over 12 weeks.

MicroCT Analysis

The percent of bone volume that formed in the defect was obtained by microCT (Fig. V-3A). Group Free_10 had significantly higher bone formation (5.0 ± 3.4%) compared to Groups P-AEPZ_10 and P-AEPZ_40 (0.7 ± 0.9% and 0.5 ± 0.7%, respectively). The amount of bone healing was also analyzed by comparing the percent of bone area in the MIPs that were obtained by microCT (Fig. V-3B). As observed for the bone volume results, Group Free_10 had a significantly higher amount of bone area (21.9 ± 15.7%) compared to Groups P-AEPZ_10 and P-AEPZ_40 (5.0 ± 5.9 and 2.6 ± 3.0%, respectively).

The MIPs were also used to evaluate the extent of bony bridging and union based on the guide shown in Table V-2, and the average scores are shown in Figure V-4A. Groups P-AEPZ_10 and P-AEPZ_40 had average scores of around 1 (1.3 ± 0.9 and 0.9 ± 0.9, respectively), whereas the other groups had scores closer to 2 (1.9 to 2.3).
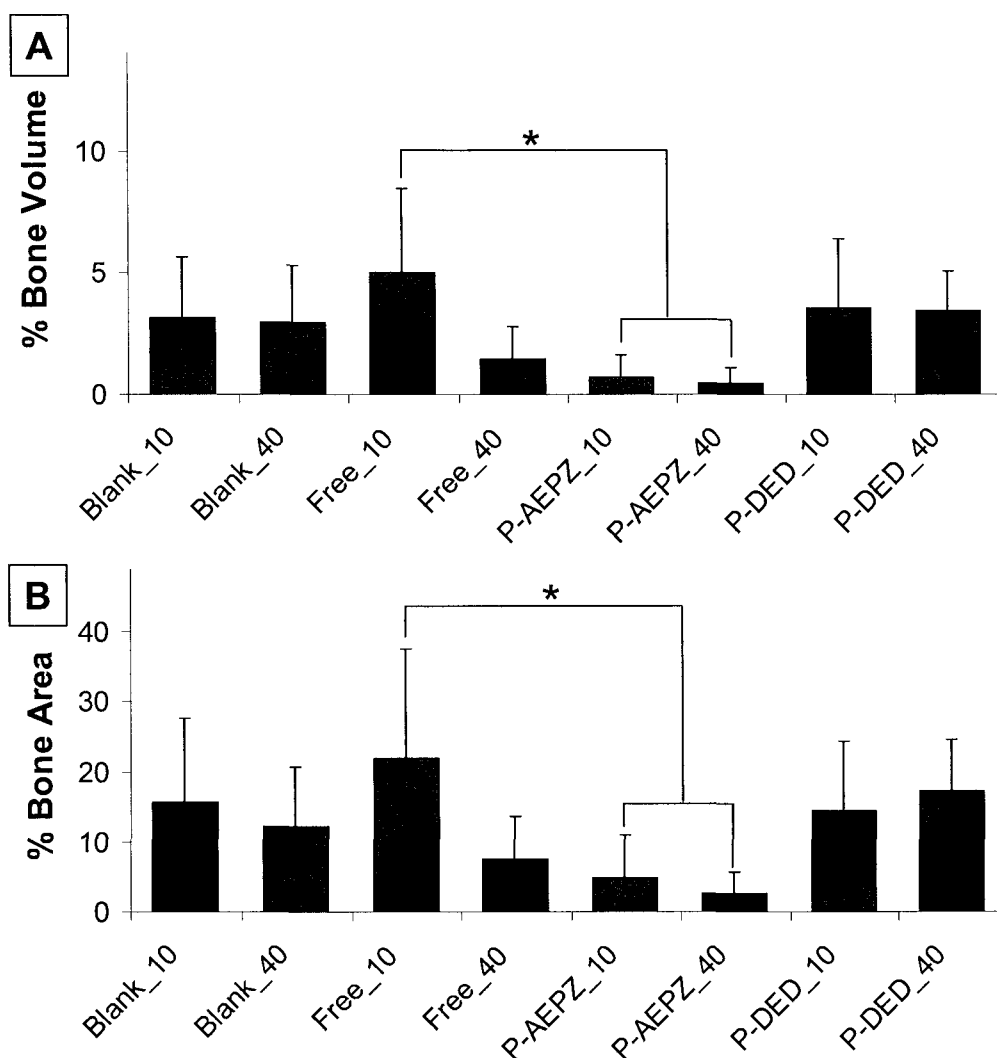
Figure V-3 Percent bone (A) volume formed within an 8 mm diameter and 1.5 mm thick cylindrical VOI as measured by microCT and (B) area formed within an 8 mm diameter circular ROI of the MIPs as measured by microCT at 12 weeks. The results are expressed as means ± standard deviation for n = 7-9. * represents a statistically significant difference between groups (p<0.05).
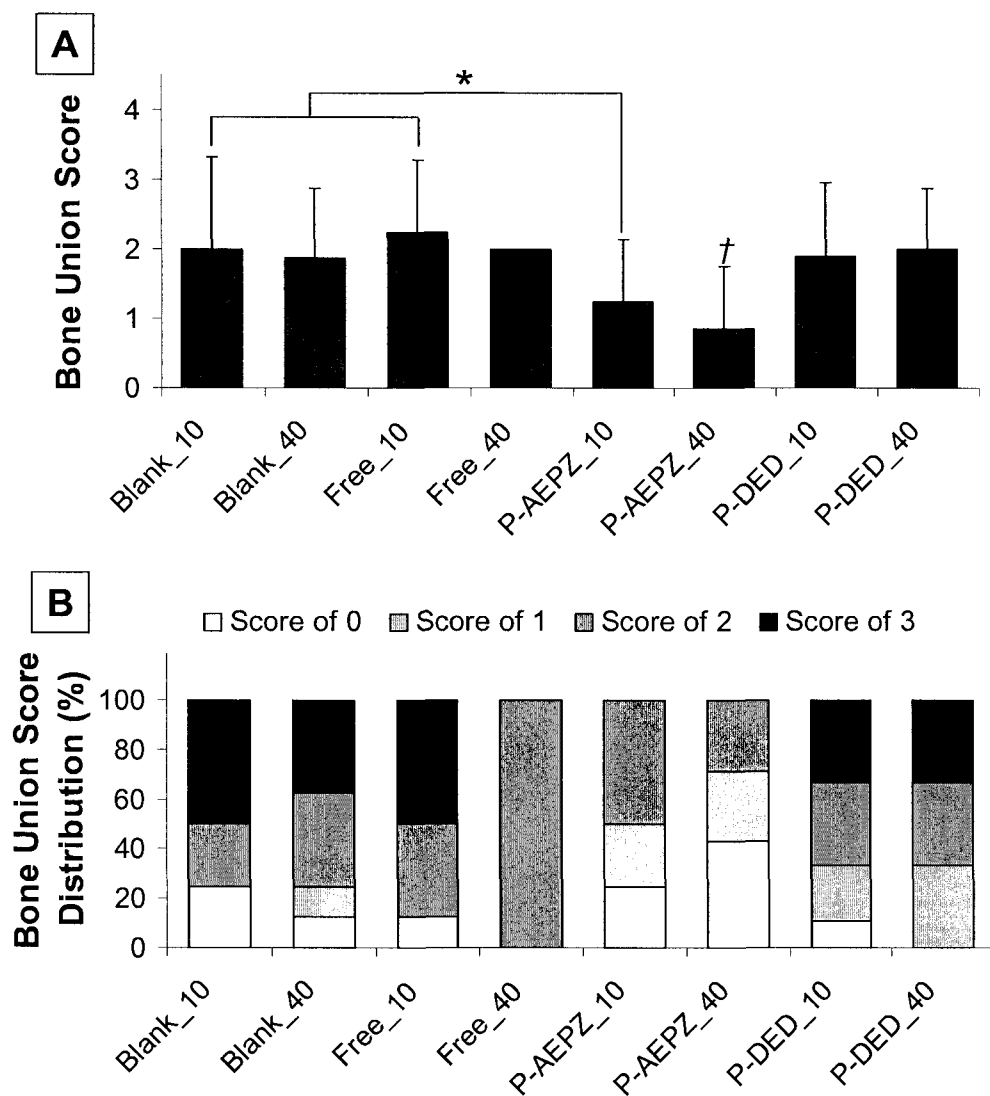
Figure V-4 (A) Average bone union score within the defect as measured by assessing MIPs obtained by microCT at 12 weeks. The results are expressed as means ± standard deviation for n = 7-9. [†] represents a statistically significant difference between one group from all other groups (p<0.05) excluding the group with the same TAPP treatment (i.e., P-AEPZ_10 and P_AEPZ_40 are not significantly different from each other). * represents a statistically significant difference between groups (p<0.05). (B) Bone union score distribution.

The extent of bony bridging and union in Group P-AEPZ_10 (1.3 ± 0.9) was significantly lower than Groups Blank_10 and Free_10 (2.0 ± 1.3 and 2.3 ± 1.0, respectively). The extent of bony bridging and union in Group P-AEPZ_40 (0.9 ± 0.9) was significantly lower than all the other groups (1.9 to 2.3), excluding Group P-AEPZ_10.
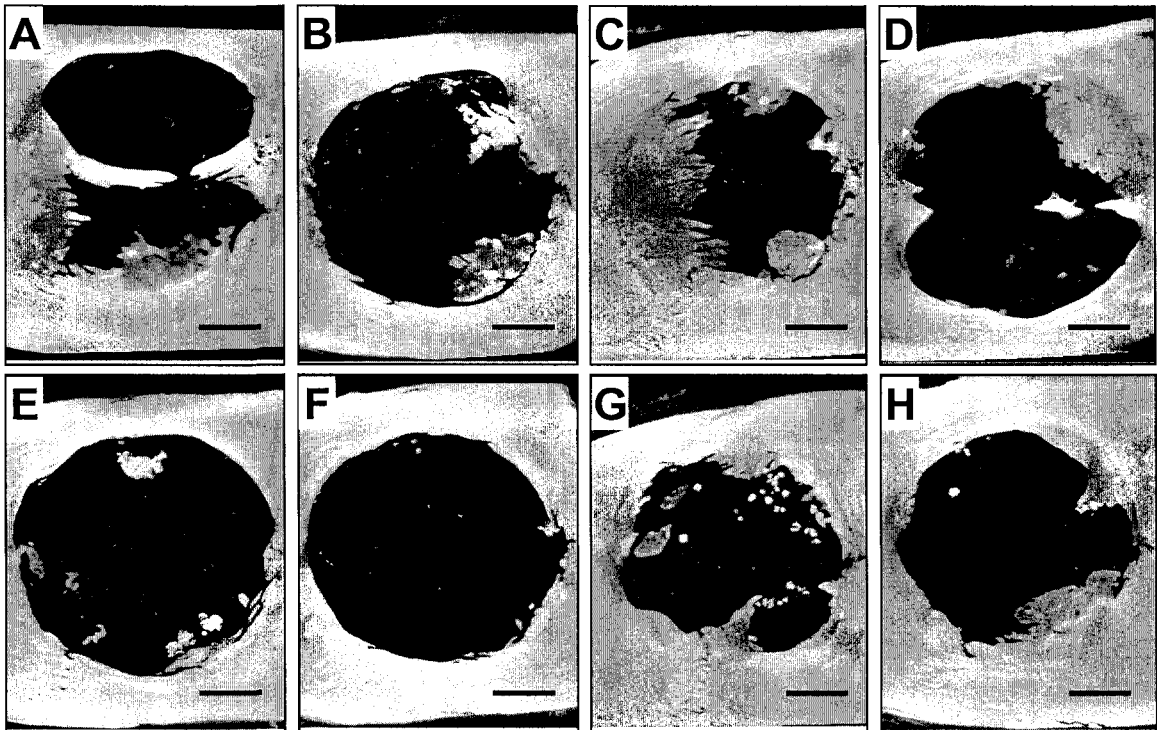
Figure V-5 Representative images of MIPs of rat cranial defects obtained by microCT at 12 weeks. (A) Group Blank_10: 6.0% bone volume, 25.6% bone area, bone score = 3. (B) Group Blank_40: 3.0% bone volume, 17.3% bone area, bone score = 2. (C) Group Free_10: 10.2% bone volume, 47.0% bone area, bone score = 3. (D) Group Free_40: 2.9% bone volume, 15.6% bone area, bone score = 2. (E) Group P-AEPZ_10: 1.0% bone volume, 6.2% bone area, bone score = 1. (F) Group P-AEPZ_40: 0.1% bone volume, 0.1% bone area, bone score = 0. (G) Group P-DED_10: 6.6% bone volume, 26.1% bone area, bone score = 2. (H) Group P-DED_40: 5.8% bone volume, 19.3% bone area, bone score = 2. Bar represents 2 mm.

None of the samples had total union, which corresponds to a bone score of 4 (Fig. V-4B). All the groups had at least 1 sample with a bone score of 3, which signifies partial union, except Groups Free_40 (all samples had a score of 2), P-AEPZ_10 and P-AEPZ_40. The groups containing only GMPs, Pluronic F-127 and a PPF scaffold (without any drug loaded) in this study (i.e., Groups Blank_10 and Blank_40) had comparable bone scores (2.0 ± 1.3 and 1.9 ± 1.0, respectively) to that observed by Patel et al. (Group BLANK, 2.0 ± 1.1)[18]. The bone that formed in the defects was mostly on the dural side of the cranium. The bone usually formed from the defect margins, and, in some of the animals, bone formed further towards the middle of the defect (Fig. V-5A and V-5C).

Histological Analysis

Histological analysis was performed on the samples to further investigate the tissue response to the implanted composite scaffolds. The scoring of the hard tissue response at the scaffold-bone interface and within the pores of the scaffolds was performed on the H&E sections based on the guide shown in Table V-3, and the average scores are shown in Figure V-6. Groups Free_40 and P-AEPZ_10 had significantly lower scaffold-bone interface and pore tissue scores compared to Groups Blank_10, Blank_40, Free_10, P-DED_10 and P-DED_40. Group P-AEPZ_40 had a significantly lower interface score compared to Groups Blank_10, Blank_40 and P-DED_40 and a significantly lower pore tissue score compared to Groups Blank_40, P-DED_10 and P-DED_40.
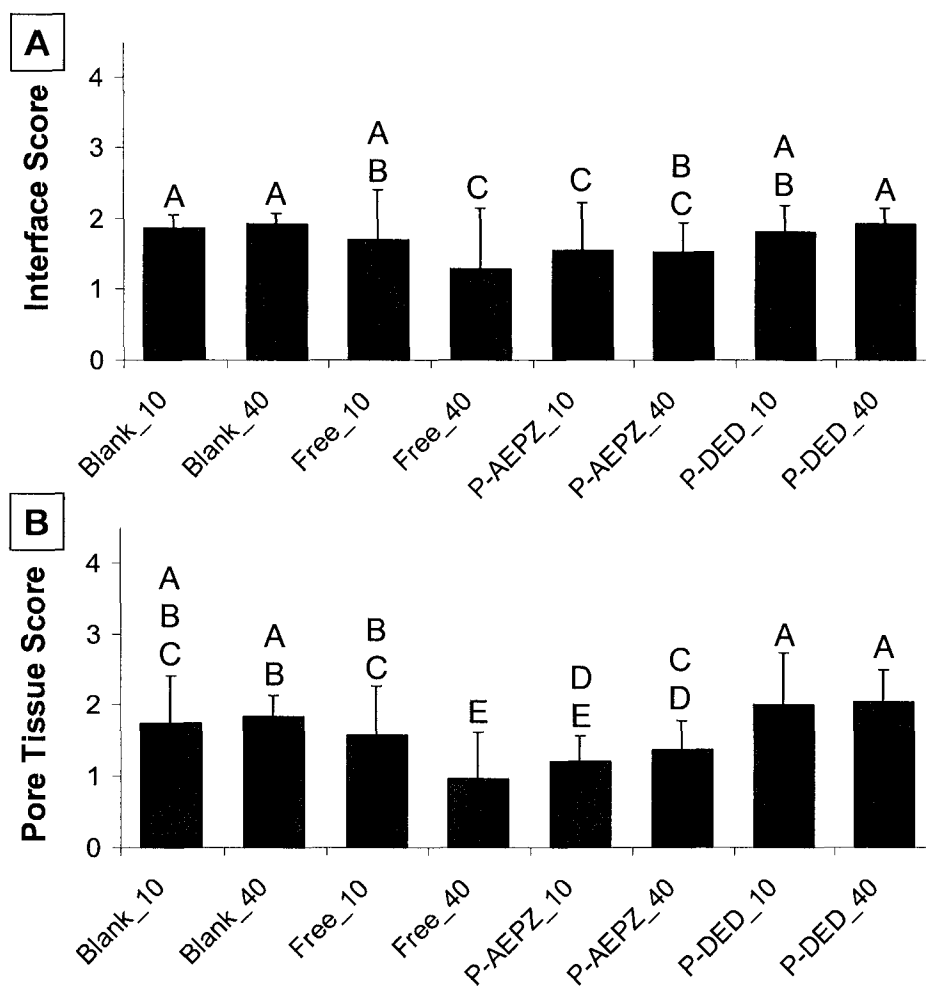
Figure V-6 Average histological scores for hard tissue response (A) at the scaffold-bone interface and (B) within the scaffold pores of the defect as assessed using H&E histological sections of rat cranial defects at 12 weeks. The results are expressed as means ± standard deviation for n = 7-9. Groups not connected with the same letter are significantly different from each other (p<0.05).

All the groups had a majority of implants that were surrounded by a fibrous tissue capsule, which corresponds to a score of 2, except for samples from Groups P-AEPZ_10 and P-AEPZ_40 (Fig. V-7A). The implants from these groups were mostly surrounded by

unorganized fibrous tissue that was not arranged in a capsule, which corresponds to a score of 1. The pores of the implants were mostly filled with immature fibrous tissue with some blood vessel formation, which corresponds to a score of 2 (Fig. V-7B). Groups P-AEPZ_10 and P-AEPZ_40, however, had more samples where the majority of the implant pores were empty or filled with fluid which corresponds to a score of 1.
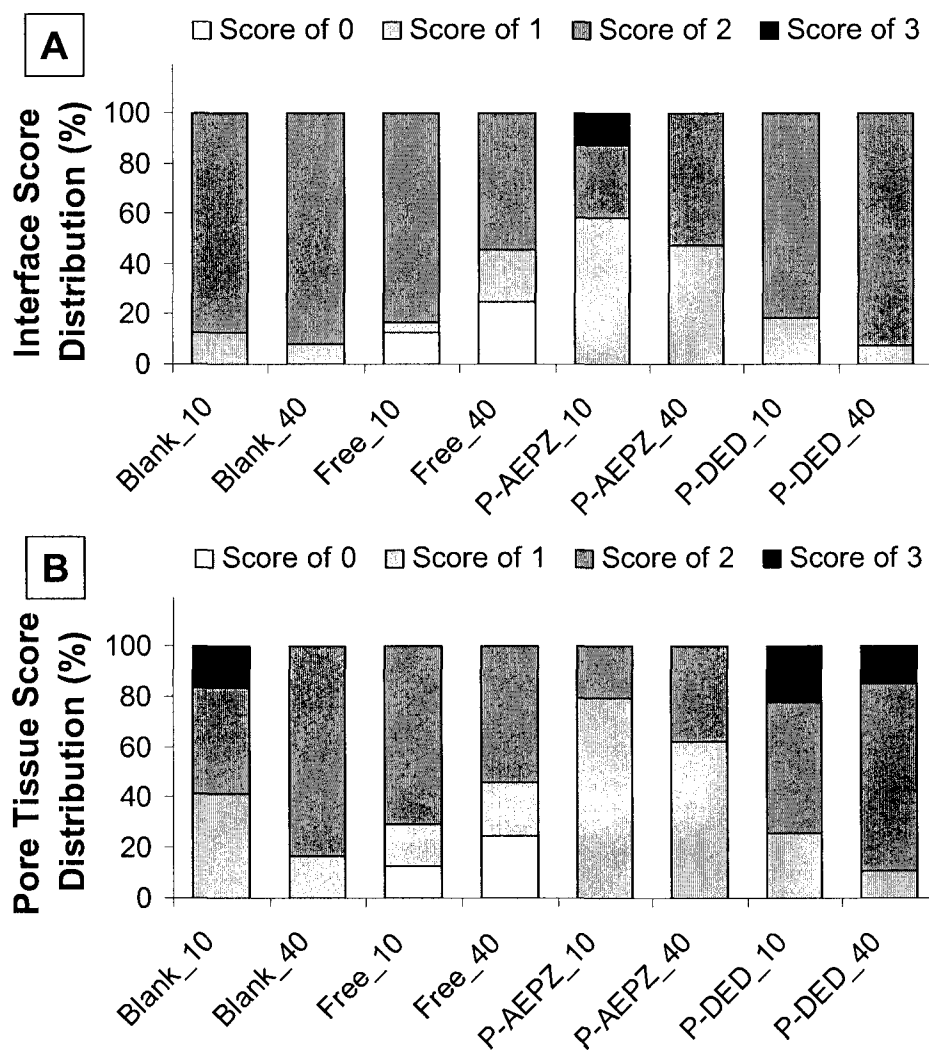
Figure V-7 Histological score distribution of hard tissue response (A) at the scaffold-bone interface and (B) within the scaffold pores of the defect as assessed using H&E histological sections of rat cranial defects at 12 weeks.

One sample from Group Free _10 and two samples from Group Free_40 had implants with pores filled with dense inflammatory tissue, which corresponds to a score of 0. The interface of these implants was surrounded by an abundance of inflammatory cells and poorly organized tissue, which corresponds to an interface score of 0.

Bone formation was mostly observed on the defect margin and on the outer surface of the implant (Fig. V-8A and V-8C) as confirmed with Von Kossa/Van Gieson staining, which stains mineralized tissue black. However, several samples also had bone formation in the pores of the scaffold (Fig. V-8H) and towards the middle of the defect. As observed by microCT, histological analysis also showed that the newly formed bone was mostly on the dural side of the defect (Fig. V-8A and V-8C). Minimal osteoid formation was observed in some samples as indicated by the dark red staining of the matrix by Goldner's Trichrome staining (shown in Supplementary Data). The osteoid matrix was observed mostly at the edge of the newly formed bone or the defect margin (i.e., host bone) and usually next to a line of osteoblasts arranged linearly along the developing bone.
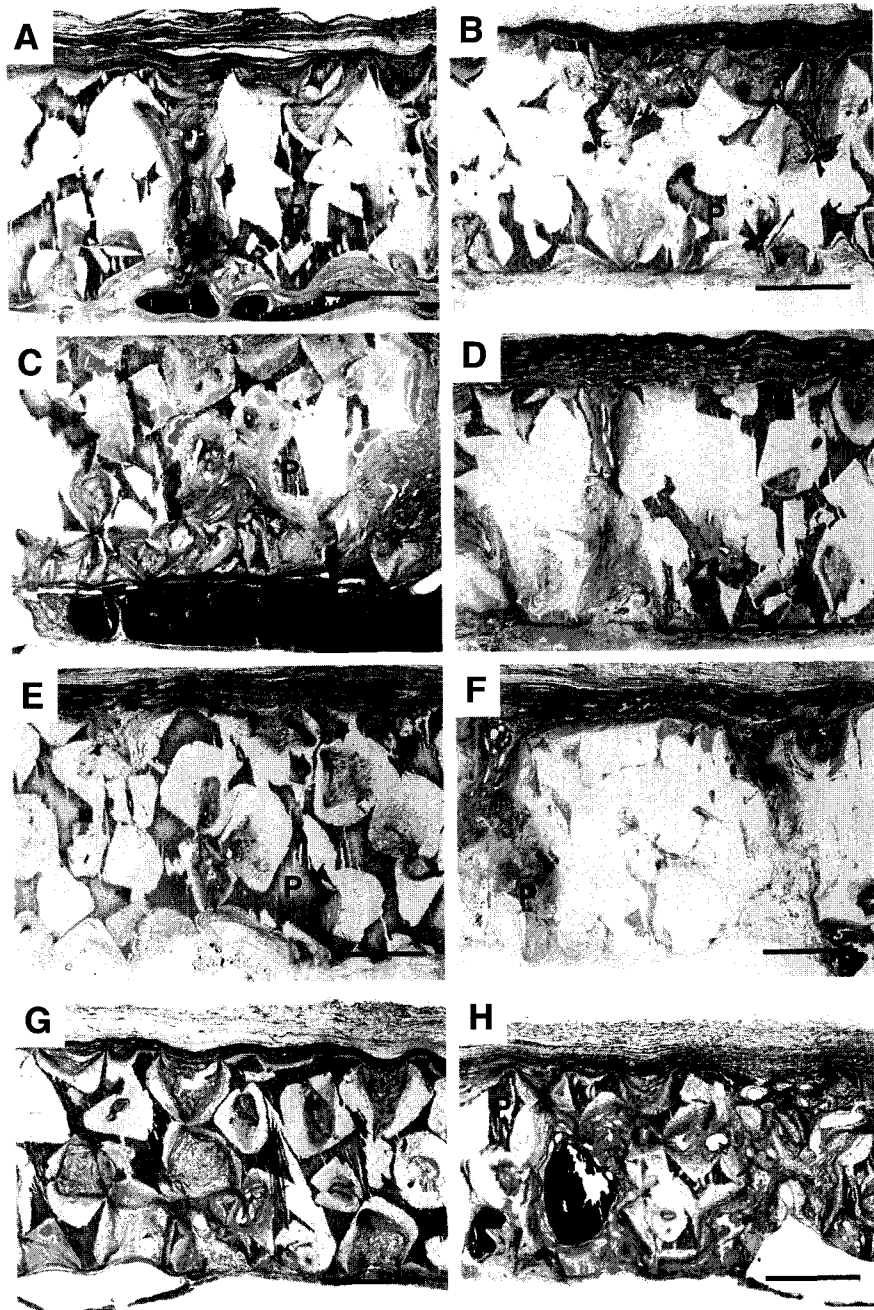
Figure V-8 Representative histological sections of samples stained with Von Kossa/Van Gieson at 12 weeks (A) Group Blank_10, (B) Group Blank_40, (C) Group Free_10, (D) Group Free_40, (E) Group P-AEPZ_10, (F) Group P-AEPZ_40, (G) Group P-DED_10 and (H) Group P-DED_40. P: PPF scaffold; B: new bone. Bar represents 500 μm.

Discussion

Porous PPF scaffolds have been used previously in our laboratory with GMPs to deliver BMP-2 in a controlled and sustained manner in a critical-size rat cranial defect[18,138]. In this work, we investigated the application of these composite scaffolds to deliver pDNA encoding BMP-2 complexed with biodegradable branched polycationic polymers, which we have previously characterized extensively[108], and evaluated their ability to enhance bone formation *in vivo* compared to the delivery of naked pDNA from these composite scaffolds.

In Vitro Plasmid DNA Release Kinetics

In the first part of this work, the release kinetics of pDNA from the composite scaffolds were evaluated *in vitro*. In the first 24 h (Phase 1), there was a large burst release of pDNA from composite scaffolds that did not contain a TAPP (i.e., Groups Free_10 and Free_40, 92.6 ± 1.1% and 88.9 ± 2.5% per day, respectively). The GMPs used in this study were synthesized from acidic gelatin and thus were negatively charged at physiological pH. Naked pDNA, which is also negatively charged due to the phosphate backbone, is not able to interact electrostatically with these GMPs, which results in inefficient loading of the GMPs with pDNA. Groups containing a TAPP (i.e., P-AEPZ_10, P-AEPZ_40, P-DED_10 and P-DED_40) only had a slight burst release in Phase 1, which could have resulted from the initial release of polyplexes not bound to the GMPs (10.7 to 14.7% per day). This initial burst release of unbounded drug in the first 24 h has also been observed when growth factors were delivered from a similar composite scaffold[138,139]. The TAPP/pDNA polyplexes (300:1 weight ratio) have a net positive

charge[108], thus, are able to interact electrostatically with the negatively charged acidic GMPs. This results in a potentially stronger binding and more efficient loading of the pDNA to the GMPs.

Following the initial burst release in Phase 1, the mechanism for the release of growth factors from these composite scaffolds is usually dominated by the enzymatic degradation of the GMPs [138,139]. Although release of the drug from the GMPs by diffusion or dissociation through a change in environment (such as a change in ionic concentration) can occur, enzymatic degradation of the GMPs is the more likely mechanism for the drug release[154]. If the pDNA release mechanism from GMPs was the same as that observed previously with growth factors, the pDNA release would also be dominated by the degradation of the GMPs. In this study, we found that the GMP crosslinking density (which influences the degradation kinetics of the GMPs) did not affect the release profiles of the pDNA and that the pDNA release depended on the known degradation rates of the TAPPs instead. Thus, beyond the initial release of polyplexes not bound to the GMPs in Phase 1 and the minimal release of intact polyplexes through diffusion or dissociation, the remaining pDNA in polyplexes that were bounded to the GMPs were likely released from the composite scaffolds as naked pDNA or in polyplexes with a lower amount of polymer (i.e., lower polymer/pDNA weight ratio), as fragments of the polymer had to degrade to dislodge and release the pDNA from the GMPs.

A previous *in vitro* degradation study in our laboratory has shown that ~80% of the esters in P-AEPZ and P-DED degrade after 3 days and 14 days at pH 7.4, respectively[108]. The actual amount of ester in the TAPPs that has to be degraded to lead

to release of the pDNA in the polyplexes is unknown. Nonetheless, it is hypothesized that the higher degradation rate of P-AEPZ compared to P-DED will cause polyplexes formed with P-AEPZ to have a higher pDNA release rate compared to those formed with P-DED. In Phase 2, the significantly higher pDNA release rate for Groups P-AEPZ_10 and P-AEPZ_40 compared to the other groups indicates that in 1 to 3 d, enough ester groups in P-AEPZ had degraded to result in a burst release of pDNA (31 to 32% per day). As suggested from the ester degradation rate of P-AEPZ (80% ester degraded after 3 d), a high amount of esters in P-AEPZ may be degraded during this phase, as well as in the following phases (i.e., Phase 3 and 4). Thus, the pDNA released from Groups P-AEPZ_10 and P-AEPZ_40 beyond Phase 1 were more likely naked pDNA or polyplexes with a lower amount of polymer (i.e, lower polymer/pDNA weight ratio).

Compared to P-AEPZ, P-DED, which has a significantly lower degradation rate (80% ester degraded after 14 d), should have a lower amount of esters that are degraded in Phase 2 and should not have reached the amount necessary to dislodge or release the pDNA from the polyplexes that are bound to the GMPs. Thus, unlike groups containing P-AEPZ (which released 31 to 32% per day), the significantly lower amount of pDNA released in Phase 2 by groups containing P-DED (9 to 10% pDNA per day) should mostly be in the polyplex form, which could have been released through diffusion or dissociation of polyplexes that have less stable electrostatic interactions with the GMPs. However, at the later phases (i.e., Phase 3 and 4), the release of pDNA from composite scaffolds containing P-DED were more likely released as naked pDNA or pDNA with less fragments of polymer, as P-DED would have degraded enough to dislodge or release the encapsulated pDNA at these later time points. At the end of the study, almost the

entire loaded dose of pDNA (93 to 98%) from Groups Free_10, Free_40, P-AEPZ_10 and P-AEPZ_40 had been released, which was significantly higher than the amount of pDNA release from Groups P-DED_10 and P-DED_40 (74-82%). Thus, there was likely more pDNA (18 to 26%, approximately 1/4 to 1/5 of the total loaded pDNA) remaining in the composite scaffolds from these groups that could potentially be released beyond the 30 day endpoint of the present study. Although the study design did not allow for the differentiation between pDNA of different extents of complexation (i.e., fully complexed, partially complexed and uncomplexed pDNA), the release data (free DNA detected after the 14 day incubation) coupled with the known TAPP degradation kinetics indicate that the pDNA release was dependent upon the TAPP degradation. The slower degradation rate of P-DED was able prevent the release of a large amount of pDNA too early during the delivery process and may also have been able to prolong the condensation and protection of the pDNA in the polyplexes. This is beneficial for the delivery of pDNA encoding BMP-2, as a later expression of BMP-2 is usually observed for osteoprogenitor cell differentiation *in vitro*[155] and bone formation *in vivo*[156].

As opposed to the release of growth factors from GMPs[18,138,139,142], the enzymatic degradation rates of the GMPs did not significantly affect the pDNA release kinetics, although different GMPs degradation rates were observed. The TAPPs were degrading and releasing the pDNA faster than the GMPs were degrading and releasing the whole polyplexes. In this work, after 30 days, all the 10 mM GMP particles were degraded for the samples containing naked pDNA and polyplexes formed with P-AEPZ; however, they were not fully degraded for samples containing polyplexes formed with P-DED. The slower degradation rate of 10 mM GMPs in this study compared to the previous study

where they were completely degraded within 9 days[142] suggests that the polyplexes may be shielding the GMPs from enzymatic degradation. The polyplexes formed with P-DED (i.e., TAPP with a lower degradation rate), which can stay attached to the GMPs for a longer time, were able to better shield the GMPs from degradation compared to polyplexes formed with P-AEPZ (i.e., TAPP with a higher degradation rate) and free pDNA. Although the release kinetics *in vivo* may differ from the results obtained *in vitro*, the *in vitro* analysis provides a predictive model and contextual data for the interpretation of the results from the *in vivo* bone formation study.

In Vivo Bone Formation

In the second part of this work, the ability of pDNA encoding BMP-2 complexed with a TAPP and delivered from a composite scaffold consisting of GMPs and a porous PPF scaffold to induce bone formation in a critical-size rat cranial defect was evaluated. We hypothesized that the delivery of pDNA complexed and condensed with a biodegradable polycationic polymer instead of in the free form (i.e., naked pDNA) would result in higher pDNA transfection and BMP-2 protein expression, which would be reflected by greater bone formation. However, the results from this study indicated that the addition of the biodegradable TAPP component to the delivery system did not improve the ability of the composite scaffolds to induce bone formation, even compared to composite scaffolds that did not contain pDNA (i.e., Groups Blank_10 and Blank_40) (Fig. V-3 and V-4). The reason for this observation is unclear as several factors are involved during the pDNA delivery as well as wound healing processes. We hypothesized that, even though a polycationic polymer vector component was

incorporated into the delivery system, the low amount of bone formation observed could have resulted from the unsuccessful delivery of most of the loaded pDNA in an intact polyplex form. As suggested from the results in the *in vitro* release kinetics study, excluding the initial burst release of unbound polyplexes and the minimal release of polyplexes through diffusion or dissociation from the GMPs, the pDNA released from these composite scaffolds was primarily naked pDNA or in polyplexes with a lower amount of polymer (i.e, lower polymer/pDNA weight ratio) which could have resulted from the degradation of the TAPPs. The release of the pDNA in the free or partially complexed form at the defect site results in a decrease in transfection efficiency[77,107,108] and increases the possibility of pDNA degradation by enzymes, nucleases[157-159] and the low pH (~4)[15] in the wound healing environment. Even though the pDNA released from the composite scaffolds may have resulted in some BMP-2 protein production, the composite scaffolds in this study may have not delivered enough complexed and undegraded pDNA to allow for a sufficient amount and duration of protein expression to induce bone formation[25,44].

It is promising to see that some of the samples had bone growth even towards the middle and not just on the periphery of the defect. As seen by others in the literature who delivered BMP in the protein[18] or gene[77,106] form in a critical-size rat cranial defect, the bone that formed was mostly on the dural side of the cranium instead of on the periosteal side. The sagittal sinus of the rat runs in the center of the defect, under the dura mater, and could be a source of progenitor cells to the defect area[106] which could have resulted in the higher amount of bone observed on the dural side. Histological evaluation demonstrated that a majority of the implants were surrounded by a thin layer of fibrous

tissue on the periosteal side and at the defect border between the implant and host bone. Some implants were also surrounded by a thin layer of fibrous tissue on the dural side.

Compared to the other groups, Groups P-AEPZ_10 and P-AEPZ_40 had implants that were surrounded with less fibrous tissue on the dural side and had less tissue ingrowth in the pores of the implants (Fig. V-8E and V-8F, respectively) which was reflected in the hard tissue response score distribution (Fig. V-7B). The lower scores for hard tissue response for Groups P-AEPZ_10 and P-AEPZ_40 are consistent with the significantly lower percent bone formation (volume and area, Fig. V-3A and V-3B, respectively) and bone union score (Fig. V-4A) observed with microCT compared to some of the other groups.

In general, among the samples that had a pore tissue score of 2 and 3, implants from Groups P-DED_10 and P-DED_40 had comparably more tissue ingrowth where almost all the pores were filled with fibrous tissue (Fig. V-8G and V-8H, respectively). The higher amount of tissue ingrowth observed in Groups P-DED_10 and P-DED_40 suggests that these groups may have enhanced the production of BMP-2, which has the capability of initiating the recruitment of cells to the defect site. As seen in the *in vitro* release study, groups containing P-DED (i.e. Groups P-DED_10 and P-DED_40) were able to prolong the release of pDNA and may also have delivered more of the pDNA in the intact polyplex form due to the slower degradation rate of P-DED; however the effect of polyplex release kinetics on bone formation remains unknown.

Conclusions

In this work, pDNA complexed with biodegradable branched polymers were delivered from a composite containing acidic GMPs and a porous PPF scaffold. The *in vitro* results showed that the degradation rate of the polycationic polymers can control the pDNA release kinetics. The *in vivo* results showed that the premature degradation of polycationic polymers may trigger the release of naked pDNA with minimal effect on bone formation in a critical-size rat cranial defect. The collective results showed that the degradation rate of different polymers in a pDNA carrier would affect not only its delivery but most importantly its transfection capability and therapeutic effect *in vivo*.

Supplementary Data
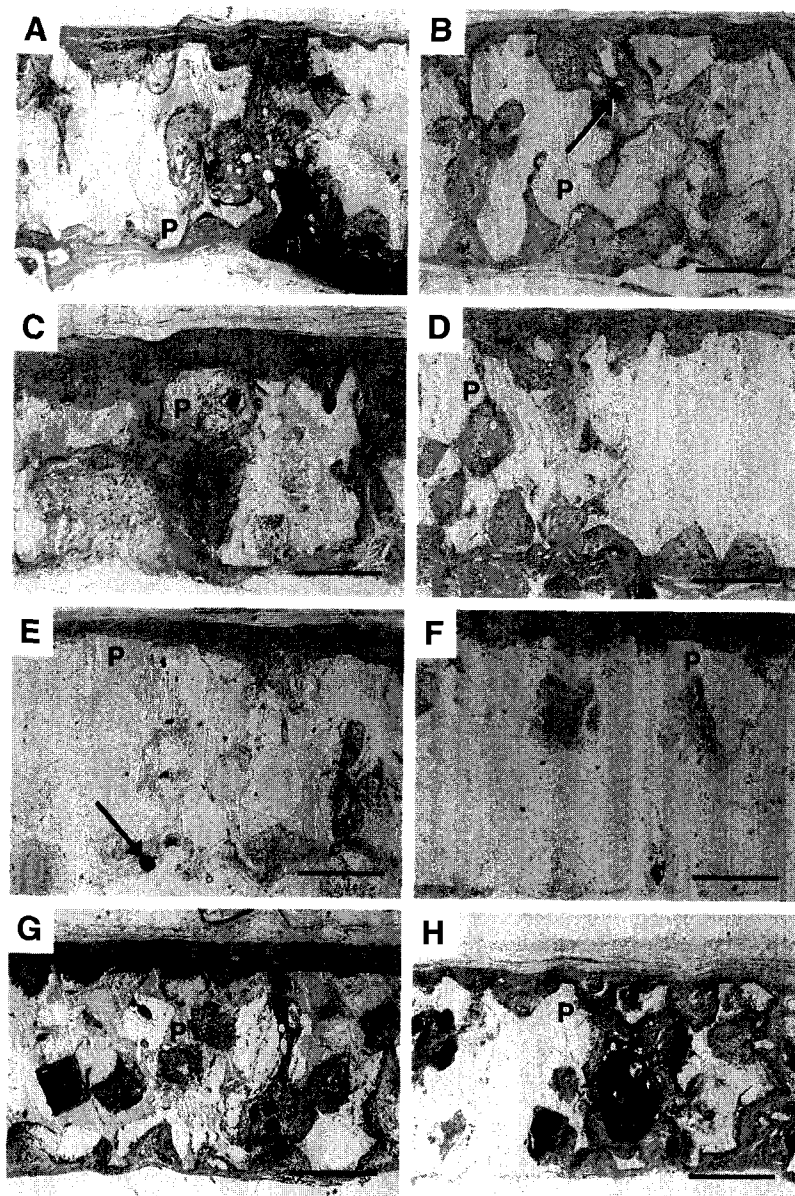
Supplementary Figure V-1 Representative histological sections of samples stained with H&E at 12 weeks. (A) Group Blank_10, (B) Group Blank_40, (C) Group Free_10, (D) Group Free_40, (E) Group P-AEPZ_10, (F) Group P-AEPZ_40, (G) Group P-DED_10 and (H) Group P-DED_40. P: PPF scaffold; B: new bone; Black arrows: GMP. Bar represents 500 μm.
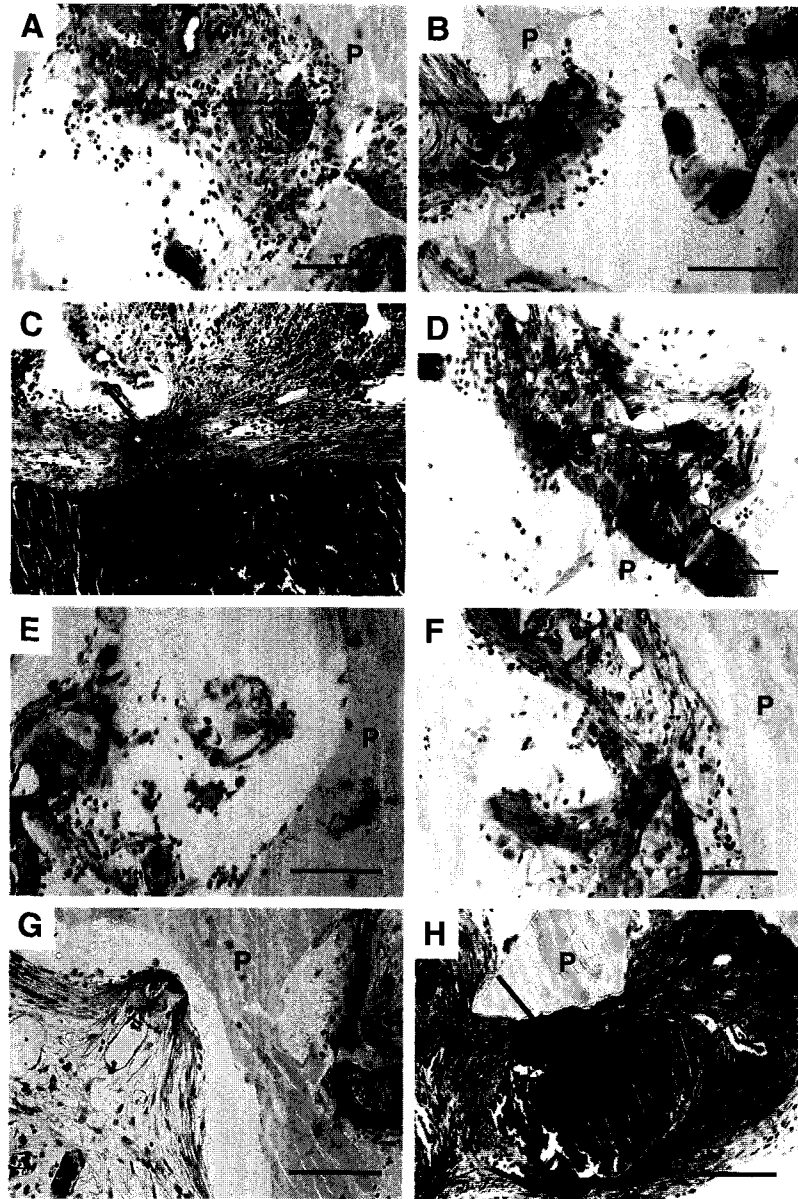
Supplementary Figure V-2 Representative histological sections of samples stained with Goldner's Trichrome at 12 weeks. (A) Group Blank_10, (B) Group Blank_40, (C) Group Free_10, (D) Group Free_40, (E) Group P-AEPZ_10, (F) Group P-AEPZ_40, (G) Group P-DED_10 and (H) Group P-DED_40. P: PPF scaffold; B: new bone; Black arrows: osteoid. Bar represents 100 μm.

CHAPTER VI

OVERALL CONCLUSIONS

In this work, biodegradable branched polycationic polymers were synthesized from different amine and triacrylate monomers by Michael addition polymerization to evaluate the effects of altering certain polymer properties on characteristics which are important for gene delivery. These biodegradable polycationic polymers were then incorporated into a composite scaffold carrier to evaluate these vectors in a bone tissue engineering system.

In the first specific aim, the effects of the hydrophilic spacer lengths in the polymer on characteristics which are important for gene delivery were investigated by varying the triacrylate monomer used in the synthesis. We found that the incorporation of hydrophilic spacers resulted in high cell viability upon exposure to the polymer and increased the ester degradation rate of the polymer. This study demonstrated that hydrophilic spacers could be incorporated into polycationic polymers to reduce their cytotoxicity and enhance their degradability, which may facilitate the continued development of polymeric non-viral gene delivery vectors.

In the second specific aim, the effects of the amine basicities in the polymer on characteristics which are important for gene delivery were investigated by varying the amine monomers used in the synthesis. We found that amines that dissociated above pH 7.4 and were available for pDNA complexation, were a key parameter for effective pDNA condensation and transfection. This study indicated that one would need to investigate the amount of amines that dissociate in specific pH ranges relevant for

autocatalytic degradation, pDNA complexation and endosomal escape instead of only examining the total amount of amine in the polymer.

In the third and last specific aim, the TAPP/pDNA polyplexes were incorporated into a composite containing GMPs and a porous PPF scaffold to develop a bone tissue engineering system with the ability to control the release of pDNA and enhance bone formation *in vivo*. We found that the pDNA release kinetics *in vitro* were not affected by the crosslinking density of the GMPs (which influences the degradation kinetics of the GMPs) but depended, instead, on the degradation rates of the TAPPs. Besides the initial loss of polyplexes not bound to the GMPs and the minimal release of polyplexes through diffusion or dissociation from the GMPs, the pDNA was likely released as naked pDNA or as part of an incomplete polyplex, following the degradation of fragments of the polycationic polymer. Furthermore, we found that composite scaffolds containing TAPP/pDNA polyplexes did not result in enhanced bone formation compared to those containing naked pDNA. The results suggested that the degradation rate of different polymers would affect not only pDNA delivery but most importantly its transfection capability and therapeutic effect *in vivo*.

The biodegradable TAPPs evaluated in this work are promising candidates for non-viral gene delivery and the findings of this work can be used for the design of non-viral vectors with tailored structural and degradative characteristics as needed for specific applications. This work demonstrated that the premature degradation of the polycationic polymers may lead to the early release of naked pDNA with minimal effect on bone formation in a defect site. Thus, a gene delivery system consisting of biodegradable polycationic polymers should be designed to release the pDNA in an intact polyplex form.

In designing a successful gene therapy system for bone tissue engineering, the gene delivery vector and the carrier for the polyplexes (i.e., scaffold or composite scaffold) are both important factors to take into consideration, and they have to be suitable for one another. To ensure that the polyplexes formed with the biodegradable polycationic polymers are released in an intact form, a composite which is able to protect the polycationic polymer from degradation before the pDNA is released should be considered.

The polymers synthesized in this work have relatively low molecular weight (1 to 3 kDa) and thus degrade faster compared to higher molecular weight polymers. Polyplexes formed with these low molecular weight polymers may be able to stay intact during the *in vitro* transfection process where the cells were directly exposed to the polyplexes. However, for *in vitro* or *in vivo* gene therapy approaches where the polyplexes are first released from a scaffold, the polyplexes may take a longer time to reach the cells. Thus, a slower degrading polymer may be needed for these gene therapy systems to ensure that the polyplexes stay intact during the delivery process.

CHAPTER VII

LIST OF REFERENCES

1. LeGeros, R. Z., Properties of osteoconductive biomaterials: calcium phosphates. *Clin Orthop Relat Res* **2002**, (395), 81-98.

2. Wise, D. L.; Trantolo, D. J.; Altobelli, D. E.; Yaszemski, M. J., *Encyclopedic Handbook of Biomaterials and Bioengineering*. Marcel Dekker, Inc: New York, 1995.

3. Jee, W. S. S., Cell and tissue biology, a textbook of histology. In Weiss, L., Ed. Urban and Schwarzenberg: Baltimore, 1988.

4. Jee, W. S. S., Orthopaedics, principles of basic and clinical science. In Worrell, R., Ed. CRC Press: Boca Raton, 1999.

5. Frost, H. M., *Introduction to a new skeletal physiology*. Pajaro Group: Pueblo, 1995.

6. Li, X. J.; Jee, W. S. S., Integrated Bone Tissue Anatomy and Physiology. In *Current Topics in Bone Biology*, Chen, D., Ed. World Scientific Publishing Co. Pte. Ltd.: 2005; pp 11-56.

7. Caterson, E. J.; Tuan, R. S.; Bruder, S. P., Cell-Based Approaches to Orthopedic Tissue Engineering. In *Orthopedic Tissue Enginnering*, Caplan, A. I., Ed. Marcel Dekkar, Inc.: 2004; pp 21-50.

8. Cheng, H.; Jiang, W.; Phillips, F. M.; Haydon, R. C.; Peng, Y.; Zhou, L.; Luu, H. H.; An, N.; Breyer, B.; Vanichakarn, P.; Szatkowski, J. P.; Park, J. Y.; He, T. C., Osteogenic activity of the fourteen types of human bone morphogenetic proteins (BMPs). *J Bone Joint Surg Am* **2003**, 85-A, (8), 1544-1552.

9. Kobayashi, T.; Kronenberg, H., Minireview: transcriptional regulation in development of bone. *Endocrinology* **2005**, 146, (3), 1012-1017.

10. Doll, B., Developmental Biology of the Skeletal System. In *Bone Tissue Engineering*, Hollinger, J. O.; Einhorn, T. A.; Doll, B. A.; Sfeir, C., Eds. CRC Press: Boca Raton, 2005; pp 3-20.

11. Wuster, C.; Heilmann, P.; Pereira-Lima, J.; Schlegel, J.; Anstatt, K.; Soballa, T., Quantitative ultrasonometry (QUS) for the evaluation of osteoporosis risk: reference data for various measurement sites, limitations and application possibilities. *Exp Clin Endocrinol Diabetes* **1998**, 106, (4), 277-288.

12. Seeman, E.; Hopper, J. L.; Bach, L. A.; Cooper, M. E.; Parkinson, E.; McKay, J.; Jerums, G., Reduced bone mass in daughters of women with osteoporosis. *N Engl J Med* **1989,** 320, (9), 554-558.

13. Dequeker, J.; Nijs, J.; Verstraeten, A.; Geusens, P.; Gevers, G., Genetic determinants of bone mineral content at the spine and radius: a twin study. *Bone* **1987,** 8, (4), 207-209.

14. Eysel, P.; Schwitalle, M.; Oberstein, A.; Rompe, J. D.; Hopf, C.; Kullmer, K., Preoperative estimation of screw fixation strength in vertebral bodies. *Spine* **1998,** 23, (2), 174-180.

15. Park, J. S.; Lakes, R. S., *Biomaterials: An Introduction.* 2nd ed.; Plenum Press: New York, 1992.

16. Bonadio, J., Tissue engineering via local gene delivery. *J Mol Med* **2000,** 78, (6), 303-311.

17. Wenig, B. M., *Atlas of Head and Neck Pathology.* Elsevier Health Sciences: Philadelphia, 1993.

18. Patel, Z. S.; Young, S.; Tabata, Y.; Jansen, J. A.; Wong, M. E.; Mikos, A. G., Dual delivery of an angiogenic and an osteogenic growth factor for bone regeneration in a critical size defect model. *Bone* **2008,** 43, (5), 931-940.

19. Kasper, F. K.; Mikos, A. G., Biomaterials and Gene Therapy. In *Molecular and Cellular Foundations of Biomaterials,* Sefton, M. V., Ed. Elsevier: San Diego, 2004; pp 131-168.

20. Nather, A., Biology of healing of large deep-frozen cortical bone allografts. In *Allografts in Bone Healing: Biology and Clinical Applications,* Philips, G. O., Ed. World Scientific Publishing C. Pte. Ltd: Singapore, 2003; Vol. 1, pp 47-67.

21. Cao, Y.; Ibarra, C.; Vacanti, C. A., Tissue engineering cartilage and bone. In *Synthetic Biodegradable Polymer Scaffolds,* Mooney, D. J., Ed. Birkhauser; Boston, 1997; pp 199-214.

22. Khan, S. N.; Lane, J. M., Bone Tissue Engineering: Basic Science and Clinical Concepts. In *Orthopedic Tissue Engineering,* Caplan, A. I., Ed. Marcel Dekker, Inc.: 2004; pp 161-178.

23. Kofron, M. D.; Laurencin, C. T., Bone tissue engineering by gene delivery. *Advanced Drug Delivery Reviews* **2006,** 58, 555-576.

24. Strong, D. M.; Friedlaender, G. E.; Tomford, W. W.; Springfield, D. S.; Shives, T. C.; Burchardt, H.; Enneking, W. F.; Mankin, H. J., Immunologic responses in human recipients of osseous and osteochondral allografts. *Clin Orthop Relat Res* **1996,** (326), 107-114.

25. Termaat, M. F.; Den Boer, F. C.; Bakker, F. C.; Patka, P.; Haarman, H. J., Bone morphogenetic proteins. Development and clinical efficacy in the treatment of fractures and bone defects. *J Bone Joint Surg Am* **2005**, 87, (6), 1367-1378.

26. Boyan, B. D.; Lohmann, C. H.; Romero, J.; Schwartz, Z., Bone and cartilage tissue engineering. *Clin Plast Surg* **1999**, 26, (4), 629-645, ix.

27. Southwood, L. L.; Frisbie, D. D.; Kawcak, C. E.; Ghivizzani, S. C.; Evans, C. H.; McIlwraith, C. W., Evaluation of Ad-BMP-2 for enhancing fracture healing in an infected defect fracture rabbit model. *J Orthop Res* **2004**, 22, (1), 66-72.

28. Chamberlain, J. R.; Schwarze, U.; Wang, P. R.; Hirata, R. K.; Hankenson, K. D.; Pace, J. M.; Underwood, R. A.; Song, K. M.; Sussman, M.; Byers, P. H.; Russell, D. W., Gene targeting in stem cells from individuals with osteogenesis imperfecta. *Science* **2004**, 303, (5661), 1198-1201.

29. Egermann, M.; Schneider, E.; Evans, C. H.; Baltzer, A. W., The potential of gene therapy for fracture healing in osteoporosis. *Osteoporos Int* **2005**, 16 Suppl 2, S120-128.

30. Makin, M., Osteogenesis Induced by Vesical Mucosal Transplant in the Guinea-Pig. *Journal of Bone and Joint Surgery-British Volume* **1962**, 44, (1), 165-193.

31. McKay, I.; Brown, K. D., *Growth Factors and Receptor: A Practical Approach*. Oxford University Press: New York, 1998.

32. Sfeir, C.; Jadlowiec, J.; Koch, H.; Campbell, P., Signaling Molecules for Tissue Engineering. In *Bone Tissue Engineering*, Hollinger, J. O.; Einhorn, T. A.; Doll, B. A.; Sfeir, C., Eds. CRC Press: Boca Raton, 2005.

33. Friedlaender, G. E.; Perry, C. R.; Cole, J. D.; Cook, S. D.; Cierny, G.; Muschler, G. F.; Zych, G. A.; Calhoun, J. H.; LaForte, A. J.; Yin, S., Osteogenic protein-1 (bone morphogenetic protein-7) in the treatment of tibial nonunions. *J Bone Joint Surg Am* **2001**, 83-A Suppl 1, (Pt 2), S151-158.

34. Southwood, L. L.; Frisbie, D. D.; Kawcak, C. E.; McIlwraith, C. W., Delivery of growth factors using gene therapy to enhance bone healing. *Vet Surg* **2004**, 33, (6), 565-578.

35. Rhee, J. M.; Boden, S. D., Opportunities in Spinal Applications. In *Bone Tissue Engineering*, Hollinger, J. O.; Einhorn, T. A.; Doll, B. A.; Sfeir, C., Eds. CRC Press: Boca Raton, 2005.

36. Winn, S. R.; Uludag, H.; Hollinger, J. O., Carrier systems for bone morphogenetic proteins. *Clin Orthop Relat Res* **1999**, (367 Suppl), S95-106.

37. Deckers, M. M.; van Bezooijen, R. L.; van der Horst, G.; Hoogendam, J.; van Der Bent, C.; Papapoulos, S. E.; Lowik, C. W., Bone morphogenetic proteins stimulate

angiogenesis through osteoblast-derived vascular endothelial growth factor A. *Endocrinology* **2002,** 143, (4), 1545-1553.

38.	Akino, K.; Mineta, T.; Fukui, M.; Fujii, T.; Akita, S., Bone morphogenetic protein-2 regulates proliferation of human mesenchymal stem cells. *Wound Repair Regen* **2003,** 11, (5), 354-360.

39.	Akino, K.; Mineta, T.; Fukui, M.; Akita, S., P-II-04 early phase regulation of human mesenchymal stem cells and the unique profile of the proliferation by bone morphogenetic protein-2. *Wound Repair Regen* **2004,** 12, A6.

40.	Reddi, A. H., Bone morphogenetic proteins, bone marrow stromal cells, and mesenchymal stem cells. Maureen Owen revisited. *Clin Orthop Relat Res* **1995,** (313), 115-119.

41.	Sakou, T., Bone morphogenetic proteins: from basic studies to clinical approaches. *Bone* **1998,** 22, (6), 591-603.

42.	Schmitt, J. M.; Hwang, K.; Winn, S. R.; Hollinger, J. O., Bone morphogenetic proteins: an update on basic biology and clinical relevance. *J Orthop Res* **1999,** 17, (2), 269-278.

43.	Sarras, M. P., Jr., BMP-1 and the astacin family of metalloproteinases: a potential link between the extracellular matrix, growth factors and pattern formation. *Bioessays* **1996,** 18, (6), 439-442.

44.	Shea, L. D.; Smiley, E.; Bonadio, J.; Mooney, D. J., DNA delivery from polymer matrices for tissue engineering. *Nat Biotechnol* **1999,** 17, (6), 551-554.

45.	Cartier, R.; Reszka, R., Utilization of synthetic peptides containing nuclear localization signals for nonviral gene transfer systems. *Gene Ther* **2002,** 9, (3), 157-167.

46.	Hosseinkhani, H.; Azzam, T.; Kobayashi, H.; Hiraoka, Y.; Shimokawa, H.; Domb, A. J.; Tabata, Y., Combination of 3D tissue engineered scaffold and non-viral gene carrier enhance in vitro DNA expression of mesenchymal stem cells. *Biomaterials* **2006,** 27, (23), 4269-4278.

47.	Niyibizi, C.; Baltzer, A.; Lattermann, C.; Oyama, M.; Whalen, J. D.; Robbins, P. D.; Evans, C. H., Potential role for gene therapy in the enhancement of fracture healing. *Clin Orthop Relat Res* **1998,** (355 Suppl), S148-153.

48.	Chen, Y., Orthopedic applications of gene therapy. *J Orthop Sci* **2001,** 6, (2), 199-207.

49.	Lieberman, J. R.; Le, L. Q.; Stevenson, S., In vivo bone induction via retroviral gene transfer of BMP-2 into a stromal cell line. *Trans Orthop Res Soc* **1997,** 43, 223.

50.	Gazit, D.; Turgeman, G.; Kelley, P.; Wang, E.; Jalenak, M.; Zilberman, Y.; Moutsatsos, I., Engineered pluripotent mesenchymal cells integrate and differentiate in regenerating bone: a novel cell-mediated gene therapy. *J Gene Med* **1999,** 1, (2), 121-133.

51.	Baltzer, A. W.; Lattermann, C.; Whalen, J. D.; Braunstein, S.; Robbins, P. D.; Evans, C. H., A gene therapy approach to accelerating bone healing. Evaluation of gene expression in a New Zealand white rabbit model. *Knee Surg Sports Traumatol Arthrosc* **1999,** 7, (3), 197-202.

52.	Benns, J. M.; Kim, S. W., Tailoring new gene delivery designs for specific targets. *J Drug Target* **2000,** 8, (1), 1-12.

53.	Azzam, T.; Domb, A. J., Current developments in gene transfection agents. *Curr Drug Deliv* **2004,** 1, (2), 165-193.

54.	Anwer, K.; Rhee, B. G.; Mendiratta, S. K., Recent progress in polymeric gene delivery systems. *Crit Rev Ther Drug Carrier Syst* **2003,** 20, (4), 249-293.

55.	De Smedt, S. C.; Demeester, J.; Hennink, W. E., Cationic polymer based gene delivery systems. *Pharmaceutical Research* **2000,** 17, (2), 113-126.

56.	Lemarchand, P.; Jaffe, H. A.; Danel, C.; Cid, M. C.; Kleinman, H. K.; Stratford-Perricaudet, L. D.; Perricaudet, M.; Pavirani, A.; Lecocq, J. P.; Crystal, R. G., Adenovirus-mediated transfer of a recombinant human alpha 1-antitrypsin cDNA to human endothelial cells. *Proc Natl Acad Sci U S A* **1992,** 89, (14), 6482-6486.

57.	Ogris, M.; Steinlein, P.; Kursa, M.; Mechtler, K.; Kircheis, R.; Wagner, E., The size of DNA/transferrin-PEI complexes is an important factor for gene expression in cultured cells. *Gene Ther* **1998,** 5, (10), 1425-1433.

58.	Pouton, C. W.; Lucas, P.; Thomas, B. J.; Uduehi, A. N.; Milroy, D. A.; Moss, S. H., Polycation-DNA complexes for gene delivery: a comparison of the biopharmaceutical properties of cationic polypeptides and cationic lipids. *J Control Release* **1998,** 53, (1-3), 289-299.

59.	Brokx, R.; Gariepy, J., Peptide- and polymer-based gene delivery vehicles. *Methods Mol Med* **2004,** 90, 139-160.

60.	Jans, D. A.; Chan, C. K.; Huebner, S., Signals mediating nuclear targeting and their regulation: application in drug delivery. *Med Res Rev* **1998,** 18, (4), 189-223.

61.	Tseng, W. C.; Haselton, F. R.; Giorgio, T. D., Mitosis enhances transgene expression of plasmid delivered by cationic liposomes. *Biochim Biophys Acta* **1999,** 1445, (1), 53-64.

62.	Puzas, J. E.; O'Keefe, R. J.; Lieberman, J. R., The orthopaedic genome: what does the future hold and are we ready? *J Bone Joint Surg Am* **2002,** 84-A, (1), 133-141.

63. Hannallah, D.; Peterson, B.; Lieberman, J. R.; Fu, F. H.; Huard, J., Gene therapy in orthopaedic surgery. *Instr Course Lect* **2003**, 52, 753-768.

64. Anderson, W. F., Human gene therapy. *Nature* **1998**, 392, 25-30.

65. Challita, P. M.; Kohn, D. B., Lack of expression from a retroviral vector after transduction of murine hematopoietic stem cells is associated with methylation in vivo. *Proc Natl Acad Sci U S A* **1994**, 91, (7), 2567-2571.

66. Peel, A. L.; Zolotukhin, S.; Schrimsher, G. W.; Muzyczka, N.; Reier, P. J., Efficient transduction of green fluorescent protein in spinal cord neurons using adeno-associated virus vectors containing cell type-specific promoters. *Gene Ther* **1997**, 4, (1), 16-24.

67. Reschel, T.; Konak, C.; Oupicky, D.; Seymour, L. W.; Ulbrich, K., Physical properties and in vitro transfection efficiency of gene delivery vectors based on complexes of DNA with synthetic polycations. *J Control Release* **2002**, 81, (1-2), 201-217.

68. Kichler, A., Gene transfer with modified polyethylenimines. *J Gene Med* **2004**, 6 Suppl 1, S3-10.

69. Byk, G.; Dubertret, C.; Escriou, V.; Frederic, M.; Jaslin, G.; Rangara, R.; Pitard, B.; Crouzet, J.; Wils, P.; Schwartz, B.; Scherman, D., Synthesis, activity, and structure--activity relationship studies of novel cationic lipids for DNA transfer. *J Med Chem* **1998**, 41, (2), 229-235.

70. Felgner, J. H.; Kumar, R.; Sridhar, C. N.; Wheeler, C. J.; Tsai, Y. J.; Border, R.; Ramsey, P.; Martin, M.; Felgner, P. L., Enhanced gene delivery and mechanism studies with a novel series of cationic lipid formulations. *J Biol Chem* **1994**, 269, (4), 2550-2561.

71. Radler, J. O.; Koltover, I.; Salditt, T.; Safinya, C. R., Structure of DNA-cationic liposome complexes: DNA intercalation in multilamellar membranes in distinct interhelical packing regimes. *Science* **1997**, 275, (5301), 810-814.

72. Mumper, R. J.; Duguid, J. G.; Anwer, K.; Barron, M. K.; Nitta, H.; Rolland, A. P., Polyvinyl derivatives as novel interactive polymers for controlled gene delivery to muscle. *Pharm Res* **1996**, 13, (5), 701-709.

73. Holtorf, H. L.; Mikos, A. G., Cationic and Non-Condensing Polymer-Based Gene Delivery. In *Pharmaceutical Perspectives of Nucleic Acid-Based Therapeutics*, S.W., K., Ed. Taylor & Francis: 2002; Vol. New York, pp 367-387.

74. Vijayanathan, V.; Thomas, T.; Thomas, T. J., DNA nanoparticles and development of DNA delivery vehicles for gene therapy. *Biochemistry* **2002**, 41, (48), 14085-14094.

75.   Tanahashi, K.; Jo, S.; Mikos, A. G., Synthesis and characterization of biodegradable cationic poly(propylene fumarate-co-ethylene glycol) copolymer hydrogels modified with agmatine for enhanced cell adhesion. *Biomacromolecules* **2002**, 3, (5), 1030-1037.

76.   Bonadio, J.; Smiley, E.; Patil, P.; Goldstein, S., Localized, direct plasmid gene delivery in vivo: prolonged therapy results in reproducible tissue regeneration. *Nat Med* **1999**, 5, (7), 753-759.

77.   Huang, Y. C.; Simmons, C.; Kaigler, D.; Rice, K. G.; Mooney, D. J., Bone regeneration in a rat cranial defect with delivery of PEI-condensed plasmid DNA encoding for bone morphogenetic protein-4 (BMP-4). *Gene Ther* **2005**, 12, (5), 418-426.

78.   Godbey, W. T.; Wu, K. K.; Mikos, A. G., Poly(ethylenimine) and its role in gene delivery. *J Control Release* **1999**, 60, (2-3), 149-160.

79.   Kloeckner, J.; Bruzzano, S.; Ogris, M.; Wagner, E., Gene carriers based on hexanediol diacrylate linked oligoethylenimine: effect of chemical structure of polymer on biological properties. *Bioconjug Chem* **2006**, 17, (5), 1339-1345.

80.   Godbey, W. T.; Wu, K. K.; Mikos, A. G., Tracking the intracellular path of poly(ethylenimine)/DNA complexes for gene delivery. *Proc Natl Acad Sci U S A* **1999**, 96, (9), 5177-5181.

81.   Luten, J.; van Nostrum, C. F.; De Smedt, S. C.; Hennink, W. E., Biodegradable polymers as non-viral carriers for plasmid DNA delivery. *J Control Release* **2008**, 126, (2), 97-110.

82.   Eldred, S. E.; Pancost, M. R.; Otte, K. M.; Rozema, D.; Stahl, S. S.; Gellman, S. H., Effects of side chain configuration and backbone spacing on the gene delivery properties of lysine-derived cationic polymers. *Bioconjug Chem* **2005**, 16, (3), 694-699.

83.   Choksakulnimitr, S.; Masuda, S.; Tokuda, H.; Takakura, Y.; Hashida, M., In-Vitro Cytotoxicity of Macromolecules in Different Cell-Culture Systems. *J Control Release* **1995**, 34, (3), 233-241.

84.   Breunig, M.; Lungwitz, U.; Liebl, R.; Goepferich, A., Breaking up the correlation between efficacy and toxicity for nonviral gene delivery. *Proc. Natl. Acad. Sci. U.S.A.* **2007**, 104, (36), 14454-14459.

85.   Wu, D. C.; Liu, Y.; Chen, L.; He, C. B.; Chung, T. S.; Goh, S. H., 2A(2)+BB ' B " approach to hyperbranched poly(amino ester)s. *Macromolecules* **2005**, 38, (13), 5519-5525.

86. Wu, D. C.; Liu, Y.; He, C. B.; Chung, T. S.; Goh, S. T., Effects of chemistries of trifunctional amines on mechanisms of Michael addition polymerizations with diacrylates. *Macromolecules* **2004**, 37, (18), 6763-6770.

87. Wu, D.; Liu, Y.; Jiang, X.; Chen, L.; He, C.; Goh, S. H.; Leong, K. W., Evaluation of hyperbranched poly(amino ester)s of amine constitutions similar to polyethylenimine for DNA delivery. *Biomacromolecules* **2005**, 6, (6), 3166-3173.

88. Lynn, D. M.; Anderson, D. G.; Putnam, D.; Langer, R., Accelerated discovery of synthetic transfection vectors: Parallel synthesis and screening of degradable polymer library. *J. Am. Chem. Soc.* **2001**, 123, (33), 8155-8156.

89. Lynn, D. M.; Langer, R., Degradable poly(beta-amino esters): Synthesis, characterization, and self-assembly with plasmid DNA. *J. Am. Chem. Soc.* **2000**, 122, (44), 10761-10768.

90. Kim, T.; Seo, H. J.; Baek, J.; Park, J. H.; Park, J. S., Synthesis of novel biodegradable quaternary amine-based cross-linked poly(beta-amino ester) and its self-assembly/disassembly with plasmid DNA. *Bull. Korean Chem. Soc.* **2005**, 26, (1), 175-177.

91. Kim, T. I.; Seo, H. J.; Choi, J. S.; Yoon, J. K.; Baek, J. U.; Kim, K.; Park, J. S., Synthesis of biodegradable cross-linked poly(beta-amino ester) for gene delivery and its modification, inducing enhanced transfection efficiency and stepwise degradation. *Bioconjug Chem* **2005**, 16, (5), 1140-1148.

92. Gosselin, M. A.; Guo, W.; Lee, R. J., Efficient gene transfer using reversibly cross-linked low molecular weight polyethylenimine. *Bioconjug Chem* **2001**, 12, (6), 989-994.

93. Yang, T. F.; Chin, W. K.; Cherng, J. Y.; Shau, M. D., Synthesis of novel biodegradable cationic polymer: N,N-diethylethylenediamine polyurethane as a gene carrier. *Biomacromolecules* **2004**, 5, (5), 1926-1932.

94. Tseng, S. J.; Tang, S. C.; Shau, M. D.; Zeng, Y. F.; Cherng, J. Y.; Shih, M. F., Structural characterization and buffering capacity in relation to the transfection efficiency of biodegradable polyurethane. *Bioconjug Chem* **2005**, 16, (6), 1375-1381.

95. Shau, M. D.; Tseng, S. J.; Yang, T. F.; Cherng, J. Y.; Chin, W. K., Effect of molecular weight on the transfection efficiency of novel polyurethane as a biodegradable gene vector. *J Biomed Mater Res A* **2006**, 77, (4), 736-746.

96. Ahn, C. H.; Chae, S. Y.; Bae, Y. H.; Kim, S. W., Biodegradable poly(ethylenimine) for plasmid DNA delivery. *J Control Release* **2002**, 80, (1-3), 273-282.

97. Fischer, D.; Bieber, T.; Li, Y.; Elsasser, H. P.; Kissel, T., A novel non-viral vector for DNA delivery based on low molecular weight, branched polyethylenimine: effect of molecular weight on transfection efficiency and cytotoxicity. *Pharm Res* **1999**, 16, (8), 1273-1279.

98. Hedley, M. L., Formulations containing poly(lactide-co-glycolide) and plasmid DNA expression vectors. *Expert Opin Biol Ther* **2003**, 3, (6), 903-910.

99. Walter, E.; Moelling, K.; Pavlovic, J.; Merkle, H. P., Microencapsulation of DNA using poly(DL-lactide-co-glycolide): stability issues and release characteristics. *J Control Release* **1999**, 61, (3), 361-374.

100. Wang, D.; Robinson, D. R.; Kwon, G. S.; Samuel, J., Encapsulation of plasmid DNA in biodegradable poly(D, L-lactic-co-glycolic acid) microspheres as a novel approach for immunogene delivery. *J Control Release* **1999**, 57, (1), 9-18.

101. Lim, Y. B.; Choi, Y. H.; Park, J. S., A self-destroying polycationic polymer: Biodegradable poly(4-hydroxy-L-proline ester). *J. Am. Chem. Soc* **1999**, 121, (24), 5633-5639.

102. Kircheis, R.; Wagner, E., Polycation/DNA complexes for in vivo gene delivery. *Gene Therapy and Regulation* **2000**, 1, (1), 95-114.

103. Lieberman, J. R., Gene Therapy to Enhance Bone and Cartilage Repair. In *Orthopedic Tissue Enginering*, Caplan, A. I., Ed. Marcel Dekker, Inc.: 2004; pp 305-322.

104. Franceschi, R. T., Biological approaches to bone regeneration by gene therapy. *J Dent Res* **2005**, 84, (12), 1093-1103.

105. Lim, S. H.; Liao, I. C.; Leong, K. W., Nonviral gene delivery from nonwoven fibrous scaffolds fabricated by interfacial complexation of polyelectrolytes. *Mol Ther* **2006**, 13, (6), 1163-1172.

106. Kasper, F. K.; Young, S.; Tanahashi, K.; Barry, M. A.; Tabata, Y.; Jansen, J. A.; Mikos, A. G., Evaluation of bone regeneration by DNA release from composites of oligo(poly(ethylene glycol) fumarate) and cationized gelatin microspheres in a critical-sized calvarial defect. *J Biomed Mater Res A* **2006**, 78A, (2), 335 - 342.

107. Chew, S. A.; Hacker, M. C.; Saraf, A.; Raphael, R. M.; Kasper, F. K.; Mikos, A. G., Biodegradable branched polycationic polymers with varying hydrophilic spacers for nonviral gene delivery. *Biomacromolecules* **2009**, 10, (9), 2436-2445.

108. Chew, S. A.; Hacker, M. C.; Saraf, A.; Raphael, R. M.; Kasper, F. K.; Mikos, A. G., Altering amine basicities in biodegradable branched polycationic polymers for non-viral gene delivery. *Biomacromolecules* **2010**, 11, (3), 600-609.

109. Tanahashi, K.; Mikos, A. G., Effect of hydrophilicity and agmatine modification on degradation of poly(propylene fumarate-co-ethylene glycol) hydrogels. *J. Biomed. Mater. Res., Part A* **2003,** 67, (4), 1148-1154.

110. Cherng, J. Y.; van de Wetering, P.; Talsma, H.; Crommelin, D. J.; Hennink, W. E., Effect of size and serum proteins on transfection efficiency of poly ((2-dimethylamino)ethyl methacrylate)-plasmid nanoparticles. *Pharm Res* **1996,** 13, (7), 1038-1042.

111. Breunig, M.; Lungwitz, U.; Liebl, R.; Goepferich, A., Breaking up the correlation between efficacy and toxicity for nonviral gene delivery. *Proc Natl Acad Sci U S A* **2007,** 104, (36), 14454-14459.

112. Jevprasesphant, R.; Penny, J.; Jalal, R.; Attwood, D.; McKeown, N. B.; D'Emanuele, A., The influence of surface modification on the cytotoxicity of PAMAM dendrimers. *Int J Pharm* **2003,** 252, (1-2), 263-266.

113. Mao, S.; Shuai, X.; Unger, F.; Wittmar, M.; Xie, X.; Kissel, T., Synthesis, characterization and cytotoxicity of poly(ethylene glycol)-graft-trimethyl chitosan block copolymers. *Biomaterials* **2005,** 26, (32), 6343-6356.

114. Tseng, W. C.; Fang, T. Y.; Su, L. Y.; Tang, C. H., Dependence of transgene expression and the relative buffering capacity of dextran-grafted polyethylenimine. *Mol Pharm* **2005,** 2, (3), 224-232.

115. Forrest, M. L.; Koerber, J. T.; Pack, D. W., A degradable polyethylenimine derivative with low toxicity for highly efficient gene delivery. *Bioconjug Chem* **2003,** 14, (5), 934-940.

116. Liu, Y.; Wu, D.; Ma, Y.; Tang, G.; Wang, S.; He, C.; Chung, T.; Goh, S., Novel poly(amino ester)s obtained from Michael addition polymerizations of trifunctional amine monomers with diacrylates: safe and efficient DNA carriers. *Chem Commun (Camb)* **2003,** (20), 2630-2631.

117. Lu, L.; Stamatas, G. N.; Mikos, A. G., Controlled release of transforming growth factor beta1 from biodegradable polymer microparticles. *J Biomed Mater Res* **2000,** 50, (3), 440-451.

118. Timmer, M. D.; Shin, H.; Horch, R. A.; Ambrose, C. G.; Mikos, A. G., In vitro cytotoxicity of injectable and biodegradable poly(propylene fumarate)-based networks: unreacted macromers, cross-linked networks, and degradation products. *Biomacromolecules* **2003,** 4, (4), 1026-1033.

119. Saraf, A.; Hacker, M. C.; Sitharaman, B.; Grande-Allen, K. J.; Barry, M. A.; Mikos, A. G., Synthesis and conformational evaluation of a novel gene delivery vector for human mesenchymal stem cells. *Biomacromolecules* **2008,** 9, (3), 818-827.

120. Hosseinkhani, H.; Aoyama, T.; Yamamoto, S.; Ogawa, O.; Tabata, Y., In vitro transfection of plasmid DNA by amine derivatives of gelatin accompanied with ultrasound irradiation. *Pharm Res* **2002**, 19, (10), 1471-1479.

121. Yoshii, E., Cytotoxic effects of acrylates and methacrylates: relationships of monomer structures and cytotoxicity. *J Biomed Mater Res* **1997**, 37, (4), 517-524.

122. Zhong, Z.; Song, Y.; Engbersen, J. F.; Lok, M. C.; Hennink, W. E.; Feijen, J., A versatile family of degradable non-viral gene carriers based on hyperbranched poly(ester amine)s. *J Control Release* **2005**, 109, (1-3), 317-329.

123. Breunig, M.; Lungwitz, U.; Liebl, R.; Fontanari, C.; Klar, J.; Kurtz, A.; Blunk, T.; Goepferich, A., Gene delivery with low molecular weight linear polyethylenimines. *J Gene Med* **2005**, 7, (10), 1287-1298.

124. Midoux, P.; Monsigny, M., Efficient gene transfer by histidylated polylysine/pDNA complexes. *Bioconjug Chem* **1999**, 10, (3), 406-411.

125. Dunlap, D. D.; Maggi, A.; Soria, M. R.; Monaco, L., Nanoscopic structure of DNA condensed for gene delivery. *Nucleic Acids Res* **1997**, 25, (15), 3095-3101.

126. Boussif, O.; Zanta, M. A.; Behr, J. P., Optimized galenics improve in vitro gene transfer with cationic molecules up to 1000-fold. *Gene Ther* **1996**, 3, (12), 1074-1080.

127. Godbey, W. T.; Wu, K. K.; Mikos, A. G., Size matters: molecular weight affects the efficiency of poly(ethylenimine) as a gene delivery vehicle. *J Biomed Mater Res* **1999**, 45, (3), 268-275.

128. Putnam, D.; Gentry, C. A.; Pack, D. W.; Langer, R., Polymer-based gene delivery with low cytotoxicity by a unique balance of side-chain termini. *Proc. Natl. Acad. Sci. U.S.A.* **2001**, 98, (3), 1200-1205.

129. You, Y. Z.; Manickam, D. S.; Zhou, Q. H.; Oupicky, D., Reducible poly(2-dimethylaminoethyl methacrylate): synthesis, cytotoxicity, and gene delivery activity. *J Control Release* **2007**, 122, (3), 217-225.

130. Tao, L.; Liu, J.; Tan, B. H.; Davis, T. P., RAFT Synthesis and DNA Binding of Biodegradable, Hyperbranched Poly(2-(dimethylamino)ethyl Methacrylate. *Macromolecules* **2009**, 42, 4960-4962.

131. Chen, Q. R.; Zhang, L.; Luther, P. W.; Mixson, A. J., Optimal transfection with the HK polymer depends on its degree of branching and the pH of endocytic vesicles. *Nucleic Acids Res* **2002**, 30, (6), 1338-1345.

132. Pack, D. W.; Putnam, D.; Langer, R., Design of imidazole-containing endosomolytic biopolymers for gene delivery. *Biotechnol Bioeng* **2000**, 67, (2), 217-223.

133. Kanayama, N.; Fukushima, S.; Nishiyama, N.; Itaka, K.; Jang, W. D.; Miyata, K.; Yamasaki, Y.; Chung, U. I.; Kataoka, K., A PEG-based biocompatible block catiomer with high buffering capacity for the construction of polyplex micelles showing efficient gene transfer toward primary cells. *ChemMedChem* **2006**, 1, (4), 439-444.

134. Xiong, M. P.; Bae, Y.; Fukushima, S.; Forrest, M. L.; Nishiyama, N.; Kataoka, K.; Kwon, G. S., pH-responsive Multi-PEGylated dual cationic nanoparticles enable charge modulations for safe gene delivery. *ChemMedChem* **2007**, 2, (9), 1321-1327.

135. Ahlstrom, B.; Edebo, L., Hydrolysis of the soft amphiphilic antimicrobial agent tetradecyl betainate is retarded after binding to and killing Salmonella typhimurium. *Microbiology* **1998**, 144 (Pt 9), 2497-2504.

136. Niyibizi, C.; Baltzer, A.; Lattermann, C.; Oyama, M.; Whalen, J. D.; Robbins, P. D.; Evans, C. H., Potential role for gene therapy in the enhancement of fracture healing. In *Clin Orthop Relat Res*, 1998; pp S148-153.

137. Chen, Y., Orthopedic applications of gene therapy. In *J Orthop Sci*, 2001; Vol. 6, pp 199-207.

138. Young, S.; Patel, Z. S.; Kretlow, J. D.; Murphy, M. B.; Mountziaris, P. M.; Baggett, L. S.; Ueda, H.; Tabata, Y.; Jansen, J. A.; Wong, M.; Mikos, A. G., Dose Effect of Dual Delivery of Vascular Endothelial Growth Factor and Bone Morphogenetic Protein-2 on Bone Regeneration in a Rat Critical-Size Defect Model. *Tissue Eng Part A* **2009**, 15, (9), 2347-2362.

139. Patel, Z. S.; Ueda, H.; Yamamoto, M.; Tabata, Y.; Mikos, A. G., In vitro and in vivo release of vascular endothelial growth factor from gelatin microparticles and biodegradable composite scaffolds. *Pharm Res* **2008**, 25, (10), 2370-2378.

140. Kasper, F. K.; Kushibiki, T.; Kimura, Y.; Mikos, A. G.; Tabata, Y., In vivo release of plasmid DNA from composites of oligo(poly(ethylene glycol)fumarate) and cationized gelatin microspheres. *J Control Release* **2005**, 107, (3), 547-561.

141. Kasper, F. K.; Jerkins, E.; Tanahashi, K.; Barry, M. A.; Tabata, Y.; Mikos, A. G., Characterization of DNA release from composites of oligo(poly(ethylene glycol) fumarate) and cationized gelatin microspheres in vitro. *J Biomed Mater Res A* **2006**, 78, (4), 823-835.

142. Patel, Z. S.; Yamamoto, M.; Ueda, H.; Tabata, Y.; Mikos, A. G., Biodegradable gelatin microparticles as delivery systems for the controlled release of bone morphogenetic protein-2. *Acta Biomater* **2008**, 4, (5), 1126-1138.

143. He, S.; Timmer, M. D.; Yaszemski, M. J.; Yasko, A. W.; Engel, P. S.; Mikos, A. G., Synthesis of biodegradable poly(propylene fumarate) networks with

poly(propylene fumarate)-diacrylate macromers as crosslinking agents and characterization of their degradation products. *Polymer* **2001**, 42, (3), 1251-1260.

144. Shi, X.; Sitharaman, B.; Pham, Q. P.; Liang, F.; Wu, K.; Edward Billups, W.; Wilson, L. J.; Mikos, A. G., Fabrication of porous ultra-short single-walled carbon nanotube nanocomposite scaffolds for bone tissue engineering. *Biomaterials* **2007**, 28, (28), 4078-4090.

145. Roy, D. M.; Linnehan, S. K., Hydroxyapatite Formed from Coral Skeletal Carbonate by Hydrothermal Exchange. *Nature* **1974**, 247, (5438), 220-222.

146. Kasper, F. K.; Tanahashi, K.; Fisher, J. P.; Mikos, A. G., Synthesis of poly(propylene fumarate). *Nat Protoc* **2009**, 4, (4), 518-525.

147. Moore, M. J.; Jabbari, E.; Ritman, E. L.; Lu, L.; Currier, B. L.; Windebank, A. J.; Yaszemski, M. J., Quantitative analysis of interconnectivity of porous biodegradable scaffolds with micro-computed tomography. *J Biomed Mater Res A* **2004**, 71, (2), 258-267.

148. Tabata, Y.; Hijikata, S.; Muniruzzaman, M.; Ikada, Y., Neovascularization effect of biodegradable gelatin microspheres incorporating basic fibroblast growth factor. *J Biomater Sci Polym Ed* **1999**, 10, (1), 79-94.

149. Holland, T. A.; Tessmar, J. K.; Tabata, Y.; Mikos, A. G., Transforming growth factor-beta 1 release from oligo(poly(ethylene glycol) fumarate) hydrogels in conditions that model the cartilage wound healing environment. *J Control Release* **2004**, 94, (1), 101-114.

150. Kim, H. J.; Kwon, M. S.; Choi, J. S.; Yang, S. M.; Yoon, J. K.; Kim, K.; Park, J. S., Highly effective and slow-biodegradable network-type cationic gene delivery polymer: small library-like approach synthesis and characterization. *Biomaterials* **2006**, 27, (10), 2292-2301.

151. Loscher, W.; Reissmuller, E.; Ebert, U., Anticonvulsant effect of fosphenytoin in amygdala-kindled rats: comparison with phenytoin. *Epilepsy Res* **1998**, 30, (1), 69-76.

152. Allen, F. H. J.; Runge, J. W.; Legarda, S.; Maria, B. L.; Matsuo, F.; Fischer, J. H.; Kugler, A. R.; Basson, S. M., Safety, tolerance and pharmacokinetics of intravenous fosphenytoin (Cerebyx) in status epilepticus. *Epilepsia* **1995**, 36.

153. Amling, M.; Priemel, M.; Holzmann, T.; Chapin, K.; Rueger, J. M.; Baron, R.; Demay, M. B., Rescue of the skeletal phenotype of vitamin D receptor-ablated mice in the setting of normal mineral ion homeostasis: formal histomorphometric and biomechanical analyses. *Endocrinology* **1999**, 140, (11), 4982-4987.

154. Young, S.; Wong, M.; Tabata, Y.; Mikos, A. G., Gelatin as a delivery vehicle for the controlled release of bioactive molecules. *J Control Release* **2005,** 109, (1-3), 256-274.

155. Huang, Z.; Nelson, E. R.; Smith, R. L.; Goodman, S. B., The sequential expression profiles of growth factors from osteoprogenitors [correction of osteroprogenitors] to osteoblasts in vitro. *Tissue Eng* **2007,** 13, (9), 2311-2320.

156. Lalani, Z.; Wong, M.; Brey, E. M.; Mikos, A. G.; Duke, P. J., Spatial and temporal localization of transforming growth factor-beta1, bone morphogenetic protein-2, and platelet-derived growth factor-A in healing tooth extraction sockets in a rabbit model. *J Oral Maxillofac Surg* **2003,** 61, (9), 1061-1072.

157. Pouton, C. W.; Seymour, L. W., Key issues in non-viral gene delivery. *Adv Drug Deliv Rev* **1998,** 34, (1), 3-19.

158. Choate, K. A.; Khavari, P. A., Direct cutaneous gene delivery in a human genetic skin disease. *Hum Gene Ther* **1997,** 8, (14), 1659-1665.

159. Levy, M. Y.; Barron, L. G.; Meyer, K. B.; Szoka, F. C., Jr., Characterization of plasmid DNA transfer into mouse skeletal muscle: evaluation of uptake mechanism, expression and secretion of gene products into blood. *Gene Ther* **1996,** 3, (3), 201-211.